

AD-A149 410 SINGLE INTEGRAL CONSTITUTIVE EQUATIONS FOR VISCOELASTIC 1/1
FLUIDS(U) WISCONSIN UNIV-MADISON MATHEMATICS RESEARCH
CENTER P BACH ET AL. SEP 84 MRC-TSR-2755
UNCLASSIFIED DRAG29-80-C-0041 F/G 12/1 NL

SINGLE INTEGRAL CONSTITUTIVE EQUATIONS FOR VISCOELASTIC
FLUIDS(U) WISCONSIN UNIV-MADISON MATHEMATICS RESEARCH
CENTER P BACH ET AL. SEP 84 MRC-TSR-2755
DAGG29-80-C-0041 F/G 12/1

1/1

UNCLASSIFIED

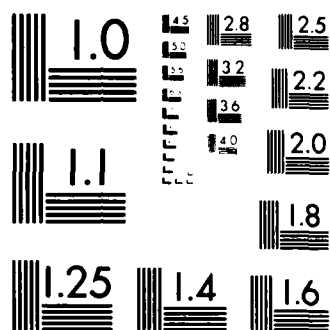
F/G 12/1

NL

END

412 WFC

RESULTS



MICROCOPY RESOLUTION TEST CHART
NATIONAL BUREAU OF STANDARDS-1963-A

AD-A149 410

MRC Technical Summary Report #2755

SINGLE INTEGRAL CONSTITUTIVE
EQUATIONS FOR VISCOELASTIC FLUIDS

Poul Bach and Ole Hassager

**Mathematics Research Center
University of Wisconsin—Madison
610 Walnut Street
Madison, Wisconsin 53705**

September 1984

(Received July 6, 1984)

DTIC FILE COPY

Approved for public release
Distribution unlimited

DTIC
SELECTED
JAN 16 1985

Sponsored by

U. S. Army Research Office
P. O. Box 12211
Research Triangle Park
North Carolina 27709

85 01 16 010

UNIVERSITY OF WISCONSIN-MADISON
MATHEMATICS RESEARCH CENTER


SINGLE INTEGRAL CONSTITUTIVE EQUATIONS FOR VISCOELASTIC FLUIDS

Poul Bach and Ole Hassager*

Technical Summary Report #2755
September 1984

ABSTRACT

It is demonstrated how the kernel functions of single integral constitutive equations may be determined from analysis of experiments in time dependent shear-free flows alone. It is assumed that the kernel functions may be factored into a product of a linear viscoelastic function and a finite-strain dependent function. No assumption is needed on the strain-dependent function except that it must be continuous within the attainable invariant space. The experimental data for ever-increasing deformations are not compatible with the assumptions inherent in single integral constitutive equations with factorized kernel functions.



AMS (MOS) Subject Classifications: 65D99, 76A10, 73G10

Key Words: Integral constitutive equations, Viscoelasticity, Rheology

Work Unit Number 2 (Physical Mathematics)

*Instituttet for Kemiteknik, Danmarks Tekniske Højskole,
DK-2800 Lyngby, Denmark

Sponsored by the United States Army under Contract No. DAAG29-80-C-0041 and the Danish Council for Scientific and Industrial Research under Grant No. 16-3475, K-822.

SIGNIFICANCE AND EXPLANATION

The characterization of the flow properties of polymeric melts represents an important and still partially unsolved problem. The "constitutive equations" used in the characterization involve unknown kernel functions of several variables that need to be determined from experiments. Usually some specific analytical form of the kernel functions with a small number of parameters is either assumed or derived from molecular arguments. In this report we show how one may determine the kernel functions of some rather general constitutive equations directly from experiments on a polymer melt. The method is analagous to the determination of the strain energy function in crosslinked rubber. The paper should be useful to the theoretical rheologist who is continually searching for "the most general" constitutive equation needed to characterize polymer melts, and to the experimental rheologist who wishes to analyze measurements with a minimum of assumptions.

Accession For	
NTIS GRA&I	<input checked="" type="checkbox"/>
DTIC TAB	<input type="checkbox"/>
Unannounced	<input type="checkbox"/>
Justification	
By	
Distribution/	
Availability Codes	
Dist	Avail and/or Special
A/1	



The responsibility for the wording and views expressed in this descriptive summary lies with MRC, and not with the authors of this report.

SINGLE INTEGRAL CONSTITUTIVE EQUATIONS FOR VISCOELASTIC FLUIDS

Poul Bach and Ole Hassager*

1. INTRODUCTION AND DEFINITION OF MODELS

The purpose of this report is to demonstrate how the kernel functions of two rather general single integral constitutive equations for viscoelastic fluids may be determined from experimental measurements. The two particular equations are:

"The factorized K-BKZ model":

$$\underline{\mathbf{I}}(t) = \int_{-\infty}^t M(t - t') \left[\frac{\partial W}{\partial \mathbf{I}_1} \underline{\chi}_{[0]} + \frac{\partial W}{\partial \mathbf{I}_2} \underline{\chi}^{[0]} \right] dt' \quad (1.1)$$

and "The factorized Rivlin Sawyers model":

$$\underline{\mathbf{I}}(t) = \int_{-\infty}^t M(t - t') [\phi_1 \underline{\chi}_{[0]} + \phi_2 \underline{\chi}^{[0]}] dt' \quad (1.2)$$

Here $\underline{\mathbf{I}}(t)$ is the stress tensor at a given particle at the current time t and $\underline{\chi}_{[0]}$ and $\underline{\chi}^{[0]}$ are strain tensors that differ from the Finger strain tensor $\underline{\mathbf{E}}$ and its inverse $\underline{\mathbf{E}}^{-1}$, respectively only by a unit tensor $\underline{\underline{\delta}}$:

$$\underline{\chi}_{[0]} = \underline{\underline{\delta}} - \underline{\mathbf{E}}; \quad \underline{\chi}^{[0]} = \underline{\mathbf{E}}^{-1} - \underline{\underline{\delta}} \quad (1.3)$$

The components of $\underline{\mathbf{E}}$ are given by $E_{ij} = (\partial x_i / \partial x'_m)(\partial x_j / \partial x'_m)$ where the x_i are the coordinates at time t of the particle with coordinates x'_i at time t' . In addition in Eqs. (1.1) and (1.2) the function M is the memory function of linear viscoelasticity related to the linear viscoelastic relaxation modulus G as follows

$$G(t) = \int_t^{\infty} M(s) ds \quad (1.4)$$

*Institutet for Kemiteknik, Danmarks Tekniske Højskole, DK2800 Lyngby, DENMARK

Sponsored by the United States Army under Contract No. DAAG29-80-C-0041 and the Danish Council for Scientific and Industrial Research under Grant No. 16-3475, K-802.

Also $\hat{\alpha}_1(I_1, I_2)$, $\hat{\alpha}_2(I_1, I_2)$ and $W(I_1, I_2)$ are nondimensional scalar functions that depend on the scalar invariants I_1 and I_2 defined by

$$I_1 = \text{tr } \underline{B}; \quad I_2 = \text{tr } \underline{B}^{-1} \quad (1.5)$$

Certainly the model in Eq. (1.1) is contained in Eq. (1.2), however for the purpose of this report it is convenient to consider it as a separate model.

In connection with the models in Eqs. (1.1) and (1.2) we note that:

i) If $W(I_1, I_2)$ and the $\hat{\alpha}_i(I_1, I_2)$, $i = 1, 2$ are analytic at $(I_1, I_2) = (3, 3)$ then the models may be approximated in slow flow by a "third order fluid" with parameters given in Bird, Armstrong and Hassager (1985).

ii) Renardy (1984) has derived sufficient conditions on W under which initial value problems based on Eq. (1.1) are always well posed, i.e. Hadamard type instability cannot occur.

iii) Hassager (1981) has derived a variational principle for Eq. (1.1) useful for simulation of creeping flow situations based on that constitutive equation.

The model in Eq. (1.1) is a factorized form of a more general model proposed independently by Kaye (1962) and Bernstein, Kearsley and Zapas (1963):

$$\underline{\tau} = \int_{-\infty}^t \left[\frac{\partial V}{\partial I_1} \underline{\gamma}_{[0]} + \frac{\partial V}{\partial I_2} \underline{\gamma}^{[0]} \right] dt' \quad (1.6)$$

where V is a scalar function of $(t - t')$, I_1 and I_2 . We call this the K-BKZ model. The arguments leading to this model may be traced back to Lodge (1964) who noted the striking similarity between the behavior of polymer melts and crosslinked natural rubber. Lodge then started with a stress-strain relation for crosslinked natural rubber obtained on the basis of a molecular theory, and then used a heuristic argument to "liquify" the relation to arrive at the "rubberlike liquid model" in Table 1.1. In the same way does Eq. (1.6) represent a heuristic "liquification" of the nonlinear stress-strain relation for incompressible isotropic materials. For example if in Eq. (1.1) one replaces $M(t - t')$ by $G_0 \delta(t' - t_0)$ one obtains the stress-strain relation for an elastic material with stress free state equal to the configuration of time t_0 and with strain energy

function (G_0W). Certainly the special status given to one particular configuration is incompatible with the concept of a fluid, and it is understood that the function V in Eq. (1.6) or M in Eq. (1.1) do not give special status to any one past configuration (but they decay to zero as $(t - t')$ tends to infinity sufficiently fast that the integrals converge).

The argumentation leading to Eq. (1.6) was questioned by Rivlin and Sawyers (1971) who instead started with the physical assumption that the effects on the stress at time t of the deformations at different past times t' are independent of each other. With this assumption it may be shown from the theory of additive functionals (Martin and Mizel (1964), Chacon and Friedman (1965)) that the most general constitutive equation for isotropic fluids is:

$$\underline{\tau}(t) = \int_{-\infty}^t [\psi_1 \underline{\gamma}^{[0]} + \psi_2 \underline{\gamma}^{[0]}] dt' \quad (1.7)$$

where the ψ 's are functions of $(t - t')$, I_1 and I_2 . We call this the Rivlin Sawyers model.

We now see that the two models to be investigated in this report, Eqs. (1.1) and (1.2) follow from the assumptions inherent in K-BKZ model and the Rivlin Sawyer model plus the additional assumptions that respectively

$$V(t - t', I_1, I_2) = M(t - t') W(I_1, I_2) \quad (1.8)$$

$$\psi_i(t - t', I_1, I_2) = M(t - t') \phi_i(I_1, I_2); \quad i = 1, 2 \quad (1.9)$$

It is at this point reasonable to ask why the seemingly arbitrary assumptions in Eqs. (1.8) and (1.9) are added to the assumptions already present in the K-BKZ and Rivlin Sawyers models. We do this for the following reasons:

- i) Two key types of molecular models, the Lodge (1956) network model on the one hand and the Curtiss Bird ($\epsilon = 0$) (1981) and Doi Edwards (1978) melt models on the other hand show such a factorization and may in fact be represented by a K-BKZ model with a potential.
- ii) Carefully performed experiments (e.g. Laun (1978), Einaga, Osaki and Kurata (1971)) indicate that at least some polymers may allow for such a factorization in simple shear deformations.

iii) From a practical point of view it may be impossible to determine a function of three independent variables on the basis of a limited number of experimental data. For this reason a number of empirical models with a limited number of parameters have been proposed, as shown in Table 1.2. These empirical relations all involve the assumption in Eq. (1.8).

Table 1.1 Examples of factorized K-BKZ models

Reference	$M(s)$	$W(I_1, I_2)$	Adjustable parameters
Lodge (1956)	$\sum_{i=1}^{\infty} \frac{M_i}{\lambda_i^2} e^{-s/\lambda_i}$	I_1	y_i, λ_i for $i = 1, 2, \dots$
Curtiss and Bird ^a (1981) with their $\epsilon = 0$.	$\frac{8}{5} N n k T \lambda^{-1} \sum_{\alpha, \text{odd}} \exp(-\pi^2 \alpha^2 s / \lambda)$	$\frac{5}{4\pi} \int \ln (\underline{B} : \underline{u}\underline{u}) d\underline{u}$	$(N n k T \lambda^{-1})$ and λ

Notes: ^aIn this model \underline{u} is a unit vector, and $\int d\underline{u}$ is an integral over a unit sphere. This model is identical in form to that of Doi and Edwards (1978), (1979)

Table 1.2 Examples factorized Rivlin Sawyers models (empirical)

Reference	Flow	ϕ_1	ϕ_2	Adjustable Parameters
Phillips (1977)	Simple Shear ^a	$(1 - \epsilon)\exp(-\alpha s)$	$\epsilon \exp(-\alpha s)$	ϵ, α
	General	(not specified)	(not specified)	note that $\epsilon = -\psi_{2,0}/\psi_{1,0}$
Wagner (1979)	Simple Shear ^a	$\exp(-ns)$	0	n, α
	General	$\exp(-n \sqrt{I - 3})$ $I = \alpha I_1 + (1-\alpha)I_2$	0	note that $\psi_2 = 0$
Papana Stasiou et al. (1983)	Simple Shear ^a	$\frac{\alpha}{\alpha + s^2}$	0	α, ρ
	General	$\frac{\alpha}{(\alpha-3) + \alpha I_1 + (1-\alpha)I_2}$	0	note that $\psi_2 = 0$

^aHere $s(t, t')$ is the "magnitude of shear", defined for $v_x = \dot{\gamma}_{yx}(t)y$, $v_y = v_z = 0$ as

$$s(t, t') = \left| \int_t^{t'} \dot{\gamma}_{yx}(t'') dt'' \right|.$$

The significance of the factorizations in Eqs. (1.8) and (1.9) is that the properties of, say, the K-BKZ model now depends on two separate functions: the linear viscoelastic memory function $M(t - t')$ and a nonlinear strain function $W(I_1, I_2)$. Standard techniques exist for the determination of M from measurements performed at small deformations (Ferry 1980). In this report we will demonstrate how $W(I_1, I_2)$ (or respectively $\phi_1(I_1, I_2)$ and $\phi_2(I_1, I_2)$) may be determined without the restrictions inherent in the empiricism in Table 1.2.

Since the nonlinear functions to be determined, $W(I_1, I_2)$ and $\phi_i(I_1, I_2)$, $i = 1, 2$, are functions of two arguments one needs experiments that cover as densely as possible the

"obtainable invariant space" given by all possible values of (I_1, I_2) subject to the incompressibility constraint. Such experiments may presently be performed in just one laboratory namely that of Meissner at the ETH in Zürich (see Meissner, Stephenson, Demarmels and Portman (1982)). The experimental method can be thought of as an analog for fluids of the method used by Rivlin and Saunders (1951) in their now classical experimental determination of the strain energy function for natural rubber.

2. KINEMATICS

We now consider the class of flows called shear-free flows. We use the notation proposed by Bird, Armstrong and Hassager (1985) but we have obtained the material data from Meissner, Stephenson, Demarmels and Portmann (1982). A comparison of the two notations is given in Table 2.1. In the notation of Bird et al. (1985), all shear-free flows may be put in the form:

$$\begin{aligned}v_x &= -\frac{1}{2}\dot{\epsilon}(t)(1+b)x \\v_y &= -\frac{1}{2}\dot{\epsilon}(t)(1-b)y \\v_z &= \dot{\epsilon}(t)z\end{aligned}\tag{2.1}$$

where $0 \leq b \leq 1$ and $\dot{\epsilon}(t)$ is any function of time.

Table 2.1: Comparison of notation in shear-free flows.

$b, \dot{\epsilon}$: parameters of Bird, Armstrong and Hassager (1985)

$m, \dot{\epsilon}_0$: parameters of Meissner, Stephenson, Demarmels and Portmann (1982)

Flow Type	b	m	Strain-rates	Material Functions
Uniaxial	0	$-\frac{1}{2}$	$\dot{\epsilon} = \dot{\epsilon}_0$	$\mu_1 = \frac{1}{3} \bar{\eta}_1^+$
biaxial	0	1	$\dot{\epsilon} = -2\dot{\epsilon}_0$	$\mu_1 = \frac{1}{3} \bar{\eta}_1^+$
plannar	1	0	$\dot{\epsilon} = -\dot{\epsilon}_0$	$\mu_1 = \frac{1}{4} \bar{\eta}_1^+$ $\mu_2 = \frac{1}{2} \bar{\eta}_2^+$
ellipsoidal	$\frac{1}{3}$	$\frac{1}{2}$	$\dot{\epsilon} = -\frac{3}{2}\dot{\epsilon}_0$	$\mu_1 = \frac{3}{4} \bar{\eta}_1^+$ $\mu_2 = \frac{3}{2} \bar{\eta}_2^+$

We have analyzed measurements taken by Demarmels (1983) on a polyisobutylene melt in start-up of the following flows: Uniaxial-, biaxial-, planar- and ellipsoidal-elongational flows. Uniaxial elongational flow is obtained by choosing $b = 0$ and $\dot{\epsilon}$ positive, and biaxial elongational flow by choosing $b = 0$, but $\dot{\epsilon}$ negative. Planar elongational, also called "pure shear flow", is obtained with $b = 1$ and $\dot{\epsilon}$ negative, and ellipsoidal elongational flow is obtained with $b = \frac{1}{3}$ and $\dot{\epsilon}$ negative.

We wish to find the displacement functions for start-up of the shear-free flow described in Eq. (1), i.e. we imagine that $\dot{\epsilon}(t) = 0$ for $t < 0$ and $\dot{\epsilon}(t) = \dot{\epsilon}$ a constant for $t > 0$. Then, for $0 \leq t' \leq t$ we get:

$$\begin{aligned} x &= x' e^{-1/2 \dot{\epsilon}(1+b)(t-t')} \\ y &= y' e^{-1/2 \dot{\epsilon}(1-b)(t-t')} \\ z &= z' e^{\dot{\epsilon}(t-t')} \end{aligned} \quad (2)$$

and for $t' < 0$ we get

$$\begin{aligned} x &= x' e^{-1/2 \dot{\epsilon}(1+b)t} \\ y &= y' e^{-1/2 \dot{\epsilon}(1-b)t} \\ z &= z' e^{\dot{\epsilon}t} \end{aligned} \quad (2.3)$$

where a fluid particle P with coordinates x_i , at the present time t , had coordinates x'_i , $i = 1, 2, 3$ at a past time t' . We define $s = t - t'$; we now calculate the displacement gradient tensor for $0 \leq t' \leq t$. In the notation of Bird, Armstrong and Hassager (1985):

$$\underline{\underline{E}}(x, t, t') = \begin{bmatrix} e^{-1/2 \dot{\epsilon}(1+b)s} & 0 & 0 \\ 0 & e^{-1/2 \dot{\epsilon}(1-b)s} & 0 \\ 0 & 0 & e^{\dot{\epsilon}s} \end{bmatrix} \quad (2.4)$$

and we find

$$\underline{\underline{E}} \cdot \underline{\underline{F}}^+ \equiv \underline{\underline{B}} = \begin{bmatrix} e^{-\dot{\epsilon}(1+b)s} & 0 & 0 \\ 0 & e^{-\dot{\epsilon}(1-b)s} & 0 \\ 0 & 0 & e^{2\dot{\epsilon}s} \end{bmatrix} \quad (2.5)$$

We now find the first invariant:

$$\begin{aligned} I_1 &\equiv \text{tr}(\underline{\underline{B}}) \\ &= e^{-\dot{\epsilon}(1+b)s} + e^{-\dot{\epsilon}(1-b)s} + e^{2\dot{\epsilon}s} \end{aligned} \quad (2.6)$$

Similarly we find:

$$\underline{\underline{\Delta}}(x, t, t') = \begin{bmatrix} e^{1/2 \dot{\epsilon}(1+b)s} & 0 & 0 \\ 0 & e^{1/2 \dot{\epsilon}(1-b)s} & 0 \\ 0 & 0 & e^{-\dot{\epsilon}s} \end{bmatrix} \quad (2.7)$$

and

$$\underline{\underline{\Delta}}^+ \cdot \underline{\underline{\Delta}} \equiv \underline{\underline{B}}^{-1} = \begin{bmatrix} e^{\dot{\epsilon}(1+b)s} & 0 & 0 \\ 0 & e^{\dot{\epsilon}(1-b)s} & 0 \\ 0 & 0 & e^{-2\dot{\epsilon}s} \end{bmatrix} \quad (2.8)$$

The notation is this of Bird, Armstrong and Hassager (1985).

Similarly we find the second invariant

$$\begin{aligned} I_2 &\equiv \text{tr}(\underline{\underline{B}}^{-1}) \\ &= e^{\dot{\epsilon}(1+b)s} + e^{\dot{\epsilon}(1-b)s} + e^{-2\dot{\epsilon}s} \end{aligned} \quad (2.9)$$

The tensors $\underline{\underline{B}}$ and $\underline{\underline{B}}^{-1}$ may be obtained for $-\infty \leq t' \leq 0$ merely putting "s" equal to "t" in Eqs. 2.5 and 2.8.

For the incompressible flows defined by (2.1) there can be only two independent material functions in start-up flow:

$$\begin{aligned} \bar{n}_1^+ &\equiv -(\tau_{zz} - \tau_{xx})/\dot{\epsilon} \\ \bar{n}_2^+ &\equiv -(\tau_{zz} - \tau_{yy})/\dot{\epsilon} \end{aligned} \quad (2.10)$$

and in fact for $b = 0$ only one independent material function can be found, as

$$\bar{n}_1^+ = \bar{n}_2^+; \quad b = 0. \quad (2.11)$$

This will become obvious when we write down the expressions for \bar{n}_1^+

$$\begin{aligned} \tilde{\varepsilon}_1^{+-} = & \int_{-\infty}^0 M(s) \{ \phi_1 [e^{2\tilde{\varepsilon}s} - e^{\tilde{\varepsilon}(1+b)s}] + \phi_2 [e^{-2\tilde{\varepsilon}s} - e^{\tilde{\varepsilon}(1+b)s}] \} dt, \\ & + \int_0^t M(s) \{ \phi_1 [e^{2\tilde{\varepsilon}s} - e^{\tilde{\varepsilon}(1+b)s}] + \phi_2 [e^{-2\tilde{\varepsilon}s} - e^{\tilde{\varepsilon}(1+b)s}] \} ds \end{aligned} \quad (2.12)$$

Similarly we find:

$$\begin{aligned} \tilde{\varepsilon}_2^{+-} = & \int_{-\infty}^0 M(s) \{ \phi_1 [e^{2\tilde{\varepsilon}s} - e^{\tilde{\varepsilon}(1-b)s}] + \phi_2 [e^{-2\tilde{\varepsilon}s} - e^{\tilde{\varepsilon}(1-b)s}] \} dt, \\ & + \int_0^t M(s) \{ \phi_1 [e^{2\tilde{\varepsilon}s} - e^{\tilde{\varepsilon}(1-b)s}] + \phi_2 [e^{-2\tilde{\varepsilon}s} - e^{\tilde{\varepsilon}(1-b)s}] \} ds \end{aligned} \quad (2.13)$$

The ϕ_i are the functions we wish to estimate.

3. ESTIMATION PROCEDURE.

We now want to find a set of parameters ϕ_{im} , which minimizes the objective function:

$$J = \sum_{i=1}^2 \sum_{n=1}^N (\bar{n}_i^+(t_n) - \tilde{n}_i^+(t_n))^2 \quad (3.1)$$

where $\bar{n}_i^+(t_n)$ are the material functions calculated by (2.12) and (2.13), and $\tilde{n}_i^+(t_n)$ are the experimental data, and N is the number of data points. The parameters ϕ_{im} will be defined below. It is possible to use an iterative minimization routine directly on the problem: $\text{Min}(J)$. However it is more advantageous first to solve the integral equations (2.12) and (2.13) for the strain functions. This allows us to solve the minimization problem directly. The following derivation leads to the same formula as given by Demarmels (1983) (except from an obvious misprint in his eq. 6-12).

We first calculate the time derivative of the material functions:

$$\begin{aligned} \dot{\epsilon} \frac{d\bar{n}_1^+}{dt} = \frac{d}{dt} \{ G(t) (\phi_1 [e^{2\dot{\epsilon}t} - e^{-\dot{\epsilon}(1+b)t}] + \phi_2 [e^{-2\dot{\epsilon}t} - e^{\dot{\epsilon}(1+b)t}]) \\ + M(t) (\phi_1 [e^{2\dot{\epsilon}t} - e^{-\dot{\epsilon}(1+b)t}] + \phi_2 [e^{-2\dot{\epsilon}t} - e^{\dot{\epsilon}(1+b)t}]) \} \end{aligned} \quad (3.2)$$

where we have defined

$$G(t) \equiv \int_{-\infty}^0 M(t-t') dt' = - \int_{\infty}^t M(s) ds.$$

we also define

$$\begin{aligned} c_{11} &\equiv e^{2\dot{\epsilon}t} - e^{-\dot{\epsilon}(1+b)t} \\ c_{12} &\equiv e^{-2\dot{\epsilon}t} - e^{\dot{\epsilon}(1+b)t} \end{aligned} \quad (3.3)$$

and we now find

$$\begin{aligned} \dot{\epsilon} \frac{d\bar{n}_1^+}{dt} = -M(t) (\phi_1 c_{11} + \phi_2 c_{12}) + G(t) \left(\frac{d\phi_1}{dt} c_{11} + \phi_1 \frac{dc_{11}}{dt} + \frac{d\phi_2}{dt} c_{12} + \phi_2 \frac{dc_{12}}{dt} \right) \\ + M(t) (\phi_1 c_{11} + \phi_2 c_{12}) = G(t) \frac{d\phi_1}{dt} \end{aligned} \quad (3.4)$$

where we have defined:

$$\phi_1 = \phi_1 c_{11} + \phi_2 c_{12}$$

The solution to Eq. (16) is found easily

$$\phi_1 = \int_0^t \frac{1}{G(s)} \dot{\epsilon} \left(\frac{d\bar{\eta}_1^+}{ds} \right) ds \quad (3.5)$$

After partial integration we have

$$\phi_1 = \frac{\dot{\epsilon} \bar{\eta}_1^+}{G(t)} + \int_0^t \frac{\dot{\epsilon}}{G(s)^2} \left(\frac{dG}{ds} \right) \bar{\eta}_1^+ ds \quad (3.6)$$

and we see that the RHS only involves the experimental data $(\bar{\eta}_1^+)$ and the known (measured) linear viscoelastic relaxations modulus $G(t)$. The LHS is linear in the strain functions. If we use the same procedure for the second material function we find:

$$\phi_2 \equiv \phi_1 c_{21} + \phi_2 c_{22} = \frac{\dot{\epsilon} \bar{\eta}_2^+}{G(t)} + \int_0^t \frac{\dot{\epsilon}}{G(s)^2} \left(\frac{dG(s)}{ds} \right) \bar{\eta}_2^+ ds \quad (3.7)$$

where

$$\begin{aligned} c_{21} &\equiv e^{2\dot{\epsilon}t} - e^{-\dot{\epsilon}(1-b)t} \\ c_{22} &\equiv e^{-2\dot{\epsilon}t} - e^{\dot{\epsilon}(1-b)t} \end{aligned} \quad (3.8)$$

Eqs. (3.6) and (3.7) can now be solved explicitly for the strain functions ϕ_1 and ϕ_2 , except for flows with $b = 0$. This implies that it is only possible to determine a linear combination of ϕ_1 and ϕ_2 if we only have data from uniaxial or biaxial longational experiments.

We now choose a specific form for the strain functions; which is the same form as used by Bach (1985) to obtain accurate approximations to the Doi-Edwards potential function:

$$\begin{aligned} \phi_1 &= \sum_{m=1}^M N_m(I_1, I_2) \phi_{1m} \\ \phi_2 &= \sum_{m=1}^M N_m(I_1, I_2) \phi_{2m} \end{aligned} \quad (3.9)$$

where ϕ_{1m} and ϕ_{2m} are the nodal values of the strain functions, and $N_m(I_1, I_2)$ are the global shape functions for the isoparametric 4-node element, i.e. the strain functions are approximated with piecewise bilinear functions. The functions are defined on an element mesh covering the allowable invariant space where data are present. We may now write eqs. (3.6) and (3.7)

$$\begin{aligned} \sum_{m=1}^M N_m(I_1, I_2) \phi_{1m} c_{11} + \sum_{m=1}^M N_m(I_1, I_2) \phi_{2m} c_{12} &= H_1(t) \\ \sum_{m=1}^M N_m(I_1, I_2) \phi_{1m} c_{21} + \sum_{m=1}^M N_m(I_1, I_2) \phi_{2m} c_{22} &= H_2(t) \end{aligned} \quad (3.10)$$

where H_1 and H_2 are the RHS of (3.6) and (3.7) respectively. The arguments of the strain functions are functions of elapsed time t : $I_1 = e^{-\dot{\epsilon}(1+b)t} + e^{-\dot{\epsilon}(1-b)t} + e^{+2\dot{\epsilon}t}$, and $I_2 = e^{\dot{\epsilon}(1+b)t} + e^{\dot{\epsilon}(1-b)t} + e^{-2\dot{\epsilon}t}$. We can calculate the H_1 and H_2 functions at every data point t_n , and if we have N data points we have a overdetermined linear equation system with $2M$ unknowns and $2N$ equations. We know that the equations (3.10) are linearly dependent for $b = 0$, and one of these may a priori be excluded from the final equation system. The least squares solution for the $2M$ parameters ϕ_{im} can now be calculated directly using any standard algorithm. We have used the IMSL-routine LLSQF. In Appendix we give a short description of the FORTRAN programs we have developed to solve the estimation problem. Here we only note that it is convenient to use

$$I_1^* = \log(I_1 - 2) \quad (3.11)$$

and

$$I_2^* = \log(I_2 - 2)$$

as the independent variables for the strain functions. We see that I_1^* and I_2^* increase linearly in time for large t , which gives a good distribution of data points in the (I_1^*, I_2^*) space. In Figure 1 we show one of the meshes we have used to describe the strain functions. Datapoints are indicated by (+). We also note that $\phi_1 = \phi_1(I_1^*, I_2^*)$ and $\phi_2 = \phi_2(I_1^*, I_2^*)$ have to obey

$$\phi_1(0,0) + \phi_2(0,0) = 1 \quad (3.12)$$

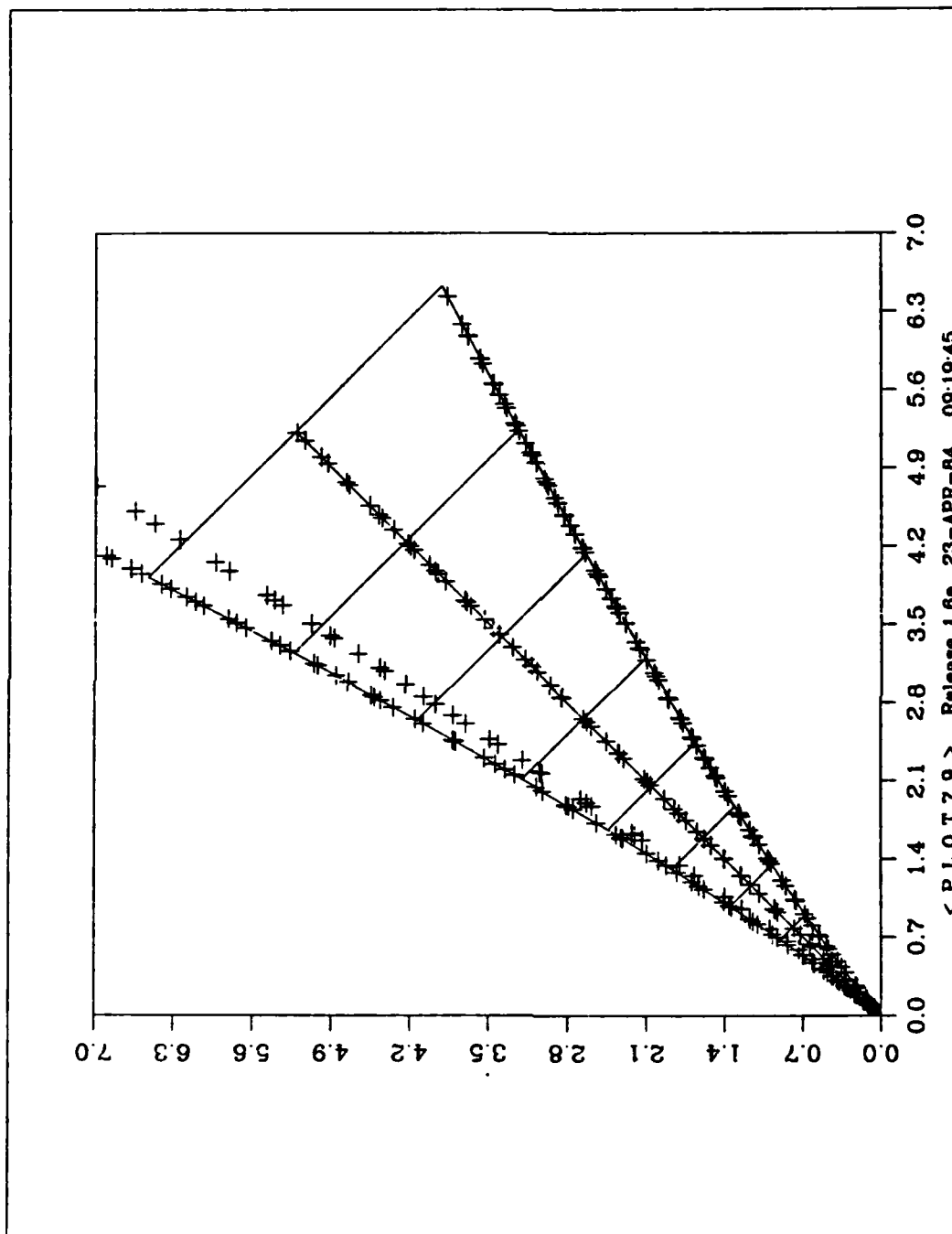


Figure 1. The data points are plotted as (+) in the invariant space (I_1^*, I_2^*) . The solid lines are an example of the meshes used. We only utilize data that lie inside the mesh. Apparently it is easier to obtain measurements for larger invariants in ellipsoidal- and biaxial extension than in uniaxial- and planar extension.

if the model shall conform with the linear viscoelastic model for very small deformations. This leaves $2N - 1$ parameters to be estimated. When we estimate the parameters in eq. (3.10), with the restriction (3.12), we find a very high (10^6) condition number for the equation system. This indicates that several of the supplied equations are numerically linearly dependent. In the two flows, uniaxial- and biaxial longational ($b = 0$), we know that it is impossible to determine other than the combination:

$$\phi = \phi_1 + \phi_2 e^{-\dot{\epsilon}t} \quad (3.13)$$

The planar data do apparently not supply the additional information needed. If the mesh is arranged as in Figure 1 the planar data do not supply any information to determine the parameters on the uniaxial branch, due to the fact that the shape functions belonging to the planar branch are all zero at the uniaxial branch. If we avoid this situation we do find a decrease in the condition number, but only a factor 10, we may conclude that it is not possible to obtain two numerically reliable and independent strain functions with the present data and model. To obtain numerically reliable parameters we simply add constraints to the strain functions by requiring equations of the form

$$\phi_1 - \alpha\phi_2 = 0, \quad (b = 0) \quad (3.14)$$

to be satisfied in least square sense for all data points on the two branches corresponding to $b = 0$. We choose α to be $5/2$, which is the value obtained for Doi-Edwards strain functions for zero deformation. When we add eq. (3.14) to the equation system we obtain a very large decrease in the condition number, from 10^5 to 10^2 . This indicates that the calculated parameters are numerically reliable, but the ultimate test of a model is of course its capability to reproduce the measured material functions. The obtained strain functions are shown on Figure 3 to Figure 6. Doi-Edwards strain functions are shown for comparison. We use the approximation to the Doi-Edwards strain functions obtained by Currie (1982). Bach (1985) has shown that the approximation do not give deviations in the viscosity functions that are larger than 5%, and this accuracy is sufficient for our present comparisons. In the following we use Curries approximation everywhere the Doi-Edwards strain functions are used. The most striking feature of the calculated strain

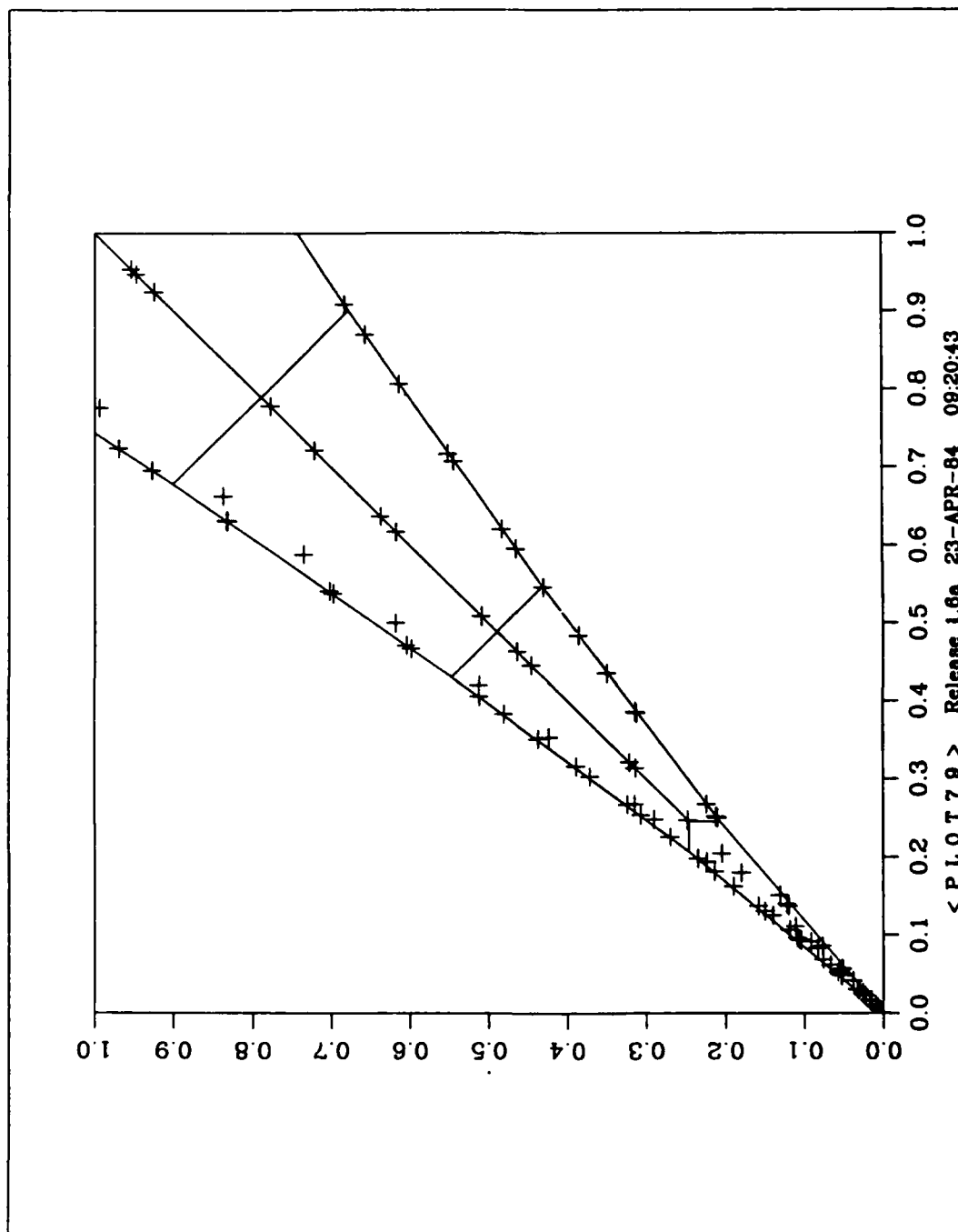


Figure 2. This is a close-up view on the distribution of data points close to zero deformations.

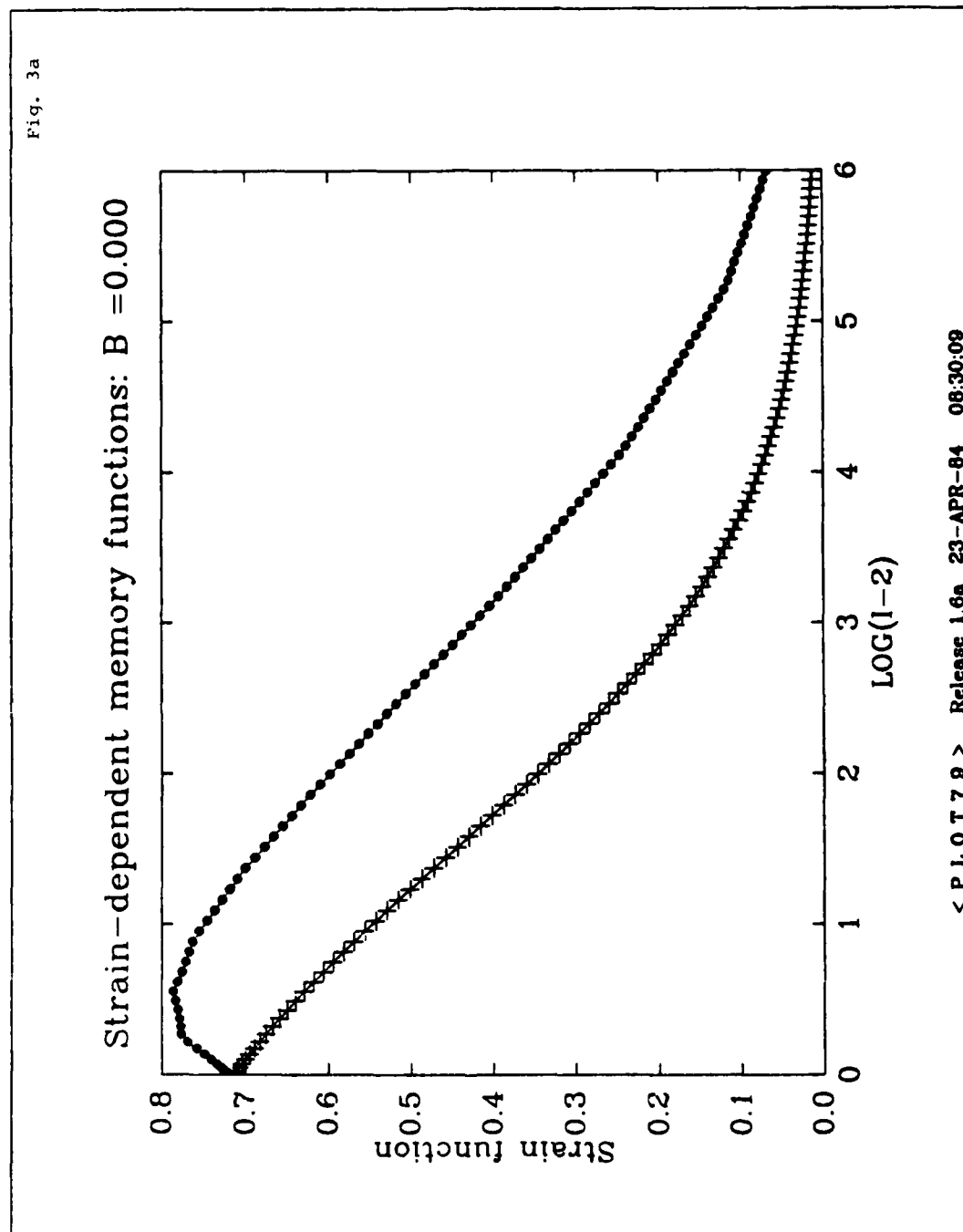
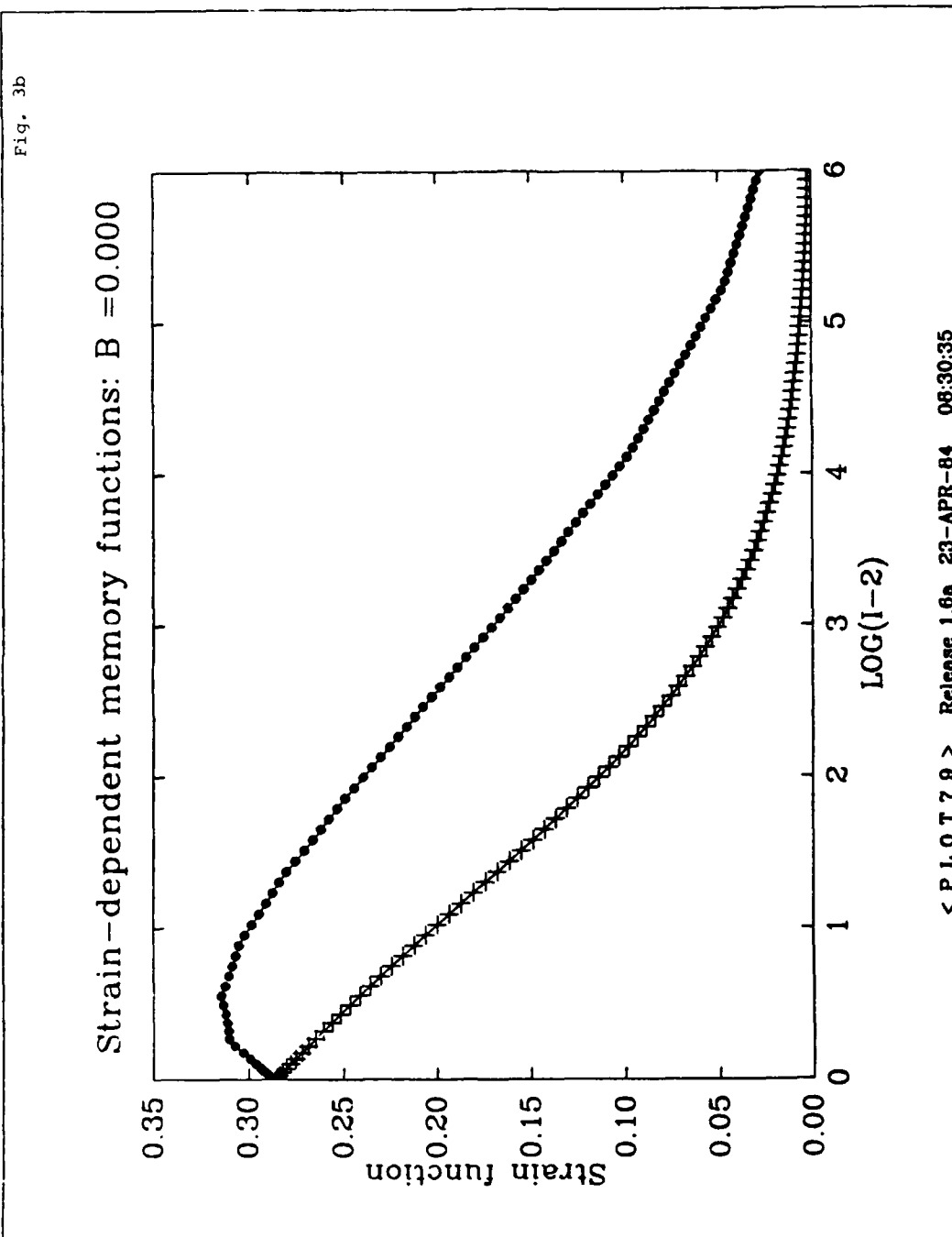
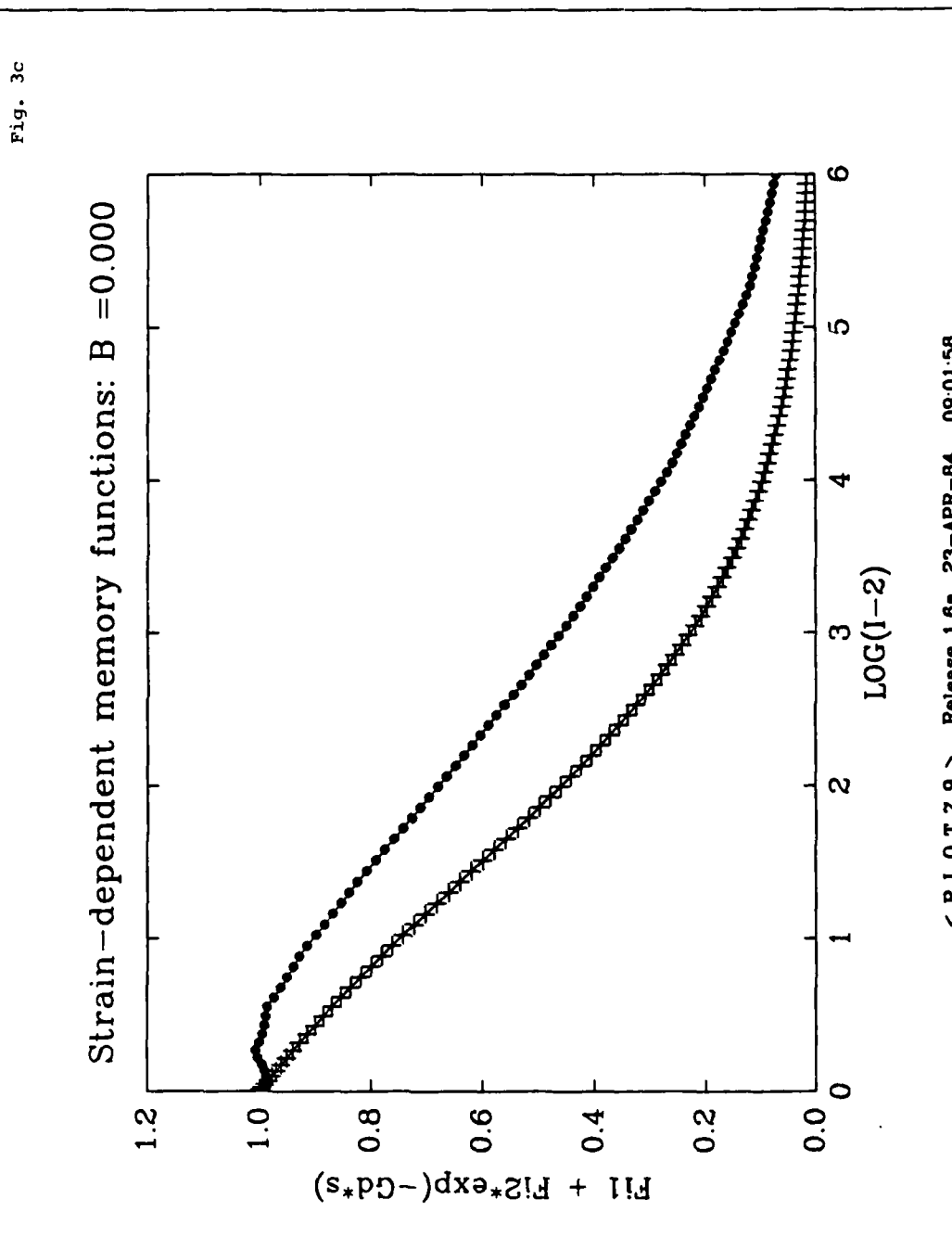


Figure 3. The optimal strain functions in comparison to the Doi-Edwards strain functions (+) in uniaxial extension ($b = 0, \dot{\epsilon} > 0$): a) ϕ_1 ; b) ϕ_2 and c) $\phi = \phi_1 + \phi_2 \cdot e^{-cs}$; where the s corresponds to the actual invariant value (see eq. (2.6)).





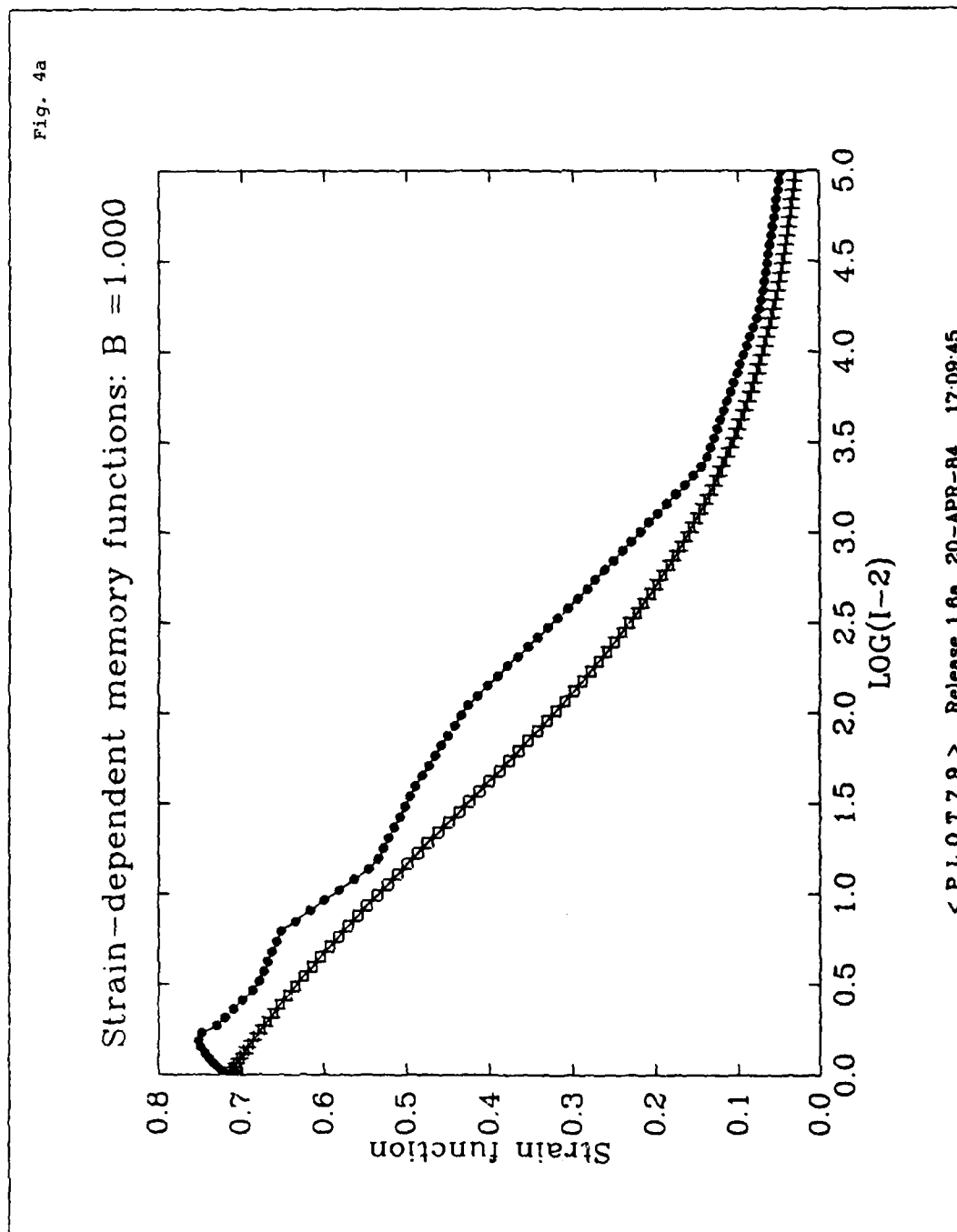
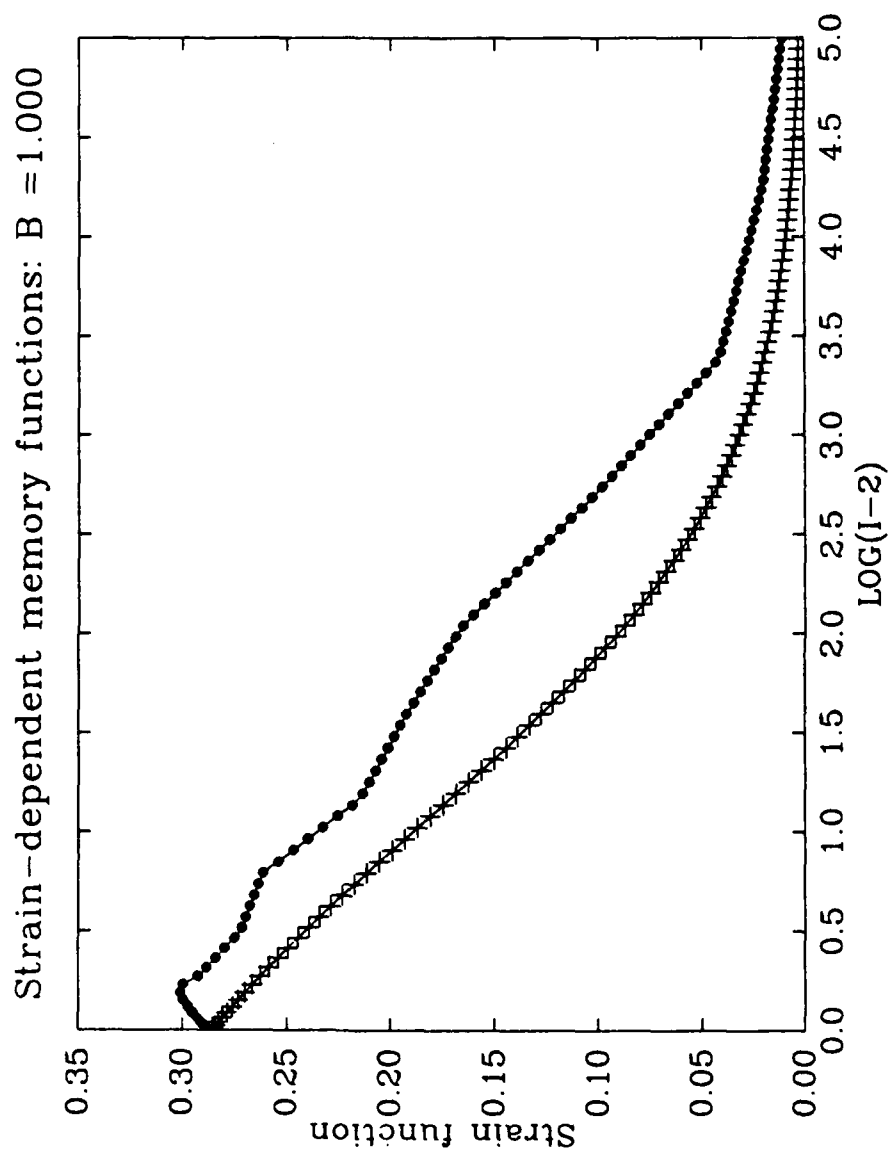


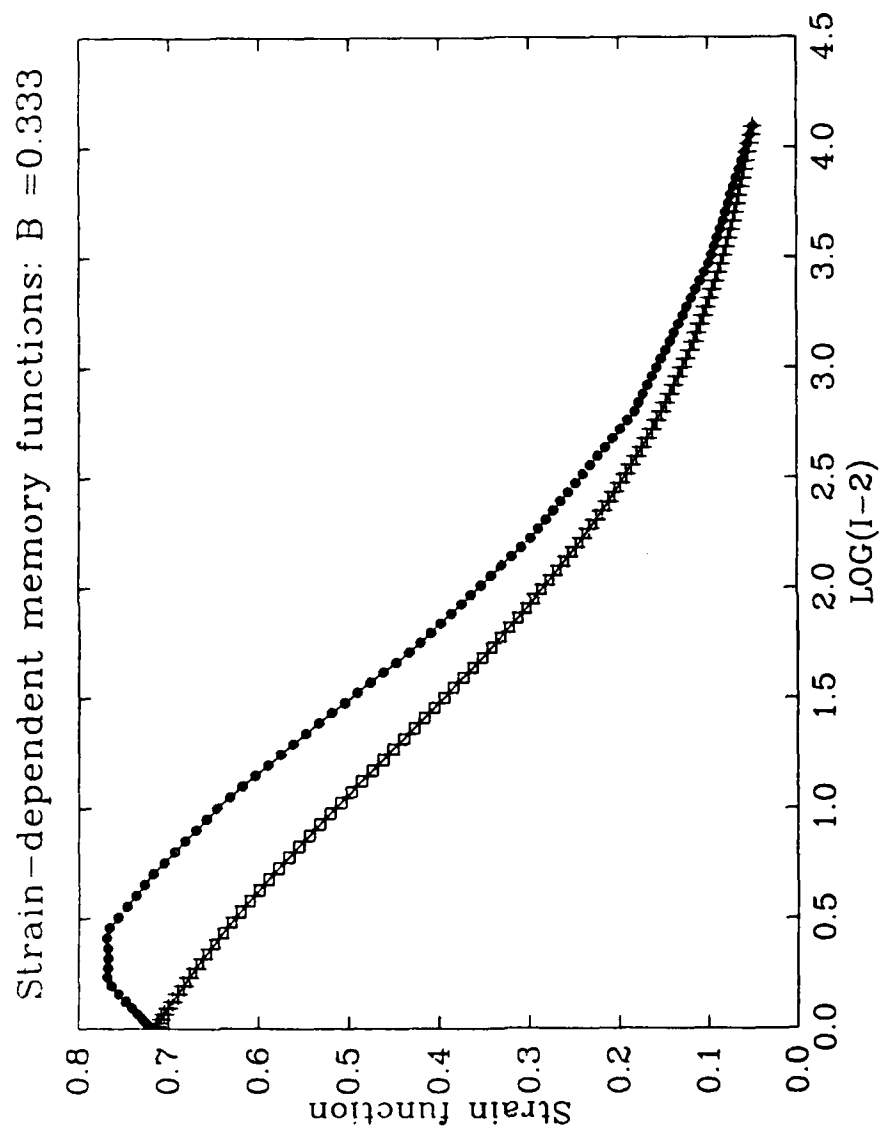
Figure 4. The optimal strain functions (O) in comparison to the Doi-Edwards strain functions (+) in planar elongational flow: a) ϕ_1 , b) ϕ_2 .

Fig. 4b



< P L O T 7 9 > Release 1.6a 20-APR-84 17:10:12

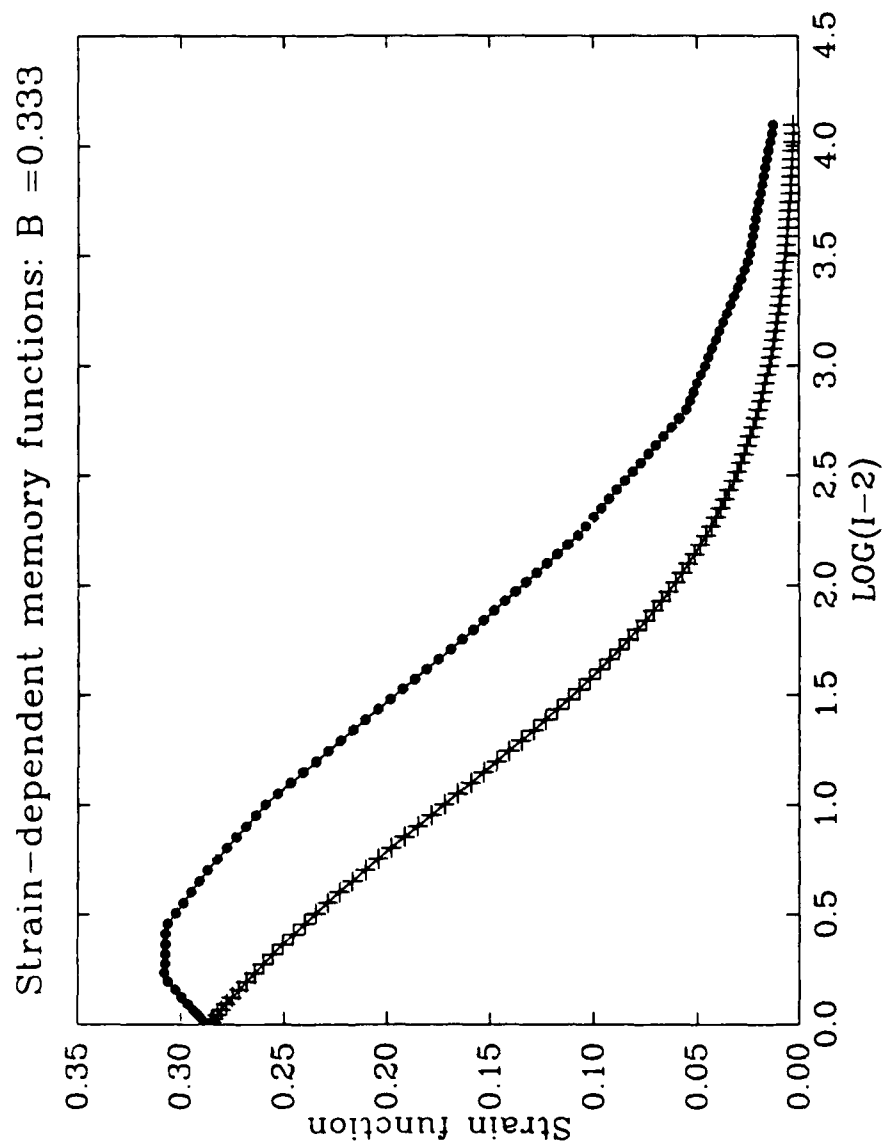
Fig. 5a



< P L O T 7 9 > Release 1.6a 23-APR-84 08:41:12

Figure 5. The optimal strain functions (0) in comparison to the Doi-Edwards strain functions (+) in ellipsoidal elongational flow ($b = \frac{1}{3}$; $\dot{\epsilon} < 0$): a) ϕ_1 and b) ϕ_2 .

Fig. 5b



< P L O T 7 9 > Release 1.6a 23-APR-84 08:41:43

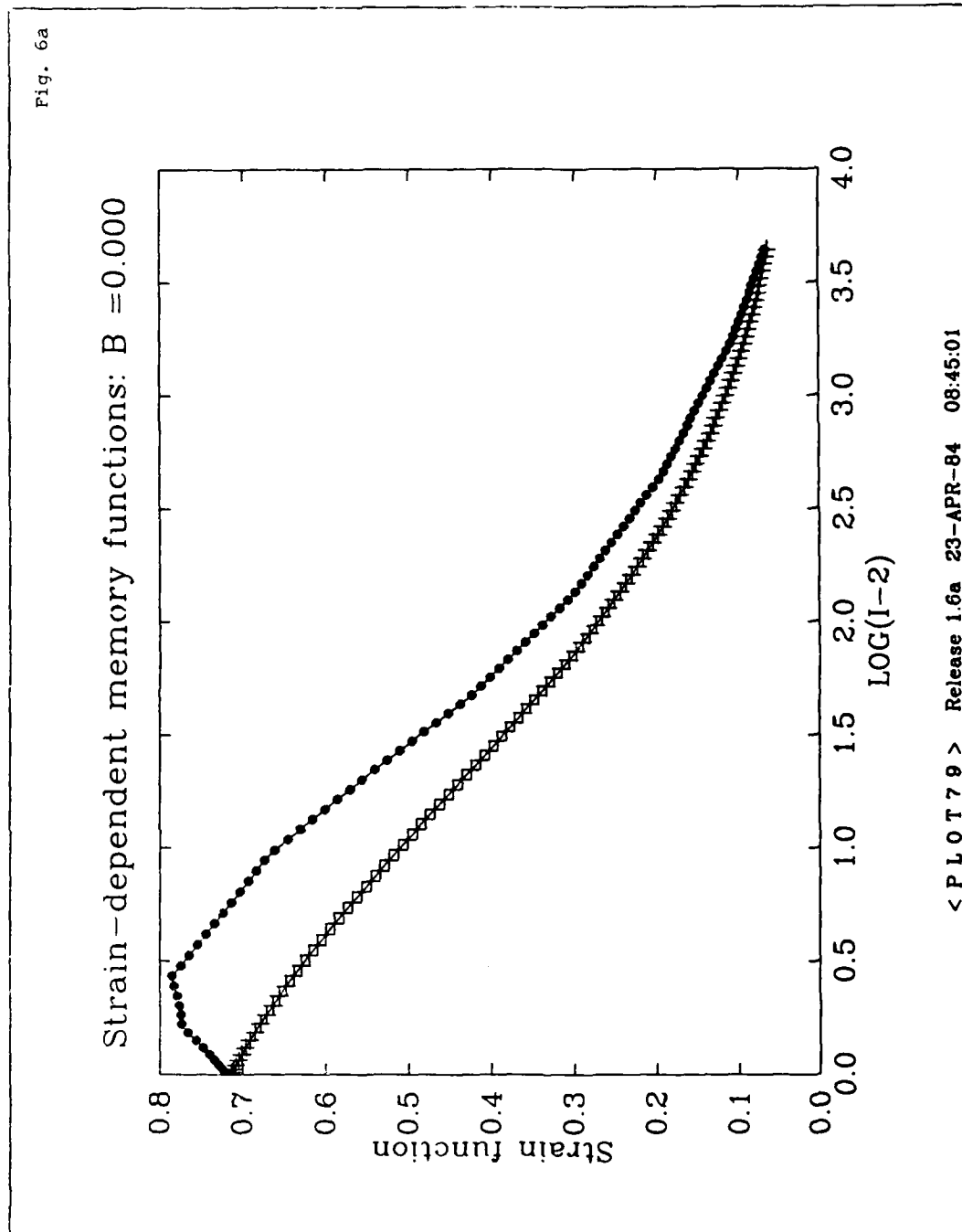
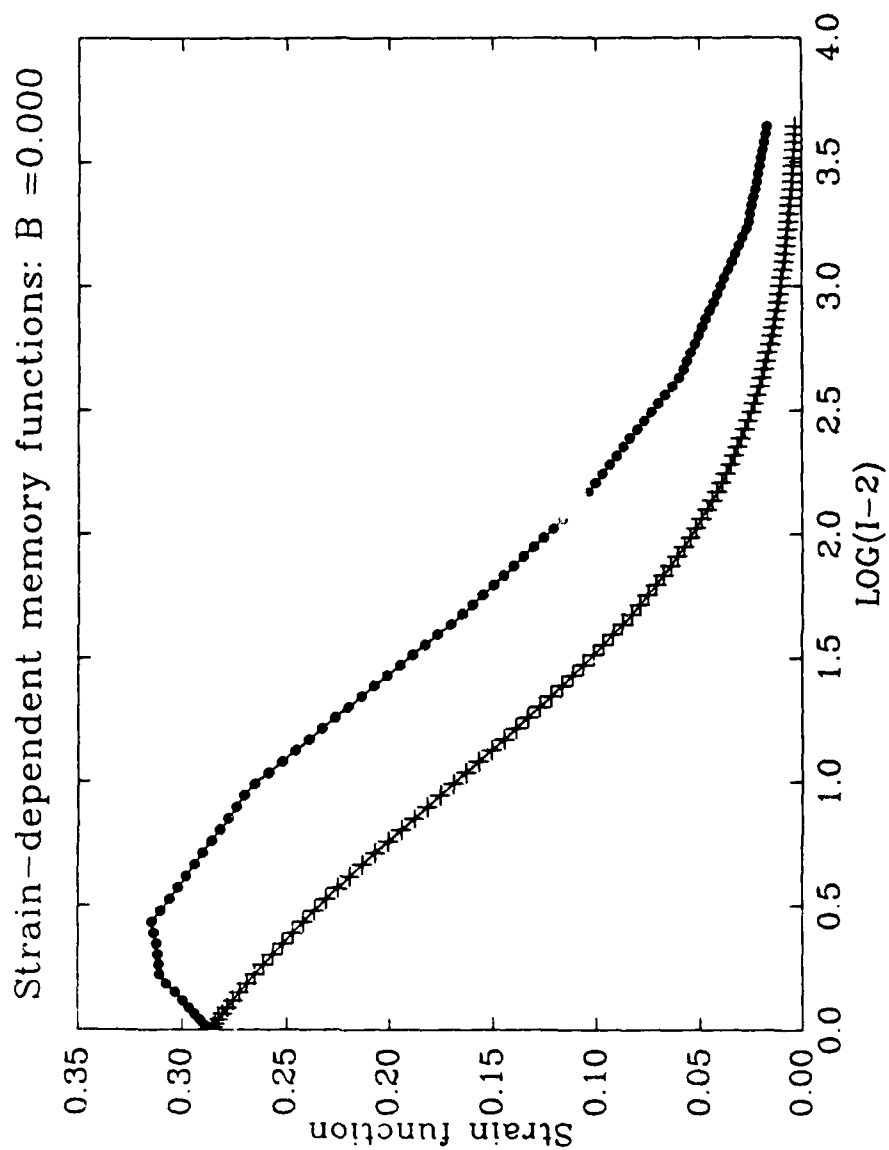


Fig. 6a

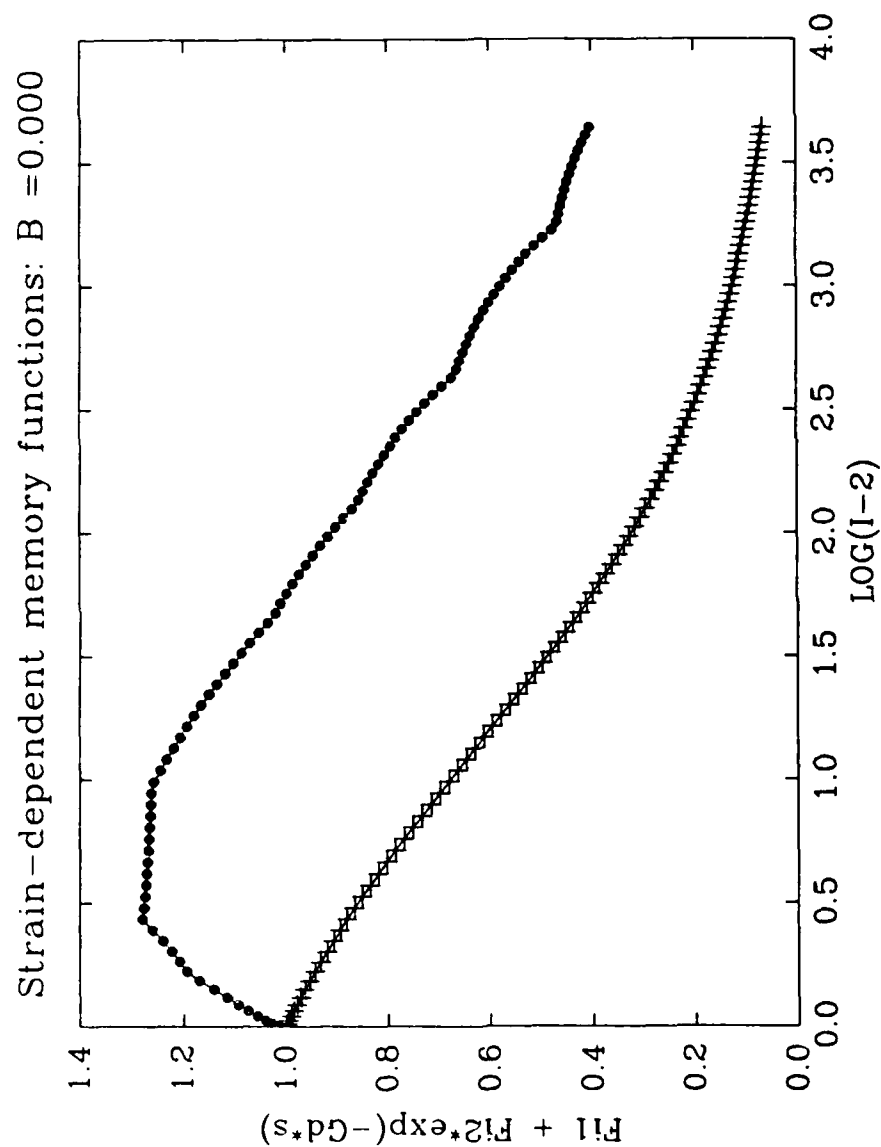
Figure 6. The optimal strain function (O) in comparison to the Doi-Edwards strain function (+) in biaxial elongational flow ($b = 0$, $\dot{\epsilon} < 0$): a) ϕ_1 , b) ϕ_2 and c) $\phi_1 + \phi_2 e^{-\epsilon s}$, where the s corresponds to the actual invariant (see eq. (2.6)).

Fig. 6b



< P L O T 7 9 > Release 1.6a 23-APR-84 08:46:15

Fig. 6c



< P L O T 7 9 > Release 1.6a 23-APR-84 09:06:54

functions is that they are not "damping"-functions. In fact they increase from the zero deformation value for small deformations. This is true for both strain functions in all flows considered. It is also obvious that the Doi-Edwards strain function would give a rather bad fit to the data. We see, for example, on Figure 2 that the Doi-Edwards strain function is typically a factor 2 smaller than the optimal strain function for I^* larger than 2, and the deviation becomes much larger as I^* increases.

The ultimate test of any model is its capability to reproduce experimental data. We have calculated the material functions in all flows considered, and plotted them together with the data on the Figures 7 to 10. The largest derivation is found where the data shows the largest derivation from the linear viscoelastic behavior, which is in uniaxial extension. The model gives a reasonably good overall fit; especially if we use the "yardstick" normally used when model predictions and data for polymer results are compared. The present polymer is very polydisperse, with a weight average molecular weight (M_w) that is 2.14 times the number average molecular weight (M_n) so that

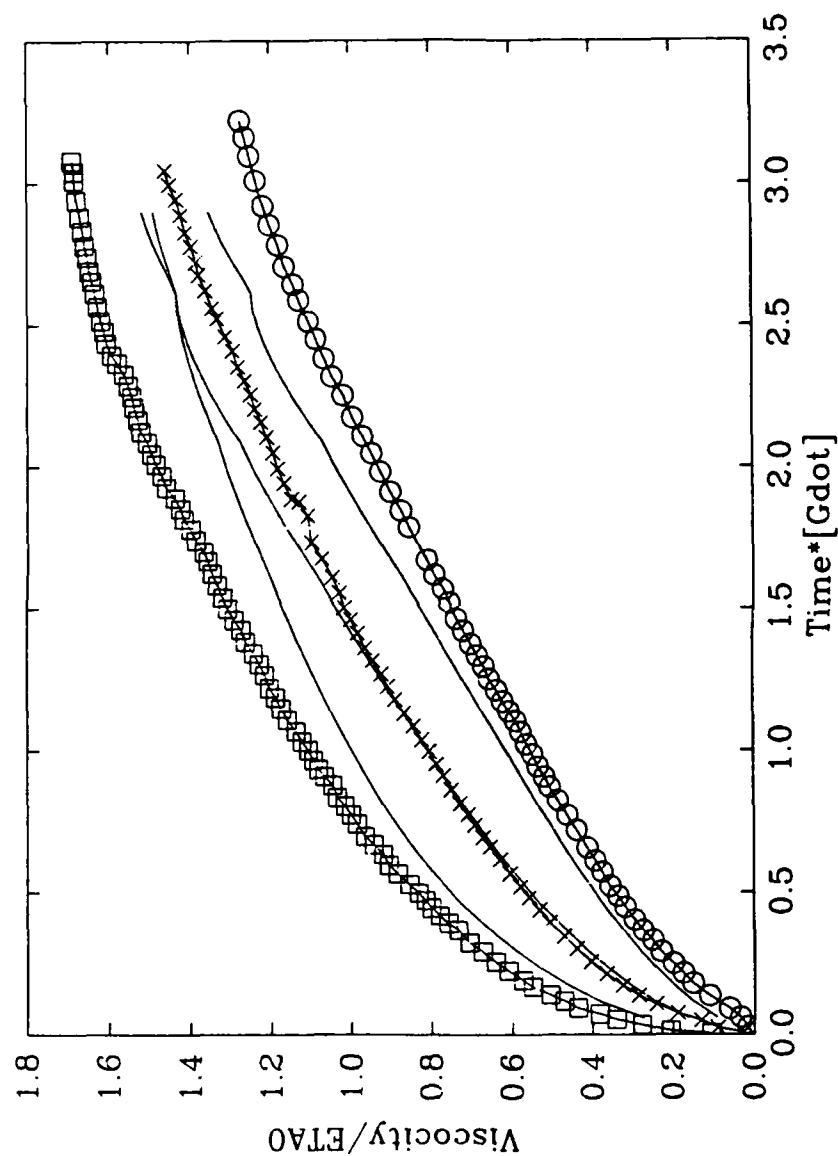
$$M_w/M_n = 2.14 .$$

We may also notice that we have used the memory function obtained by Demarmels (1983), and his procedure for calculation of this function may not be the best. He chooses the time constants a priori, and then he calculates the coefficients g_k . Whether the large deviation found by Demarmels (1983) between the calculated zero shear rate function $\eta + (t) = \sum g_k \tau_k (1 - e^{-t/\tau_k})$ and the measured function for small times is due to the estimation procedure, or due to experimental problems, as claimed by Demarmels is not clear. It is not likely though that an optimal memory function would improve the models fit to the present data significantly.

We may conclude that it is not possible to find a set of parameters in the proposed model so it interpolates the present data, but the optimal set of parameters in the least square sense is a reasonable approximation to data.

Fig. 7

$B = 0.0000$ $G\dot{\gamma} = 0.119$ 0.051 0.020



< P L O T 7 9 > Release 1.6a 20-APR-84 17:14:10

Figure 7. Comparison of model predictions (solid curves) and data (O : $\dot{\epsilon} = 0.119$; X : $\dot{\epsilon} = 0.051$ and : $\dot{\epsilon} = 0.02$) for the viscosity function in uniaxial elongational flow.

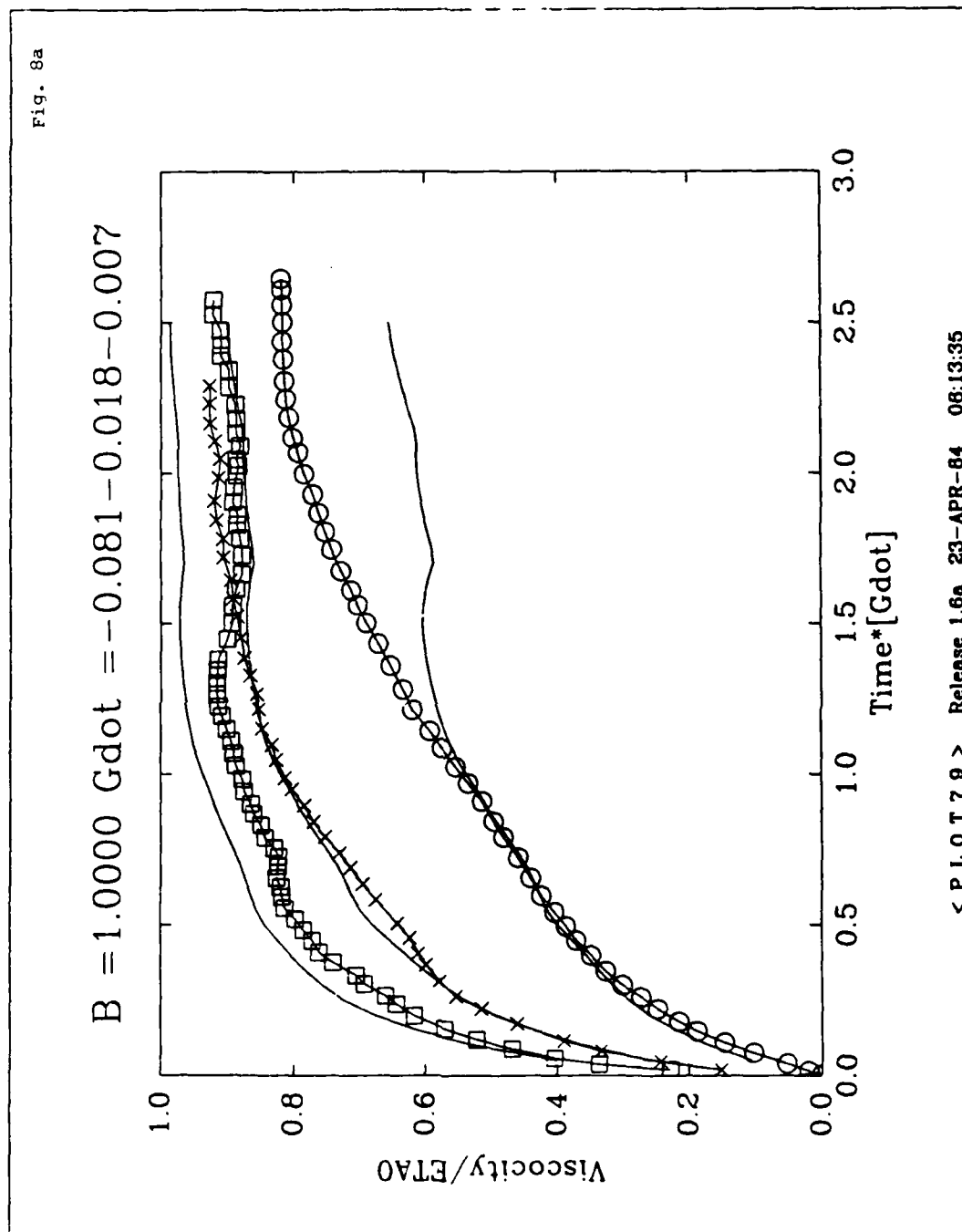
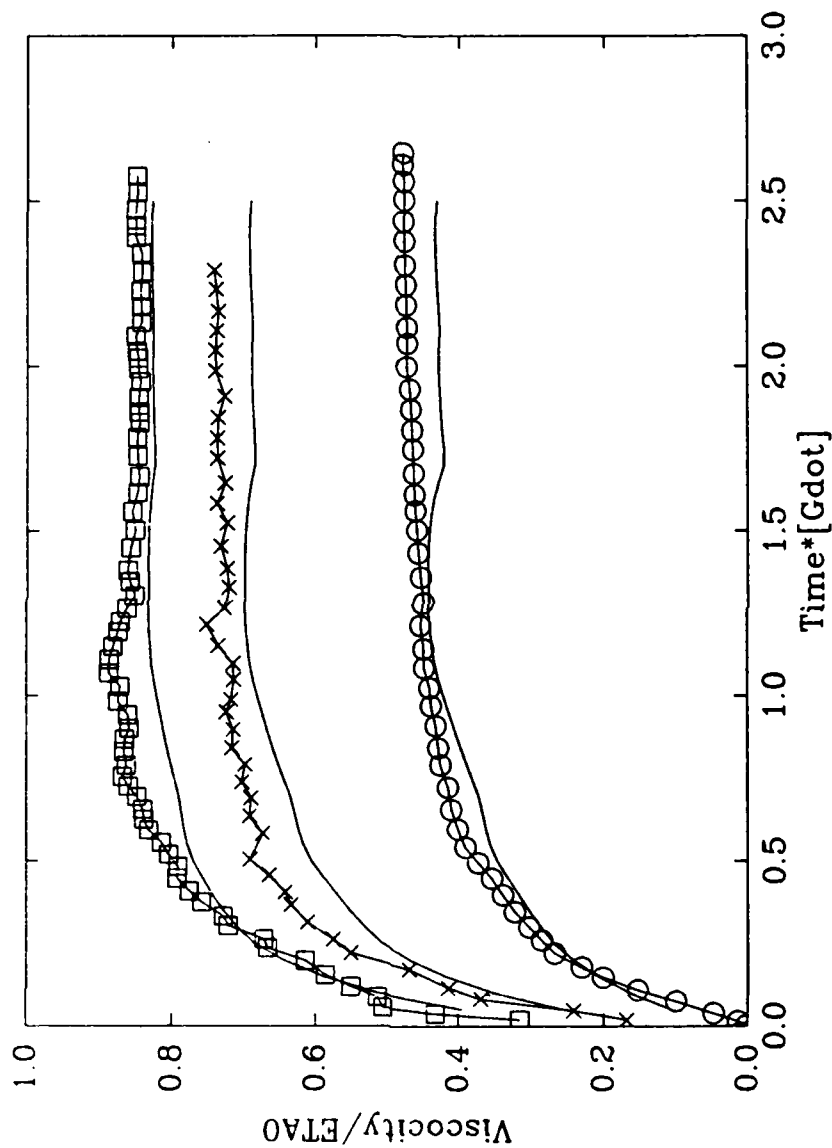


Figure 8. Comparison of model predictions (solid curves) and data (0 : $\dot{\epsilon} = -0.081$, x : $\dot{\epsilon} = -0.018$ and : $\dot{\epsilon} = -0.007$) in planar elongational flow: a) The first viscosity function; b) The second viscosity function.

Fig. 8b

$$B = 1.0000 \text{ Gdot} = -0.081 - 0.018 - 0.007$$



< P L O T 7 9 > Release 1.6a 23-APR-84 08:14:02

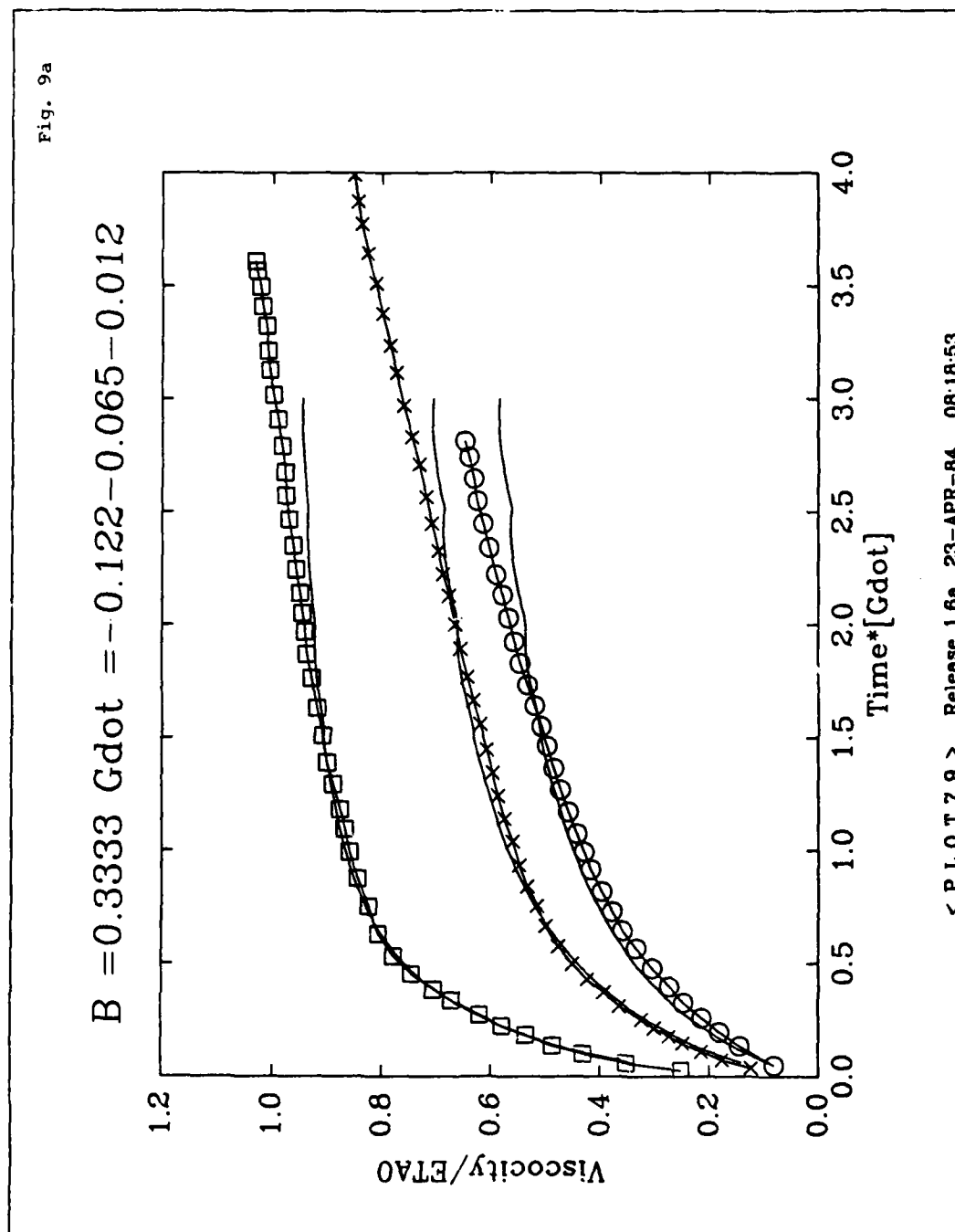
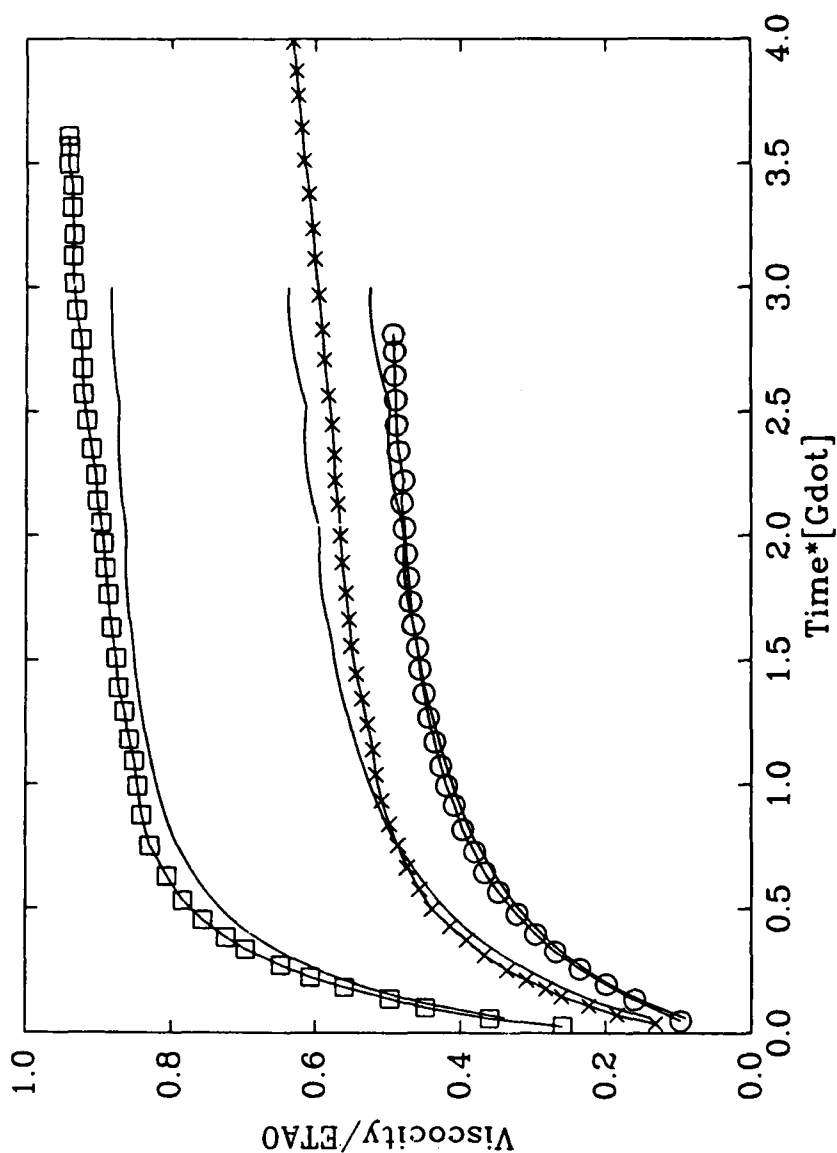


Figure 9. Comparison of model predictions (solid curves) and data (0 : $\dot{\epsilon} = -0.122$; X : $\dot{\epsilon} = -0.065$ and : $\dot{\epsilon} = -0.012$) in ellipsoidal elongational flow: a) The first viscosity function; b) The second viscosity function.

Fig. 9b

$$B = 0.3333 \quad \text{Gdot} = -0.122 - 0.065 - 0.012$$



< P L O T 7 9 > Release 1.6a 23-APR-84 08:19:20

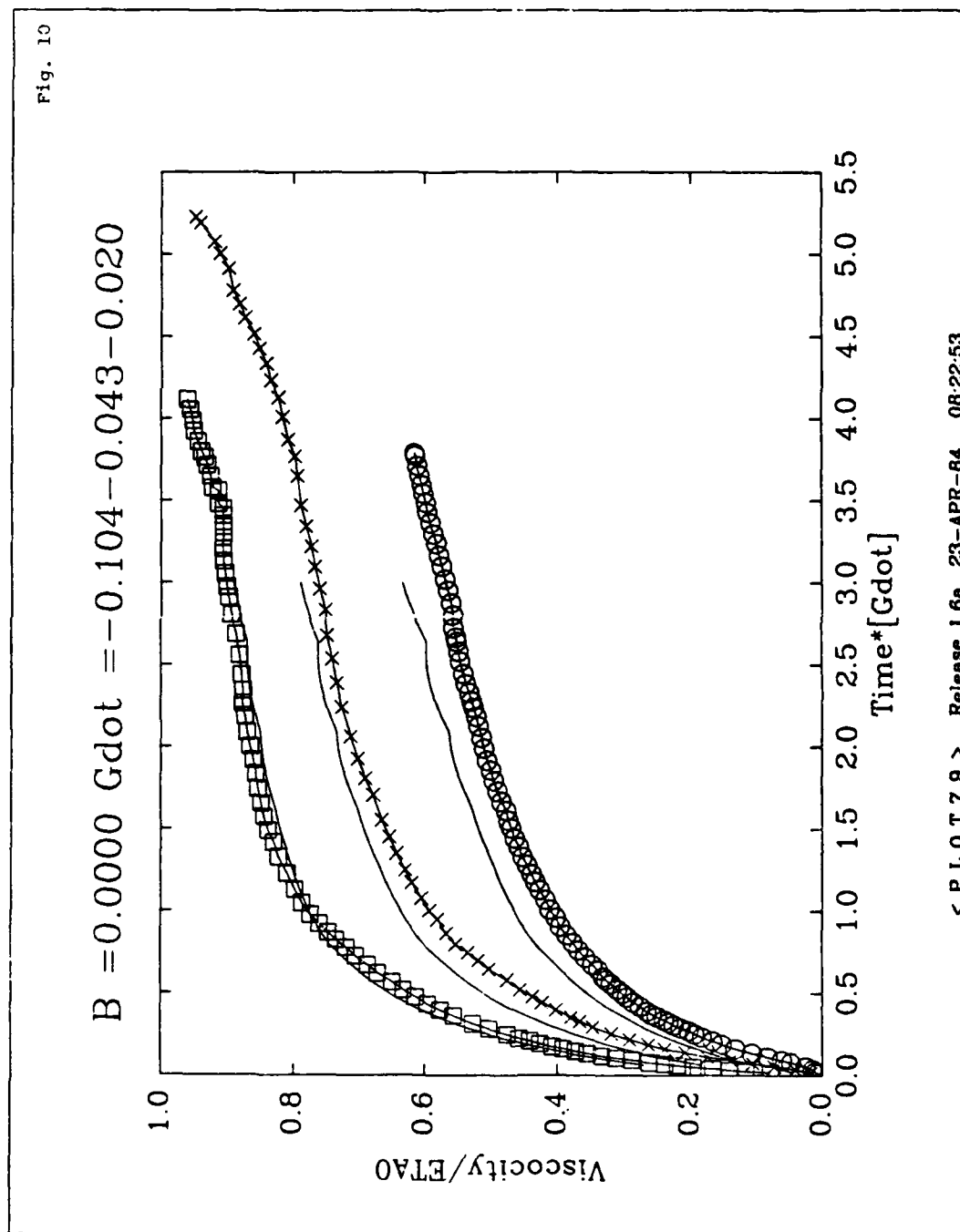


Fig. 10

Figure 10. Comparison of model predictions (solid curves) for the viscosity function, and data ($\circ : \dot{\epsilon} = -0.104$; $\times : \dot{\epsilon} = -0.043$ and $\square : \dot{\epsilon} = -0.020$) in biaxial elongational flow.

4. ESTIMATION OF W .

We now want to investigate the consequences of an assumption of the existence of a potential function W for the strain functions, i.e. that

$$\epsilon_1 = \frac{\partial W}{\partial I_1}; \quad \epsilon_2 = \frac{\partial W}{\partial I_2} \quad (4.1)$$

The W function has to be at least C^1 if the strain functions are to be continuous. Alfeld (1984) has developed a C^1 interpolant, which is a piecewise cubic function defined on a mesh of triangles. We now briefly summarize the method of Alfeld as follows: Each triangle is subdivided into three subtriangles (microtriangles), see Figure 11. On each microtriangle a cubic function is defined.

$$q(P) = \sum_{\alpha+\beta+\gamma+\delta=3} \frac{3!}{\alpha! \beta! \gamma! \delta!} c_{\alpha\beta\gamma\delta} b_1^\alpha b_2^\beta b_3^\gamma b_4^\delta \quad (4.3)$$

where

$$P = \sum_{i=1}^4 b_i v_i ;$$

is the point of evaluation. The "generalized barycentric coordinates" b_i satisfies

$$\begin{aligned} \sum_{i=1}^4 b_i &= 1 \\ \prod_{i=1}^3 b_i &= 0 \end{aligned} \quad (4.4)$$

The "Bézier ordinates" $c_{\alpha\beta\gamma\delta}$ are functions of the parameters in the Clough-Tocher scheme. The Bézier ordinates are given explicitly by Alfeld (1984). The parameters are the function values Q and the directional derivatives at all vertex nodes. The directional derivatives $\epsilon_{ij}(q)$ are defined in terms of the partial derivatives

$$D_{ij}(q) = \nabla q \cdot e_{ij} \quad (4.5)$$

where e_{ij} is the direction. The parameters we have to estimate in the polymer melt model

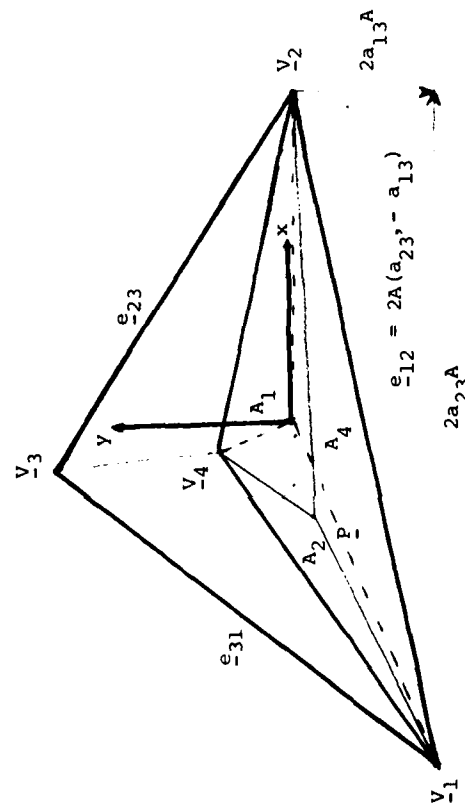


Figure 11. Each point on the macrotriangle may be expressed in terms of the generalized Barycentric coordinates introduced by Alfeld (1984): b_i ; $i = 1, 2, 3, 4$. The three of them here: $b_1 = A_1/A$, $b_2 = A_2/A$, $b_4 = A_4/A$ are the triangular coordinates of the microtriangle containing P, and the remaining coordinate (here b_3) is zero. The area of the microtriangle is $A = A_1 + A_2 + A_4$, and it is one third of the macrotriangles area.

(1.1) are the potential function values, and the partial derivatives at all corner vertices.

To calculate the strain functions everywhere on the triangular mesh we need to calculate the partial derivatives of (4.3) with respect to I_1^* and I_2^* . We find

$$\frac{\partial q}{\partial x} = \sum_{\alpha+\beta+\gamma+\delta=3} \frac{3!}{\alpha!\beta!\gamma!\delta!} c_{\alpha\beta\gamma\delta} \frac{\partial}{\partial x} (b_1^\alpha b_2^\beta b_3^\gamma b_4^\delta) \quad (4.6)$$

where x may be I_1^* or I_2^* defined in Eq. (3.11).

It is trivial, but quite lengthy, to write down all the terms that evolves from differentiation of the products, so we only give the formula for the partial derivatives of the barycentric coordinates b_i with respect to the invariants I_1^*, I_2^* .

The coordinates b_i may be expressed explicitly in I_1^*, I_2^* :

$$b_i = a_{0i} + a_{1i}(I_1^* - I_1^*(4)) + a_{2i}(I_2^* - I_2^*(4)); \quad i = 1, 2, 3$$

where $a_{0i} = \frac{1}{3}$ for all i , and

$$a_{11} = \frac{1}{2A} (I_2^*(2) - I_2^*(3)); \quad a_{21} = \frac{1}{2A} (I_1^*(3) - I_1^*(2))$$

$$a_{12} = \frac{1}{2A} (I_2^*(3) - I_2^*(1)); \quad a_{22} = \frac{1}{2A} (I_1^*(1) - I_1^*(3))$$

$$a_{13} = \frac{1}{2A} (I_2^*(1) - I_2^*(2)); \quad a_{23} = \frac{1}{2A} (I_1^*(2) - I_1^*(1))$$

See Figure 11 for a geometrical interpretation of above formula

$$(I_1^*(i), I_2^*(i)) = V_i = \text{vertex coordinates of microtriangle.}$$

We now have the simple result:

$$\frac{\partial b_i}{\partial I_1^*} = a_{1i} \quad \text{and} \quad \frac{\partial b_i}{\partial I_2^*} = a_{2i} \quad (4.7)$$

We may now formulate the estimation problem:

$$\min_{\omega} \left| \sum_{i,n} \left(\frac{\partial W}{\partial I_1^*} C_{i1} - \frac{\partial W}{\partial I_2^*} C_{i2} - H_i(\epsilon_n) \right)^2 \right| \quad (4.8)$$

where the $3M$ parameters are:

$$\begin{aligned} \omega &= \left\{ \left(W(P_1), \left(\frac{\partial W}{\partial I_1^*} \right)_{P_1}, \left(\frac{\partial W}{\partial I_2^*} \right)_{P_1} \right); \dots; \left(W(P_M), \left(\frac{\partial W}{\partial I_1^*} \right)_{P_M}, \left(\frac{\partial W}{\partial I_2^*} \right)_{P_M} \right) \right\} \\ &= \{ (\omega_{11}, \omega_{21}, \omega_{31}); \dots; (\omega_{1M}, \omega_{2M}, \omega_{3M}) \} \end{aligned} \quad (4.9)$$

where M is the number of vertices. We note that W does not enter into the objective function (4.8), and consequently we must supply at least one W value. This may be picked arbitrarily. We take

$$W(I_1^*, I_2^*) = 0 \quad \text{at} \quad (I_1^*, I_2^*) = (0, 0).$$

We want to approximate the potential function W by (4.3):

$$W(I_1^*, I_2^*) = \sum_{\alpha+R+\gamma+\lambda=3} \frac{3!}{\alpha!R!\gamma!\lambda!} c_{\alpha R \gamma \lambda} b_1^\alpha b_2^R b_3^\gamma b_4^\lambda \quad (4.10)$$

where

$$c_{\alpha R \gamma \lambda} = c_{\alpha R \gamma \lambda}(\omega)$$

$$(I_1^*, I_2^*) = b_1 V_1 + b_2 V_2 + b_3 V_3 + b_4 V_4$$

and V_i are the vertex coordinates, including the centroid (V_4), and b_i are the Barycentric coordinates of the triangle containing (I_1^*, I_2^*) .

If the model shall conform with the linear viscoelastic model for very small deformations we must require:

$$\left(\frac{\partial W}{\partial I_1^*} \right) + \left(\frac{\partial W}{\partial I_2^*} \right) = 1 \quad \text{at} \quad (I_1^*, I_2^*) = (0, 0).$$

This leaves $3M - 2$ parameters left to be estimated. The objective function is a sum of squares of cubic functions and the optimization problem is consequently supposed to be simple, and we may choose any standard unconstrained algorithm, in particular one that does not require analytical derivatives of the objective function with respect to ω . These derivatives are rather lengthy to write down.

In Appendix 1 we give a short description of the program developed to estimate the parameters \underline{w} in (4.9).

On the Figures 13 to 16 we present the calculated potential function, and its partial derivatives with respect to I_1 and I_2 . We have used following relations:

$$\left\{ \begin{array}{l} \frac{\partial W}{\partial I_1} = \frac{\partial W}{\partial I_1^*} \frac{1}{I_1 - 2} = \frac{\partial W}{\partial I_1^*} e^{-I_1^*} \end{array} \right. \quad (4.11)$$

$$\left\{ \begin{array}{l} \frac{\partial W}{\partial I_2} = \frac{\partial W}{\partial I_2^*} \frac{1}{I_2 - 2} = \frac{\partial W}{\partial I_2^*} e^{-I_2^*} \end{array} \right. \quad (4.12)$$

The invariant space has been transformed into a regular rectangular mesh, as required by the plotting routines. We use a dimensionless time $\tau = 2\dot{\epsilon}t$ as the first independent parameter, and a "flow type" parameter ξ as the other:

$$\xi = \begin{cases} +1 & \text{biaxial longational flow} \\ 0 & \text{planar longational flow} \\ -1 & \text{uniaxial longational flow} \end{cases}$$

In Figure 12 we have made a draft of the transformation, and the two different view-directions used. The zero deformation point is transformed into a line. The maximum τ value is approximately 6, which corresponds to the largest invariants in the data (see Figure 1). We also note that the different figures have different scales on the "z-axis", in fact $\left(\frac{\partial W}{\partial I_1}\right)_0 = 0.66$ and $\left(\frac{\partial W}{\partial I_2}\right)_0 = 0.34$.

We initially tested the influence of the number of polynomials used to describe W . We found no improvement using more than 3 cubic polynomials. (We tried to use up to 33 cubic polynomials).

The most characteristic feature of the $\frac{\partial W}{\partial I_1}$ - function is that in uniaxial elongational flow it increases rapidly above the zero deformation value for moderately small t , and for large t it decreases. The opposite is true for biaxial elongational flow, and here we see a monotonic decrease in time. The $\frac{\partial W}{\partial I_2}$ - function increases initially for all types of flow.

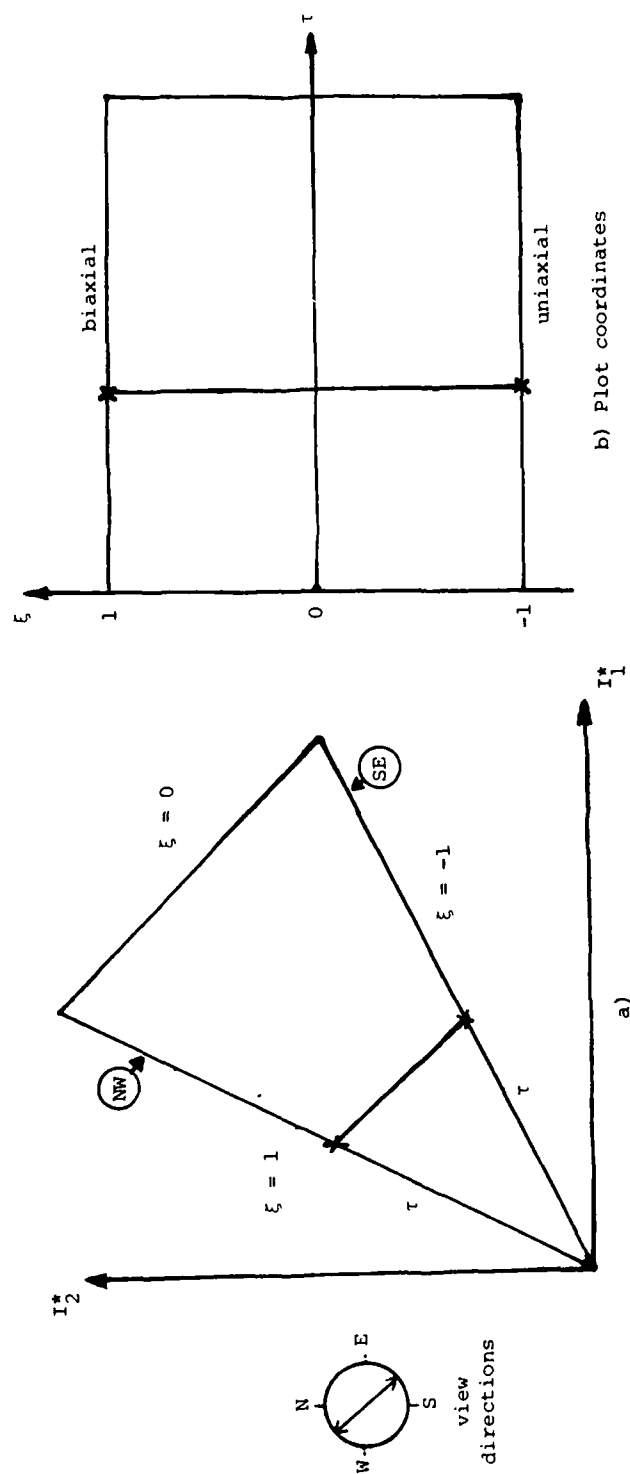


Figure 12. The covered invariant space is transformed into a rectangular and regular grid, which is required by the plotting routines. The two view directions are indicated: "Northwest" (NW), and "Southeast" (SE). All points on a line perpendicular to the planar branch ($I_1^* = I_2^*$) are transformed into a line in the (τ, η) -plane, with fixed τ . τ is a dimensionless time parameter.

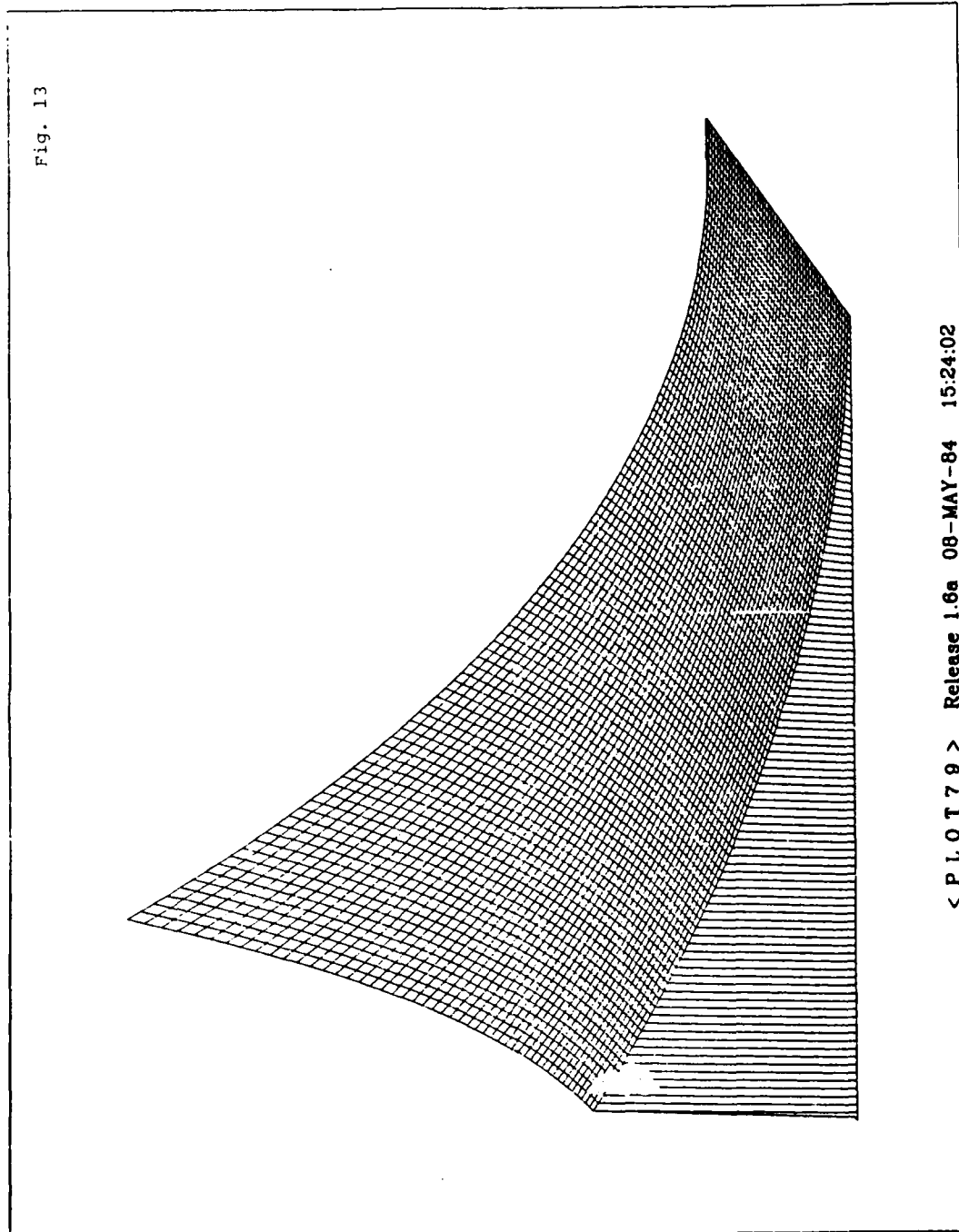
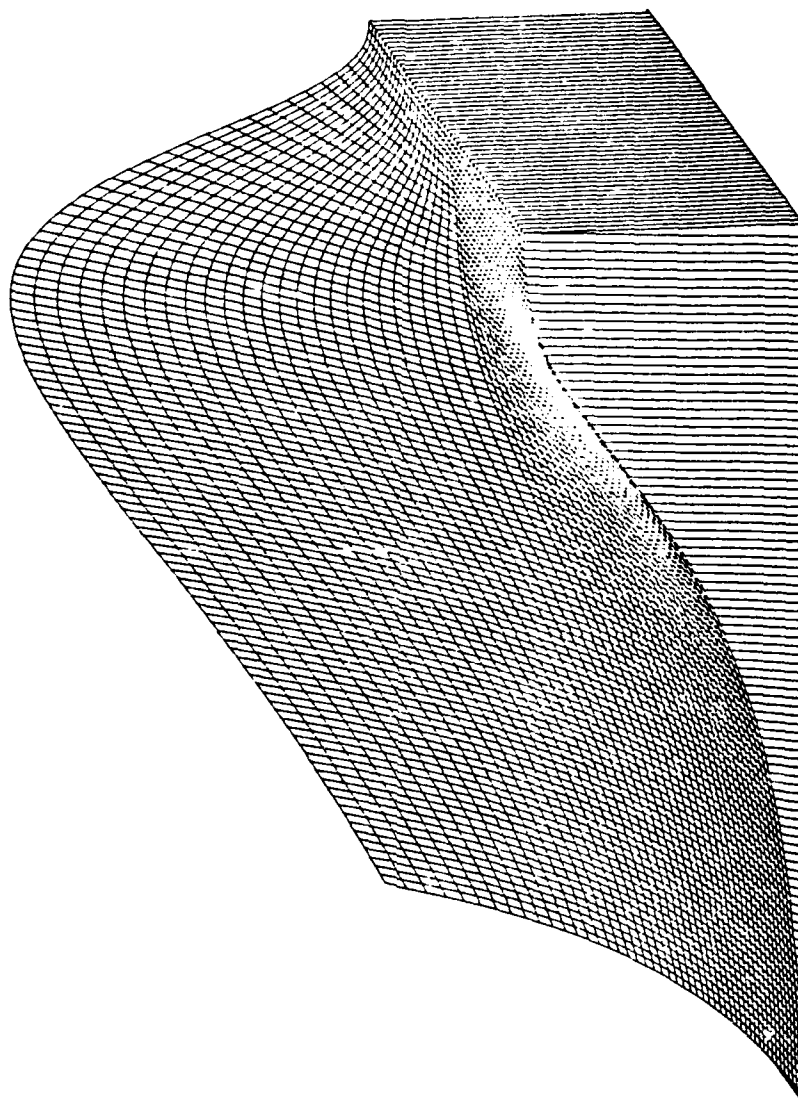


Figure 13. The potential function W is transformed into the (τ, f) plane and plotted as a surface. The view direction is Northwest (NW) (see Figure 12 for definition).

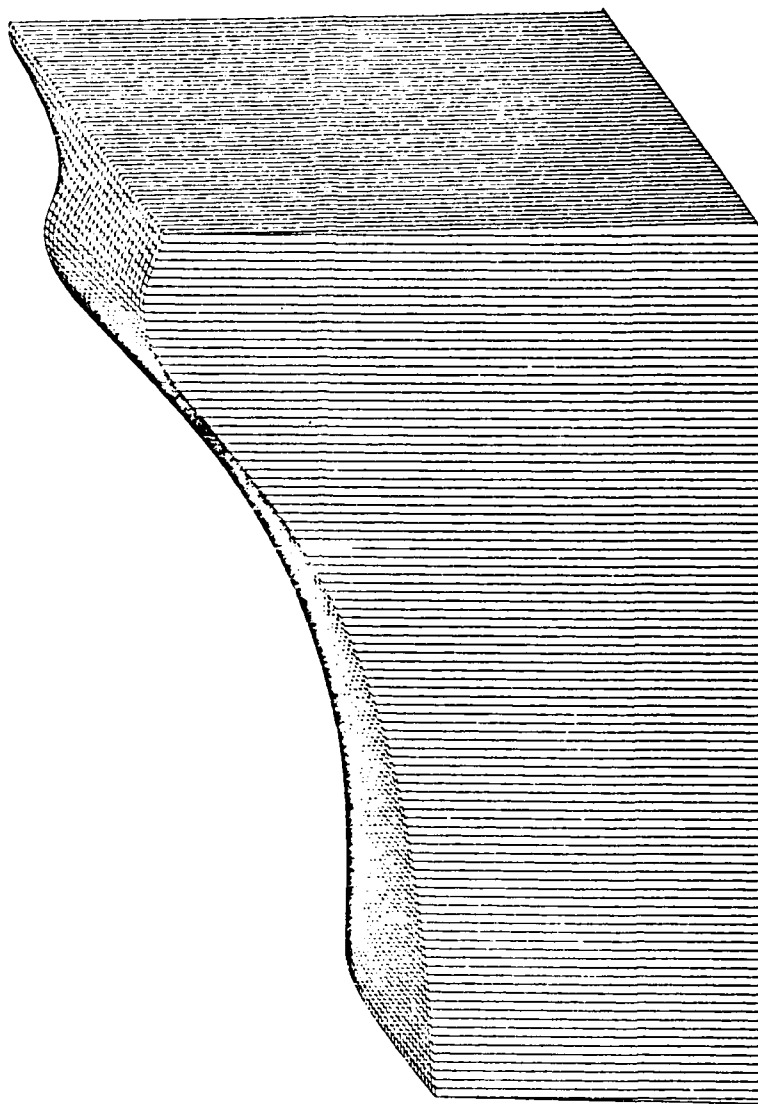
Fig. 14a



< P L O T 7 9 > Release 1.6a 08-MAY-84 15:01:05

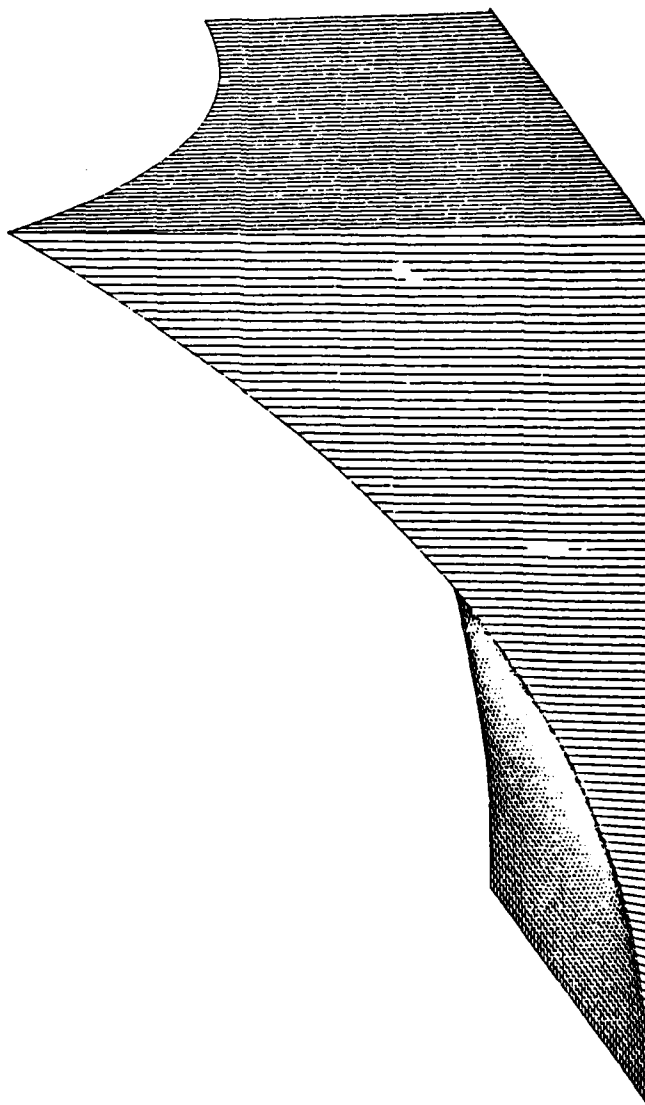
Figure 14. The derivatives are plotted in the same way as W on Figure 12: a) $\frac{\partial W}{\partial I_1}$; b) $\frac{\partial W}{\partial I_2}$.

Fig. 14b



< P L O T 7 9 > Release 1.6a 09-MAY-84 13:42:37

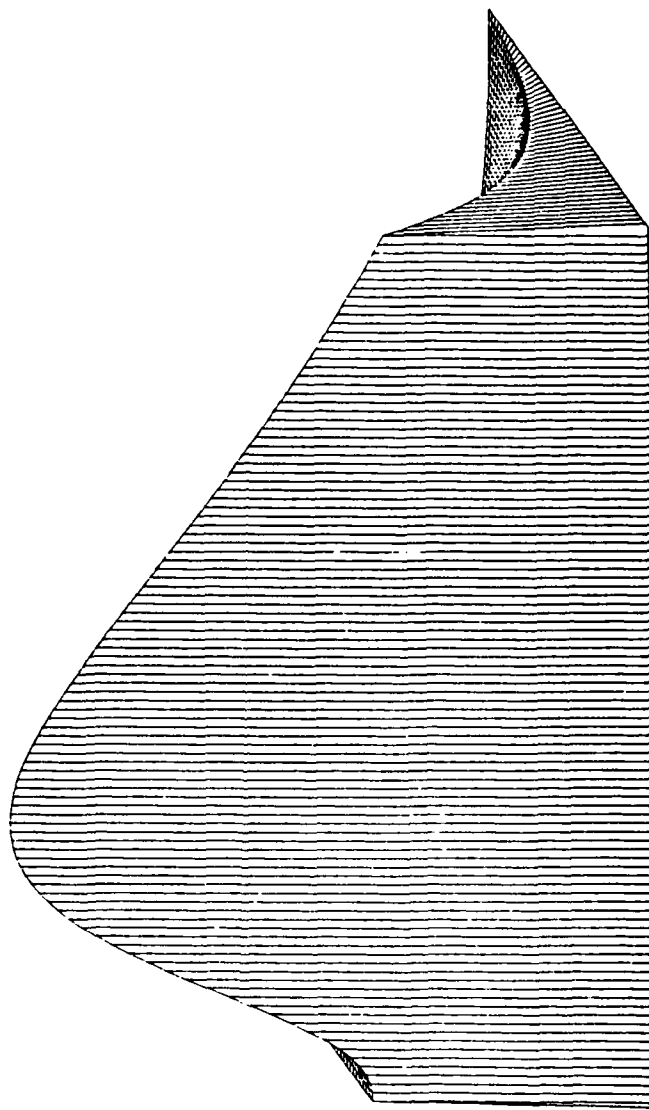
Fig. 15



< P L O T 7 9 > Release 1.6a 09-MAY-84 13:29:28

Figure 15. The W-function is plotted with view direction Southeast (SE).

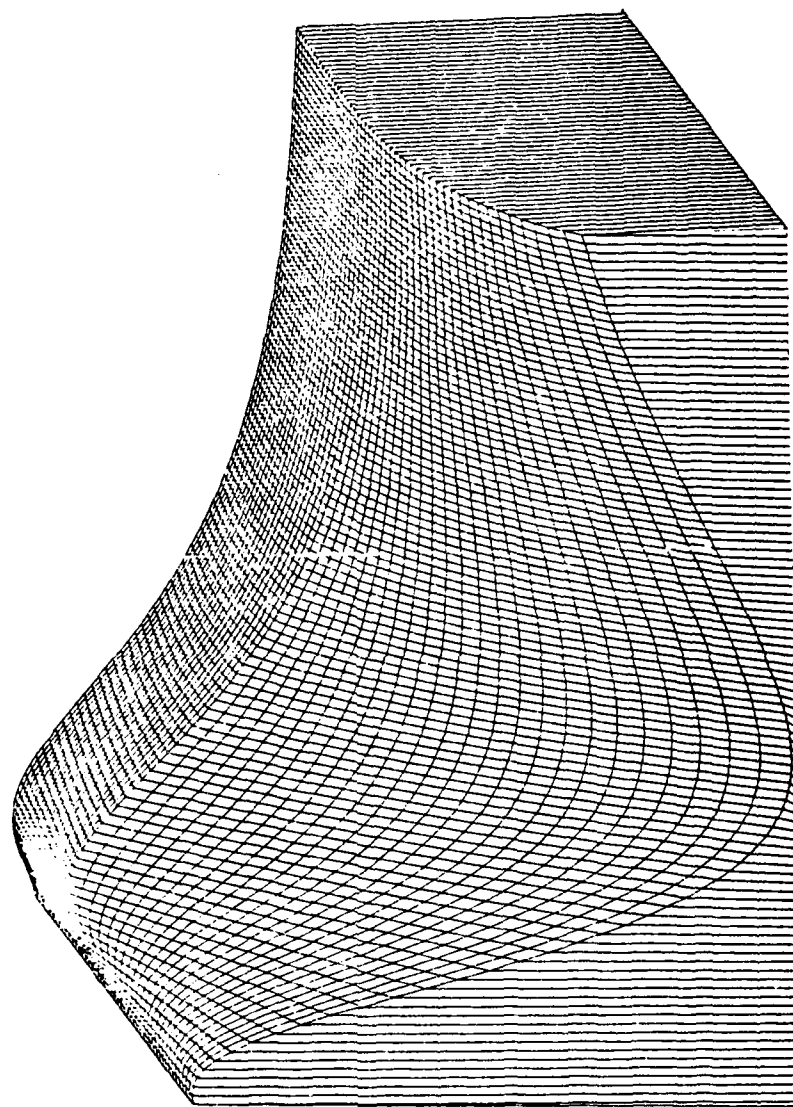
Fig. 16a



< P L O T 7 9 > Release 1.6a 09-MAY-84 13:30:36

Figure 16. The derivatives are plotted as W in Figure 15: a) $\frac{\partial W}{\partial I_1}$; b) $\frac{\partial W}{\partial I_2}$.

Fig. 16b



< P L O T 7 9 > Release 1.6a 08-MAY-84 14:54:43

To obtain an idea about how the strain function depends on the invariants we have plotted the $\frac{\partial W}{\partial I_1}$, and the $\frac{\partial W}{\partial I_2}$ - function on Figures 17 to 19 as functions of I_1 with b as discrete parameter. We have also plotted the "effective" strain function in the two extreme flows with $b = 0$. The Doi-Edwards strain functions have been plotted for comparison. We notice again the initial increase in $\left(\frac{\partial W}{\partial I_1}\right)$ in uniaxial flow. In Figure 17c the effective strain function combination is plotted, and we notice a good coincidence between the estimated strain function and Doi-Edwards for very small deformations but very soon the derivations become very large (>100%). There is no overshoot in planar extension for $\frac{\partial W}{\partial I_1}$, but now there is for $\frac{\partial W}{\partial I_2}$.

There is a very small overshoot in $\frac{\partial W}{\partial I}$ in biaxial extension. (It is too small to be seen on the 3-D plots). The effective strain function shows a larger overshoot, as it is now the $\frac{\partial W}{\partial I_2}$ - function that is the important strain function. Again there is a large deviation between the estimated strain function and the Doi-Edwards function.

Figure 20 to 23 shows how the estimated potential function describes data, both in a linear scale and in a logarithmic scale. The latter is often used as the customarily large deviations between data and model predictions look quite small on such plots.

The deviations in uniaxial flow are approximately the same as we observed for the more general model. In planar extension we see that the curve for the largest $\dot{\epsilon}$ - value has improved, but the curves for the two smallest $\dot{\epsilon}$ - values have become worse. The data, especially for the smallest $\dot{\epsilon}$ - value, do not seem to be accurate. The second viscosity function has improved for all $\dot{\epsilon}$ - values. We may notice that, although there is a large negative deviation from the linear viscoelastic behaviour for the largest $\dot{\epsilon}$ - value, the model is apparently much better to describe this kind of deviation. Again in ellipsoidal extension we see a small improvement for the largest $\dot{\epsilon}$ - value, and an overall good fit for both viscosity functions. In biaxial extension we observe the same deviations as we saw when we did not assume the existence of a potential function.

We may now conclude that a potential function "exists", in the sense that we obtain a fit to data which is as good as if we do not assume the existence. In fact we get some

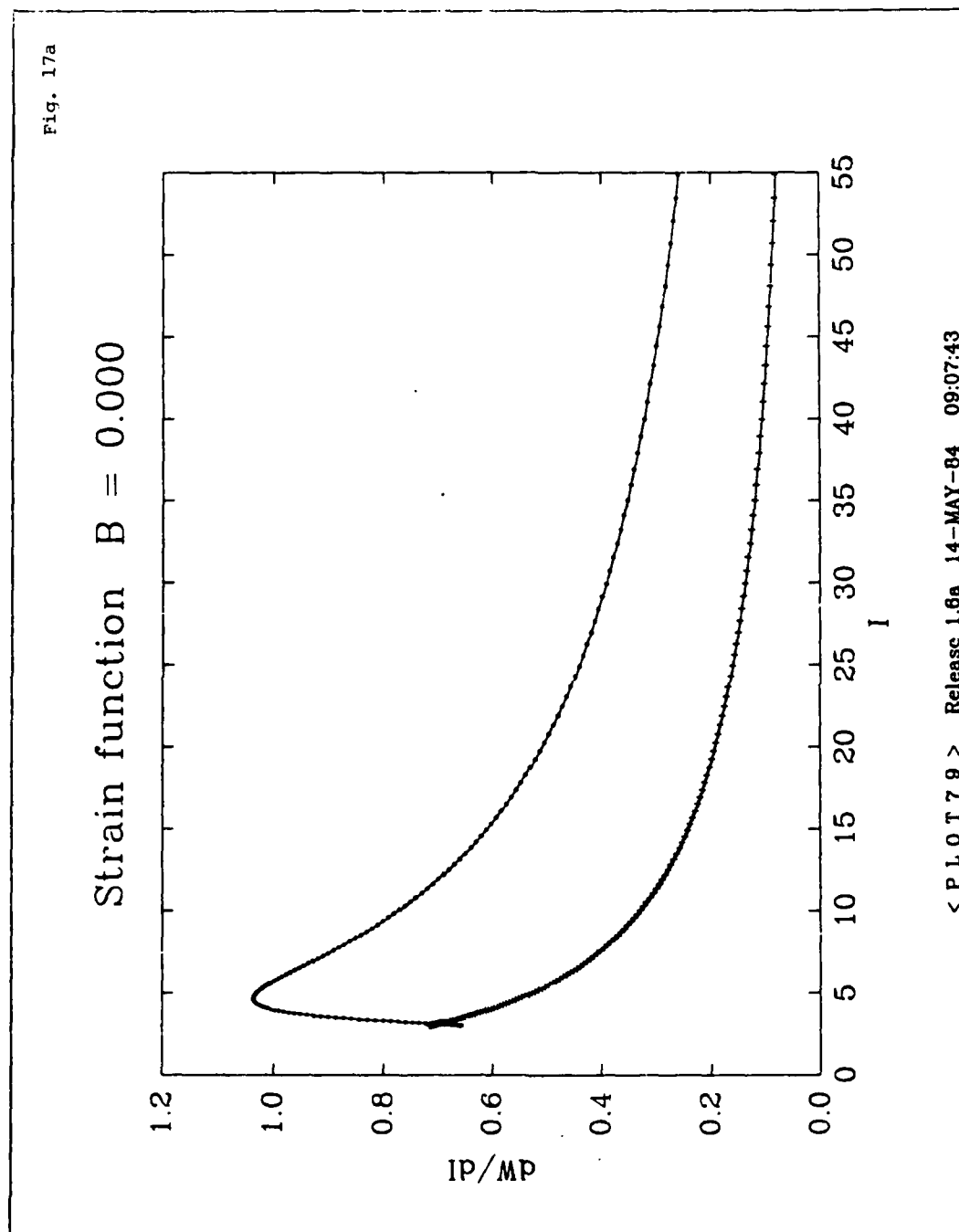
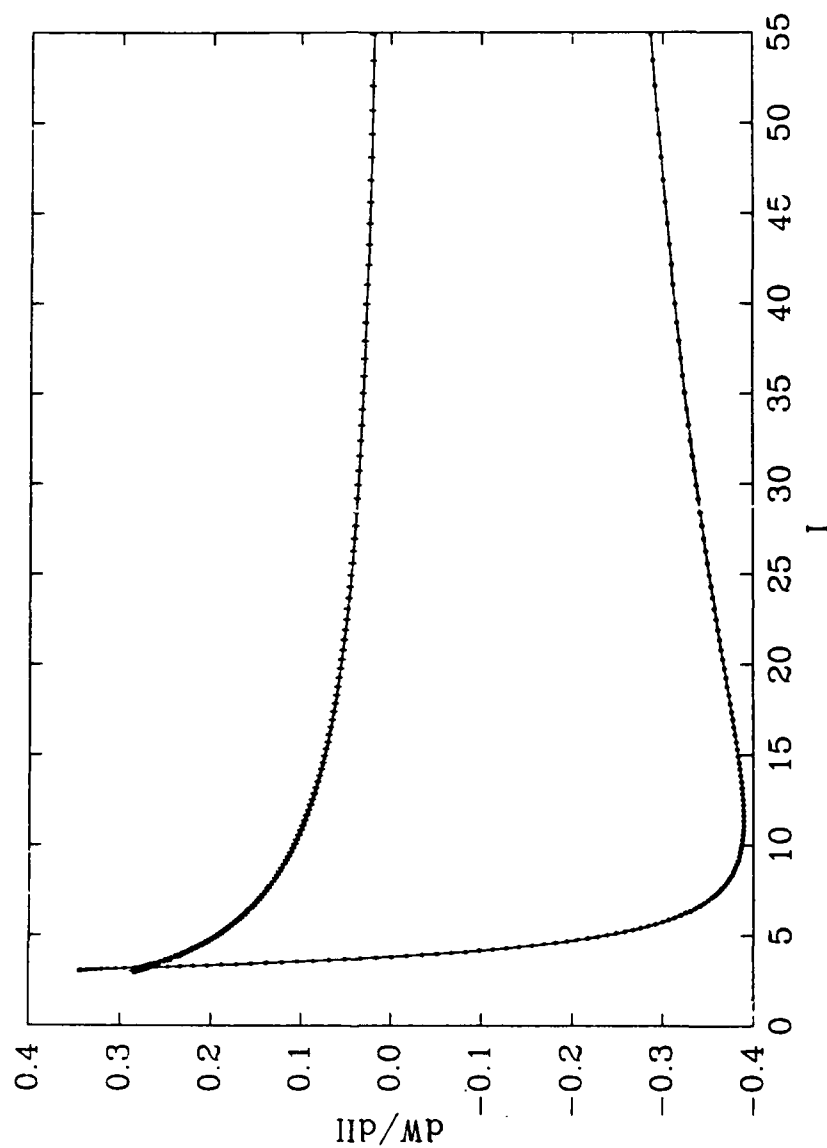


Figure 17. The strain functions are plotted as functions of I_1 in uniaxial flow: a) $\frac{\partial W}{\partial I_1}$, b) $\frac{\partial W}{\partial I_2}$, c) $\frac{\partial W}{\partial I_1} + \frac{\partial W}{\partial I_2} e^{-fs}$ where s corresponds with I_1 (see eq. (2.6)). The Doi-Edwards functions (+) are shown for comparison.

Fig. 17b

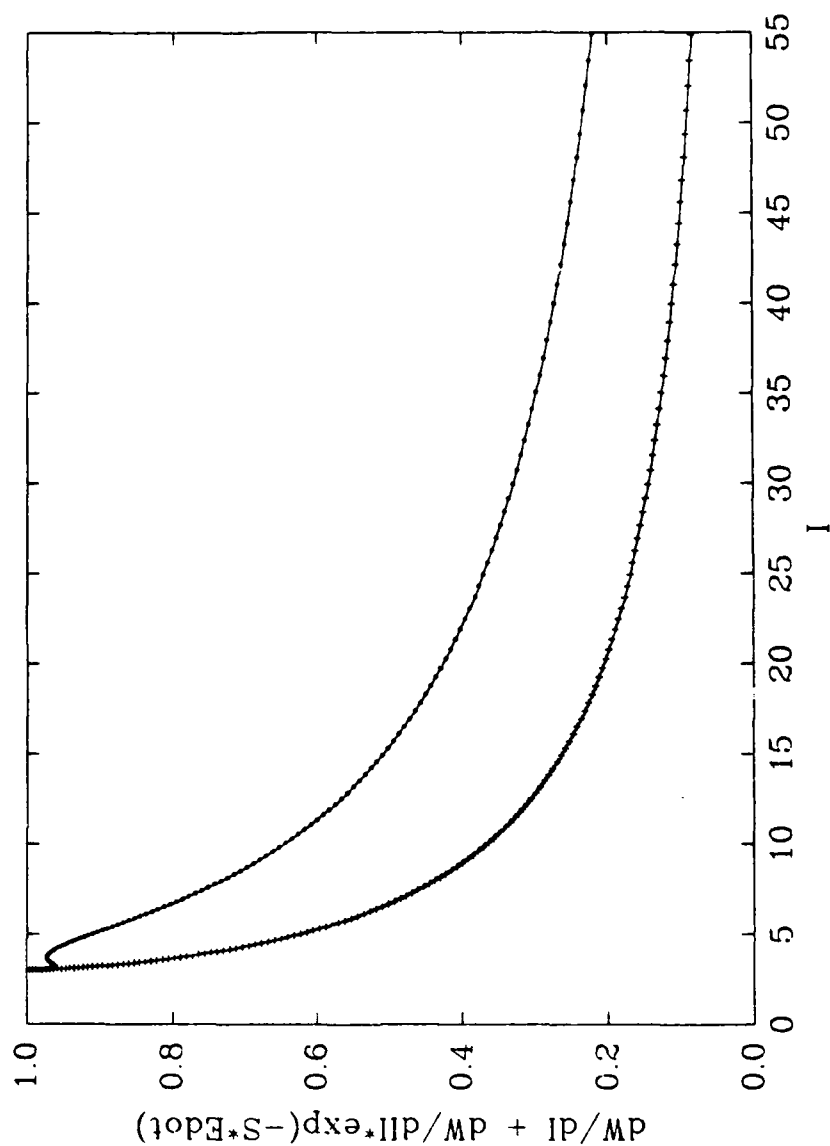
Strain function $B = 0.000$



< P L O T 7 9 > Release 1.6a 14-MAY-84 09:08:13

Fig. 17c

Strain function combination for $B = 0$.



< P L O T 7 9 > Release 1.6a 14-MAY-84 09:08:52

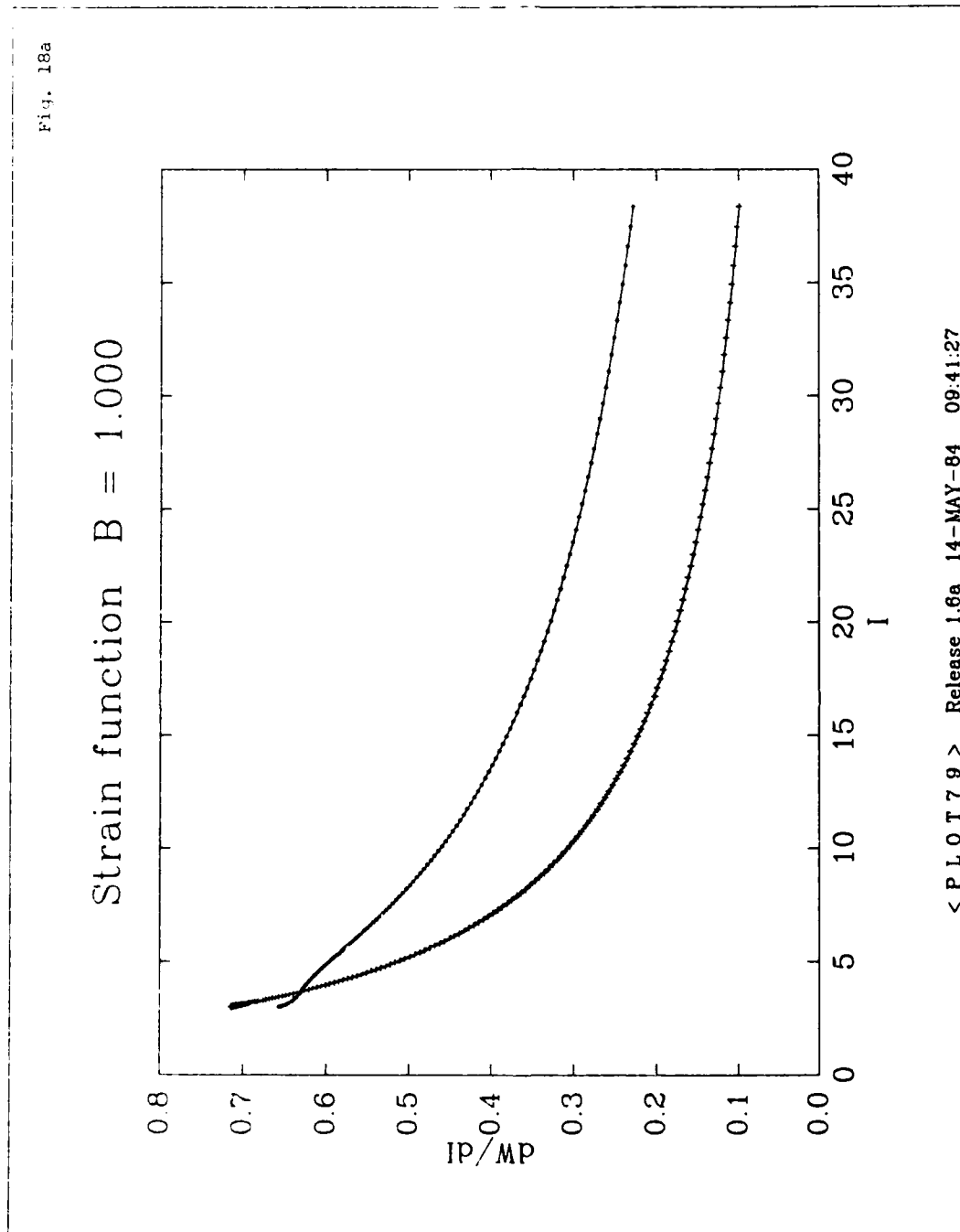
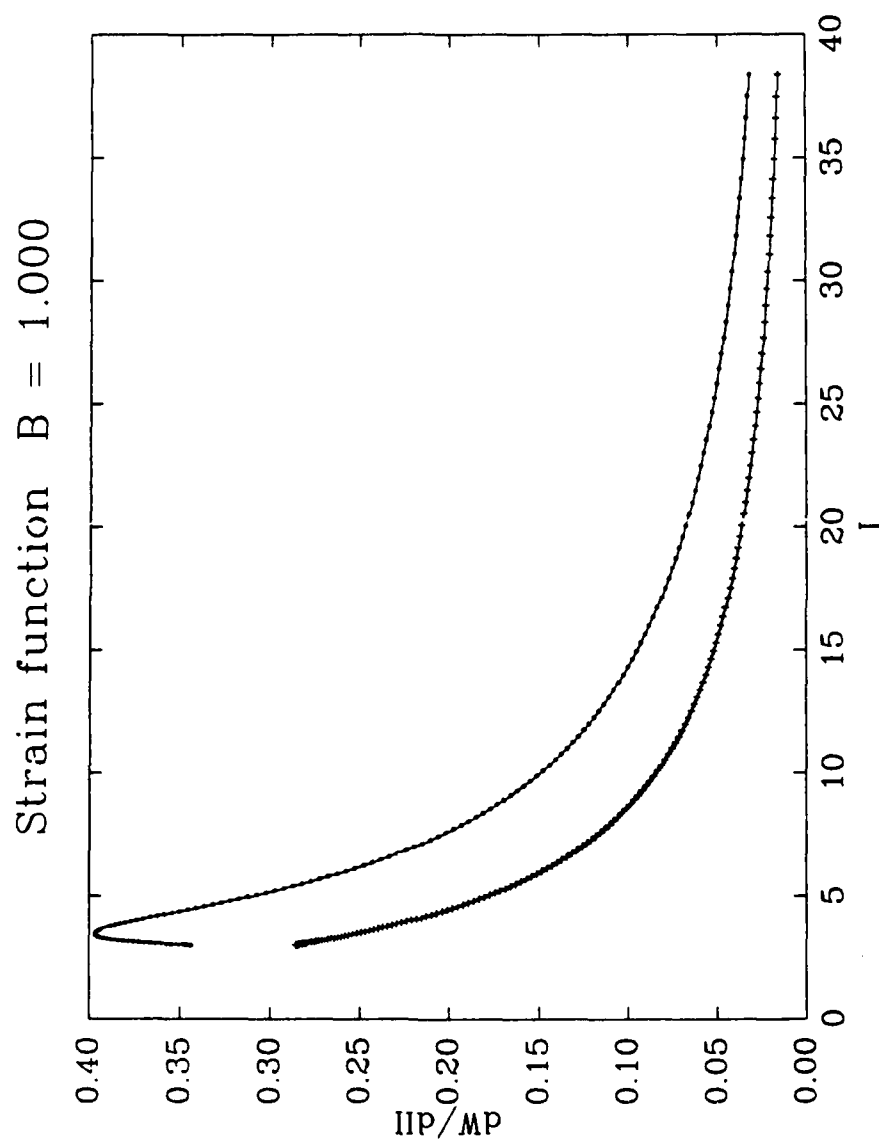


Figure 18. The strain functions are plotted as functions of I_1 in planar elongational flow:
a) $\frac{\partial W}{\partial I_1}$, b) $\frac{\partial W}{\partial I_2}$. The Doi-Edwards functions are shown for comparison.

Fig. 18b



< P L O T 7 9 > Release 1.6a 14-MAY-84 09:42:20

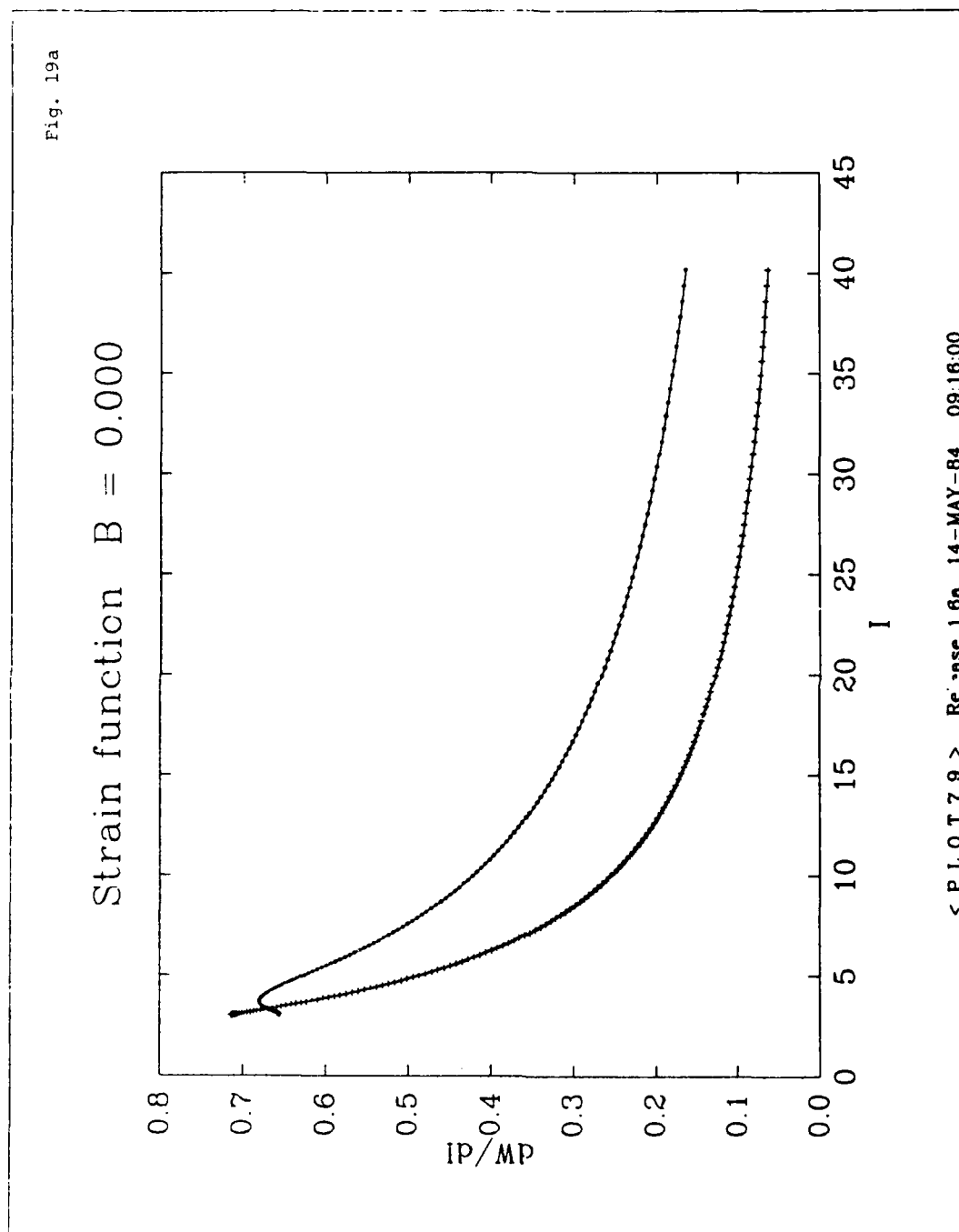
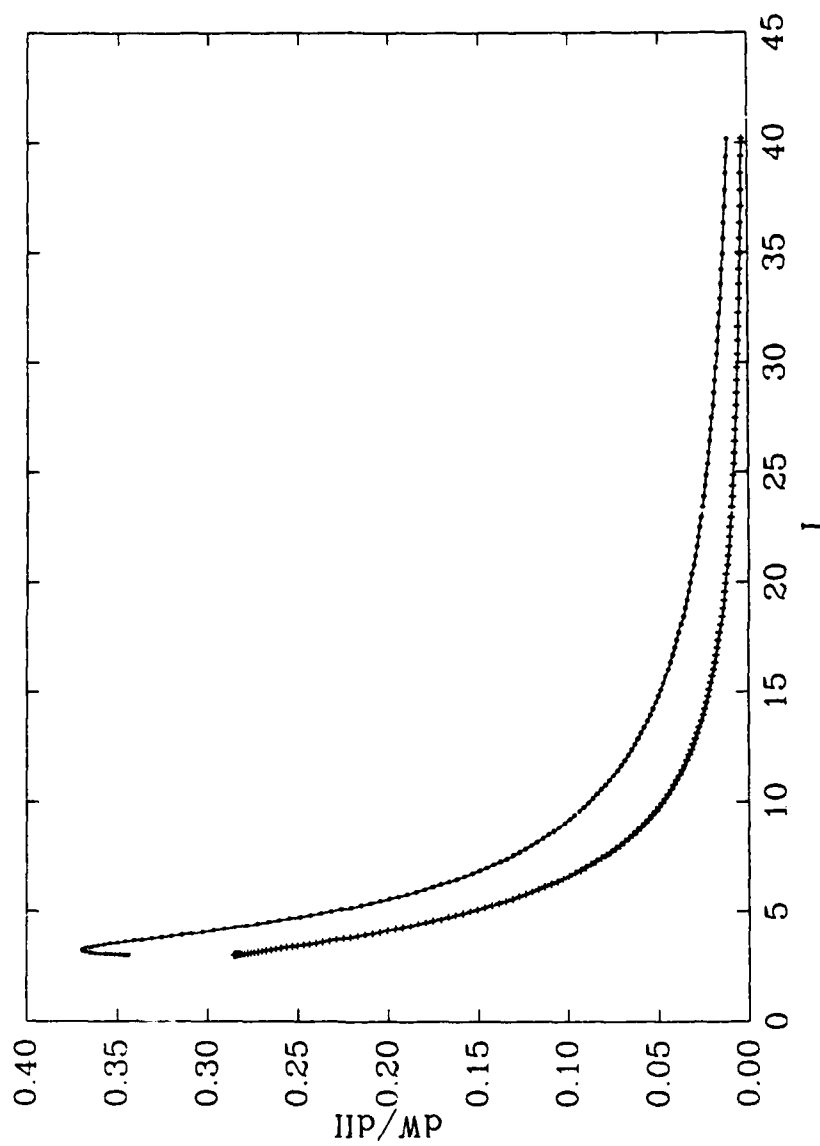


Figure 19. The strain functions are plotted as functions of I_1 in biaxial flow: a) $\frac{\partial W}{\partial I_1}$, b) $\frac{\partial W}{\partial I_2}$ and c) $\frac{\partial W}{\partial I_1} + \frac{\partial W}{\partial I_2} e^{-\epsilon s}$, where $\epsilon < 0$, and s corresponds with I_1 (see eq. (2.6)). The Doi-Edwards functions (+) are shown for comparison.

Fig. 19b

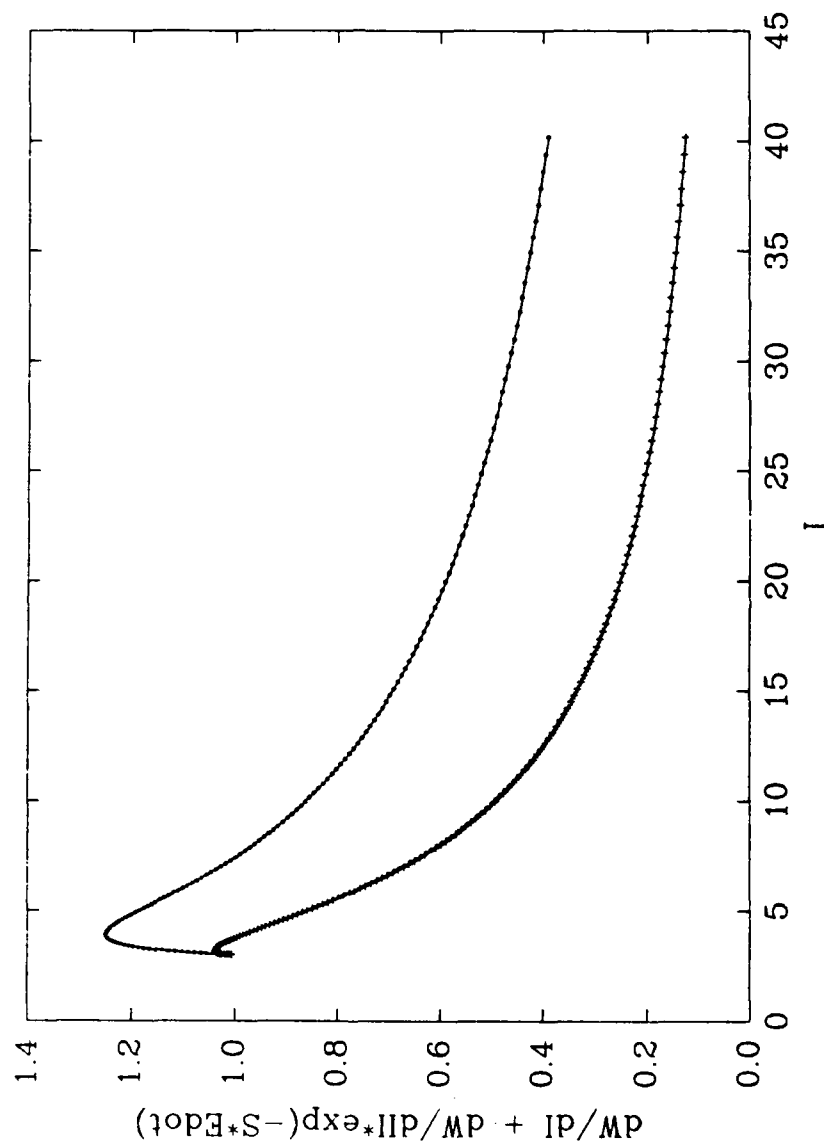
Strain function $B = 0.000$



< P L O T 7 9 > Release 1.6a 14-MAY-84 09:18:48

Fig. 19c

Strain function combination for $B = 0$.



< P L O T 7 9 > Release 1.6a 14-MAY-84 09:17:29

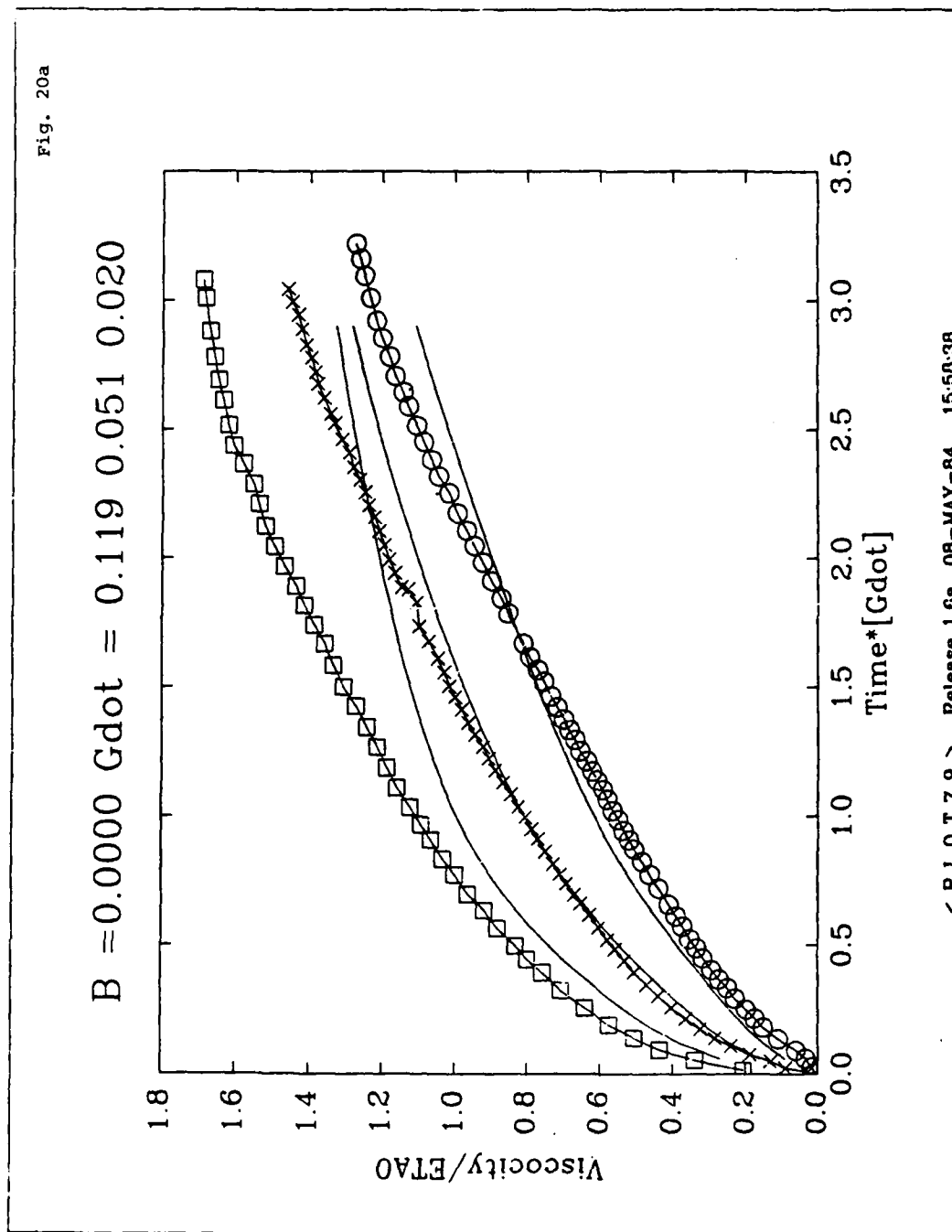
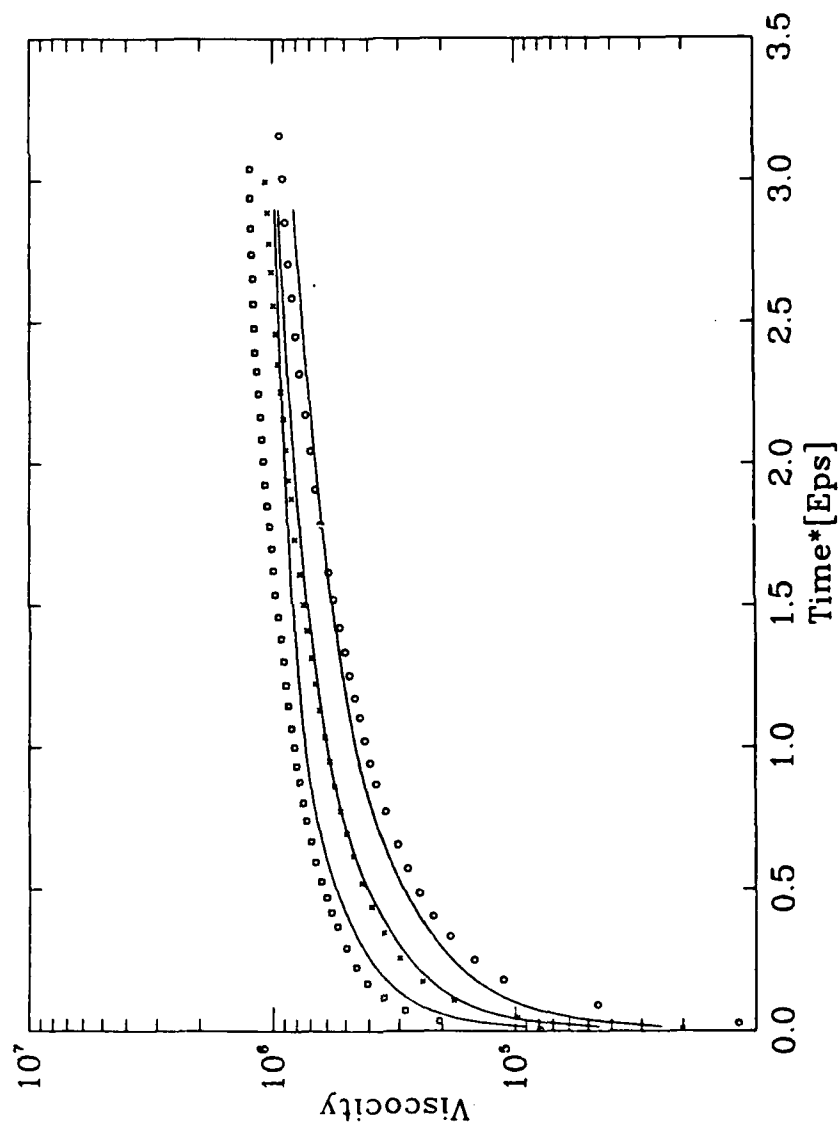


Figure 20. Comparison between model predictions (model (1.1)) (solid curves) and data (0 : $\dot{\gamma} = 0.119$, X : $\dot{\gamma} = 0.051$ and : $\dot{\gamma} = 0.020$) in uniaxial elongational flow: a) viscosity function in linear scale, b) viscosity function in logarithmic scale.

Fig. 20b

$B = 0.0000$ Eps = 0.119 0.051 0.020



< P L O T 7 9 > Release 1.6a 09-MAY-84 08:33:35

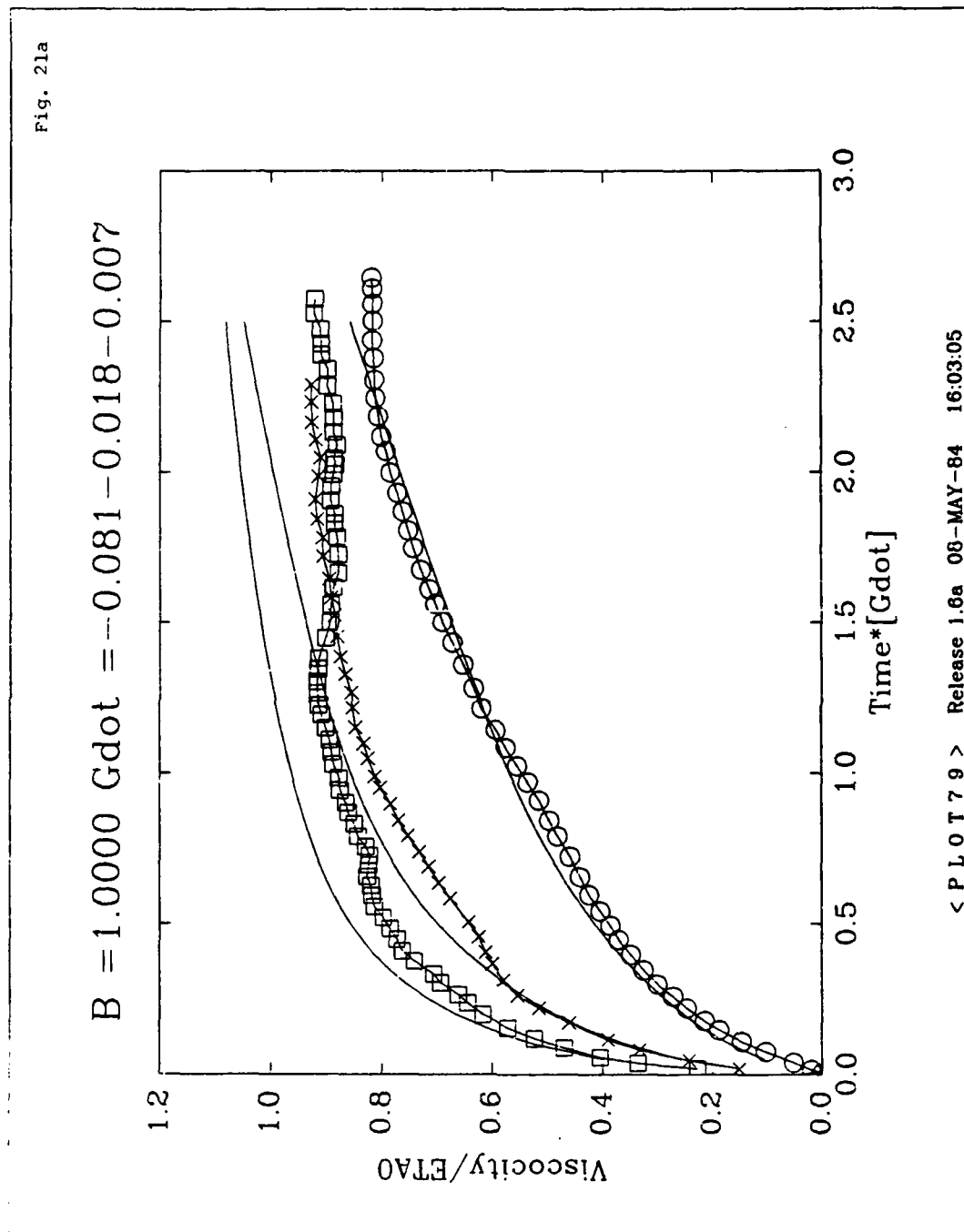
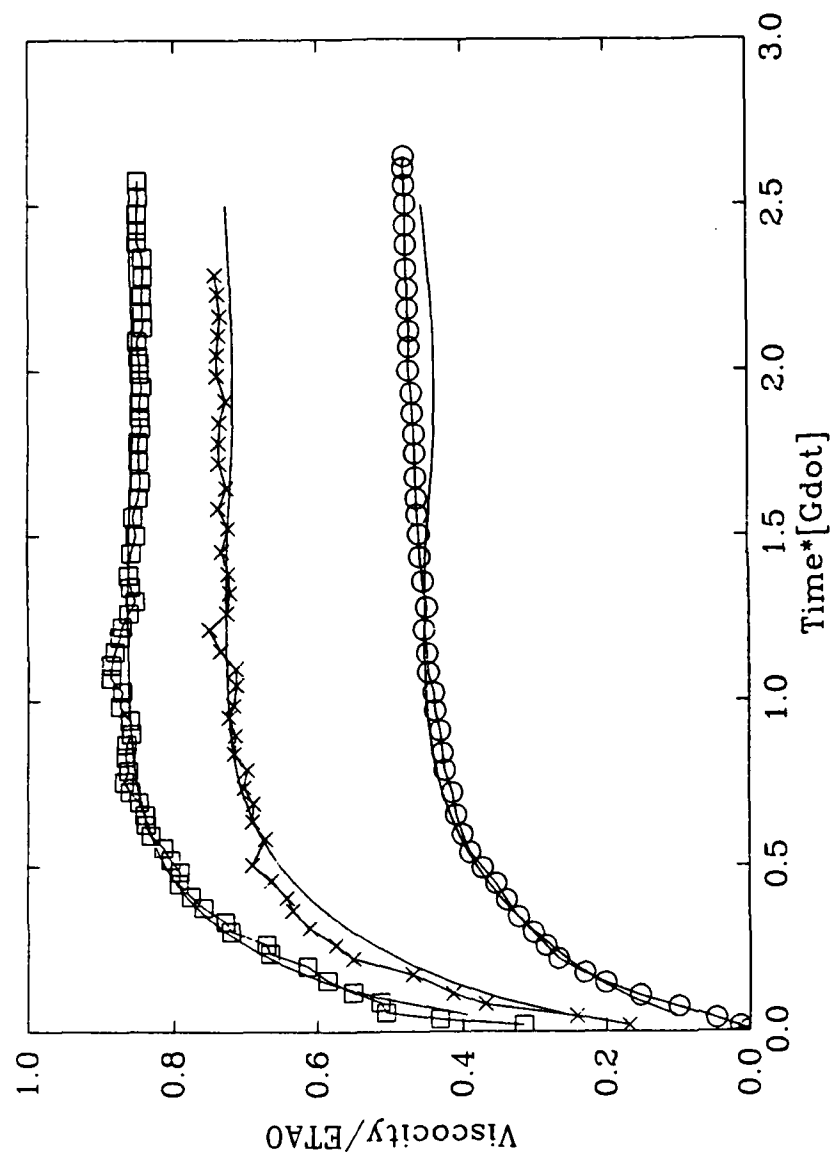


Figure 21. Comparison of model predictions (model (1.1)) and data ($\dot{\epsilon} = -0.081$, \times : $\dot{\epsilon} = -0.018$ and $\dot{\epsilon} = -0.007$) in planar elongational flow: a), c) first viscosity function, b), d) second viscosity function.

Fig. 21b

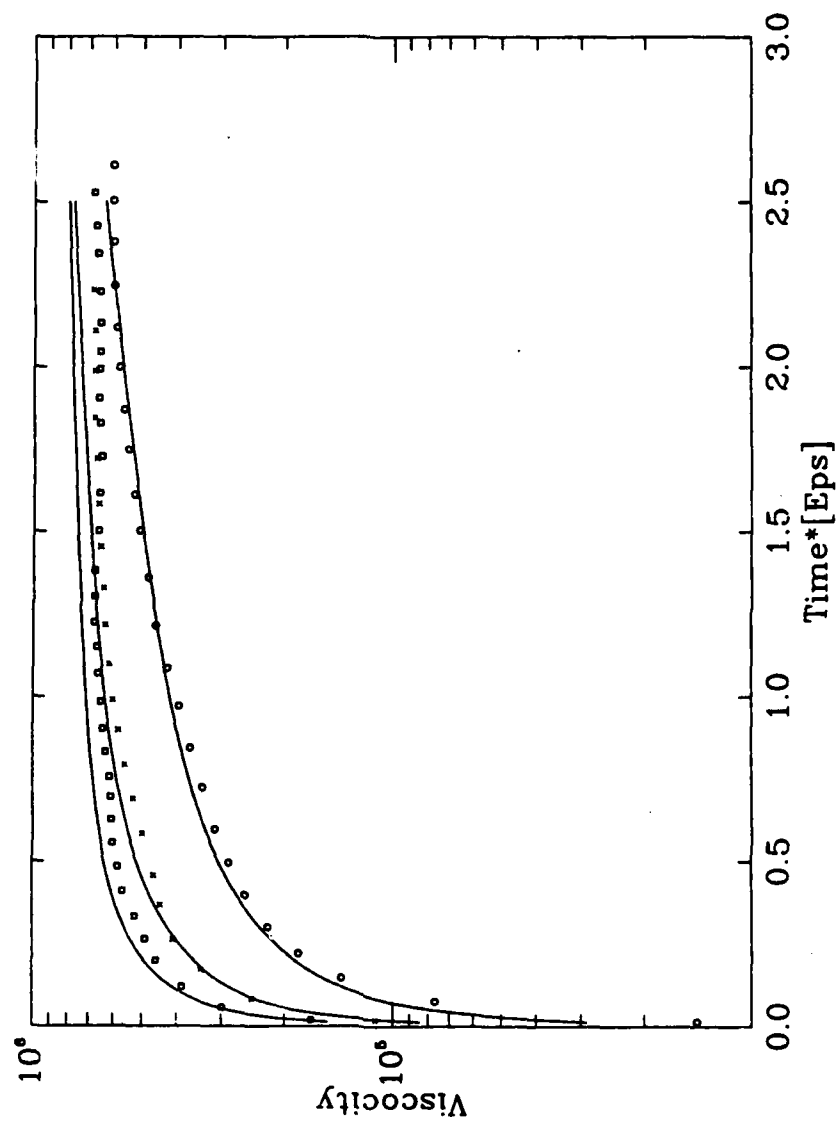
$$B = 1.0000 \text{ Gdot} = -0.081 - 0.018 - 0.007$$



< P L O T 7 9 > Release 1.6a 08-MAY-84 16:03:55

Fig. 21c

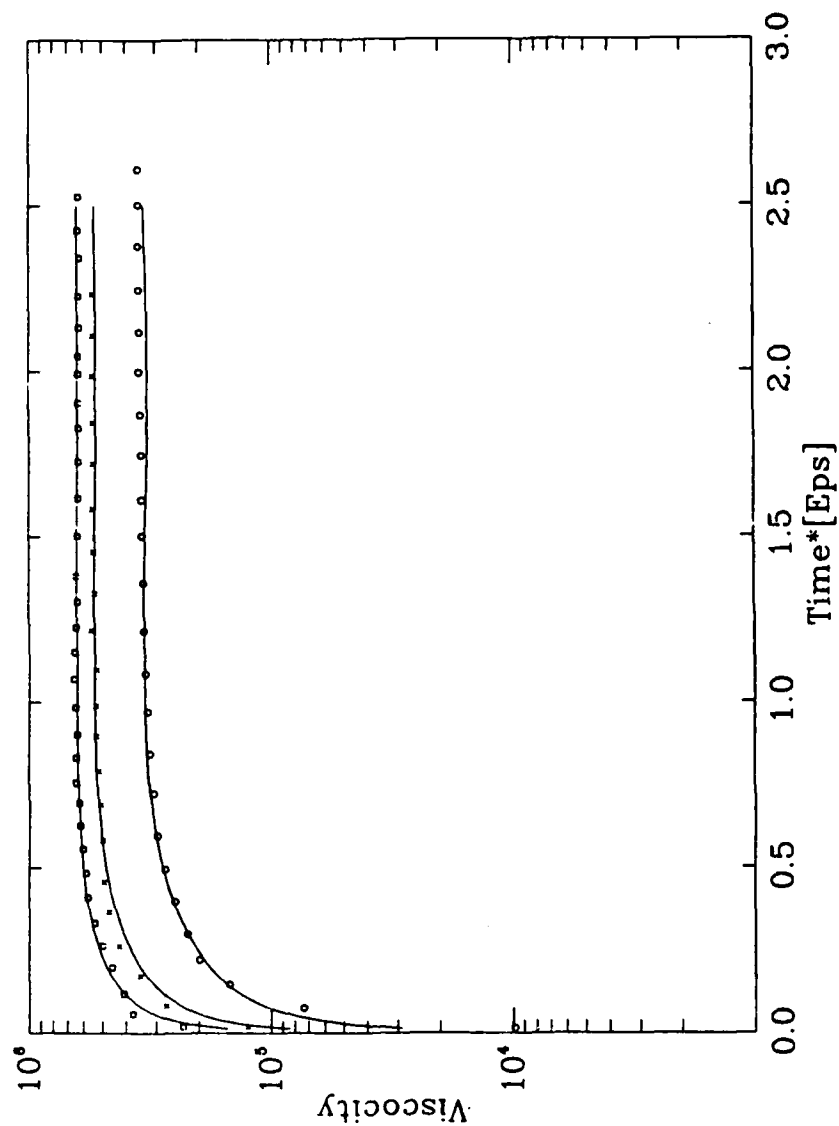
$$B = 1.0000 \text{ Eps} = -0.081 - 0.018 - 0.007$$



< P L O T 7 9 > Release 1.6a 09-MAY-84 08:38:45

Fig. 21d

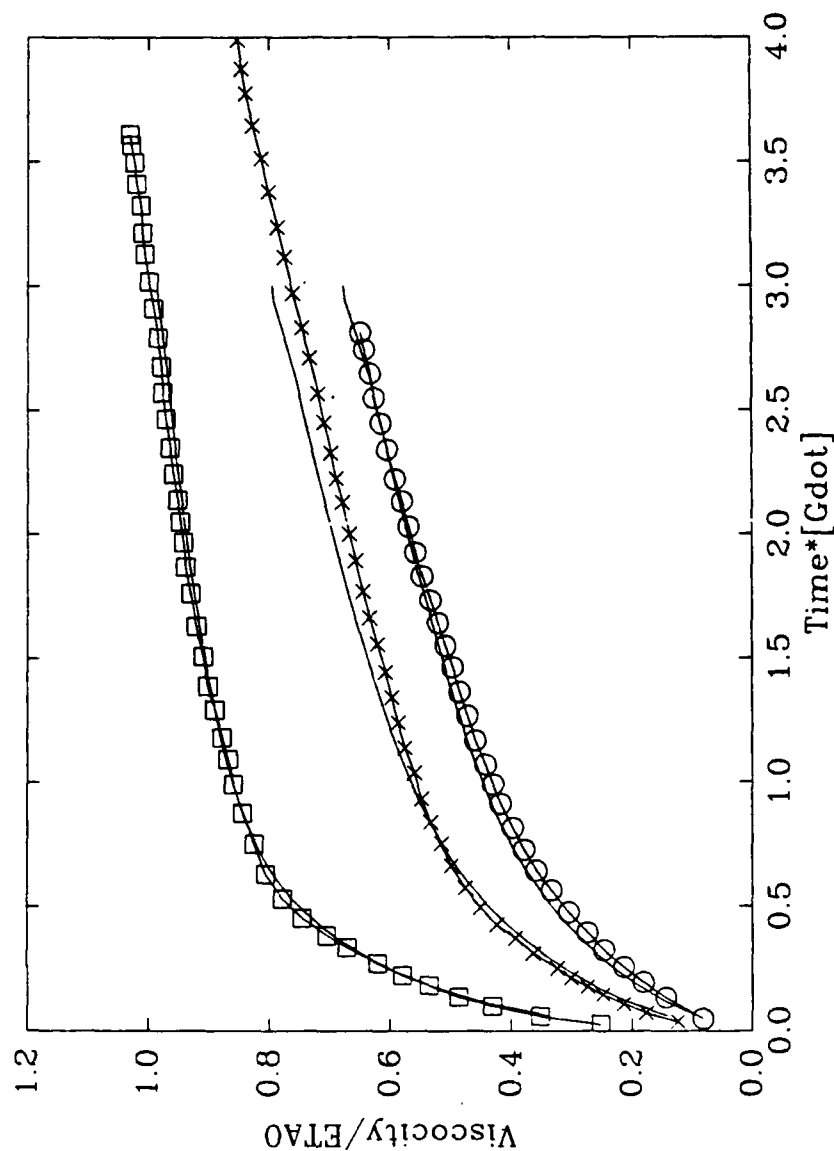
$$B = 1.0000 \text{ Eps} = -0.081 - 0.018 - 0.007$$



< P L O T 7 9 > Release 1.8a 09-MAY-84 08:39:22

Fig. 22a

$$B = 0.3333 \quad \dot{G} \dot{d} = -0.122 - 0.065 - 0.012$$

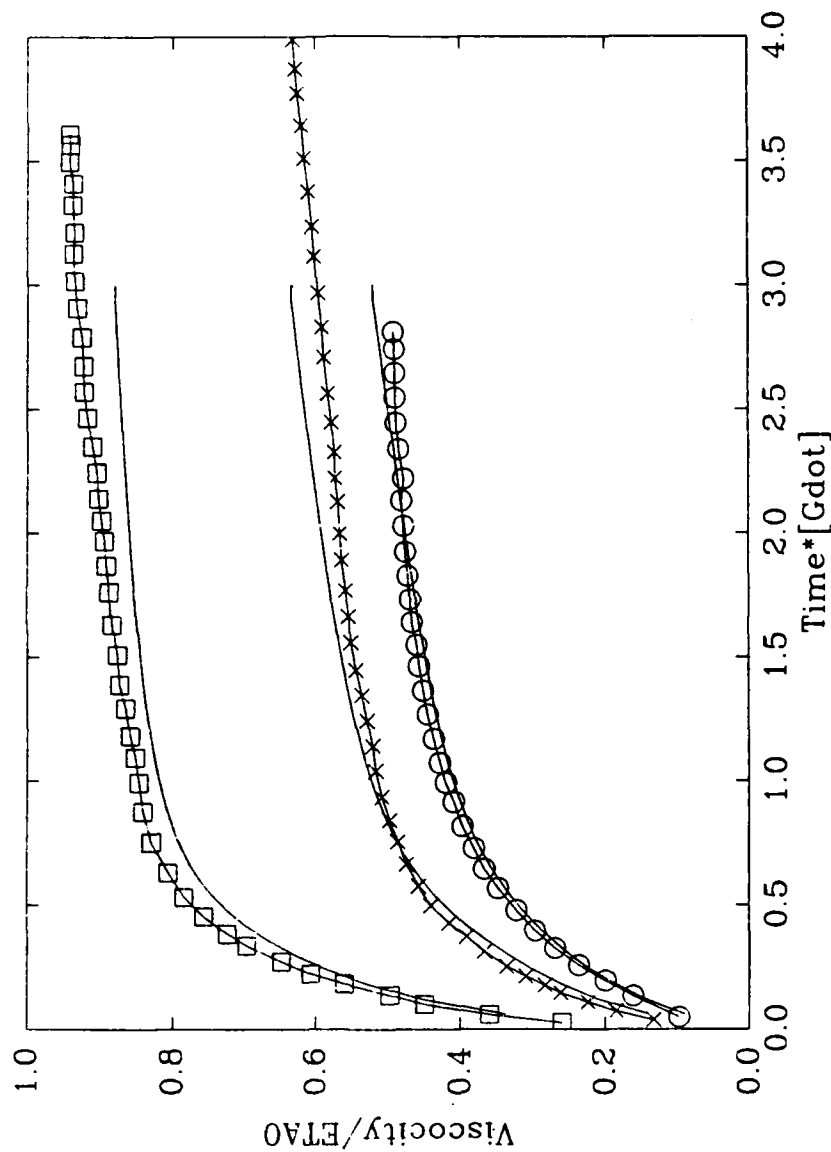


< P L O T 7 9 > Release 1.8a 08-MAY-84 16:16:26

Figure 22. Comparison of model predictions (model (1.1)) and data (0 : $\dot{\epsilon} = -0.122$, \times : $\dot{\epsilon} = -0.065$ and : $\dot{\epsilon} = -0.012$) in ellipsoidal elongational flow: a), c) first viscosity function; b), d) second viscosity function.

Fig. 22b

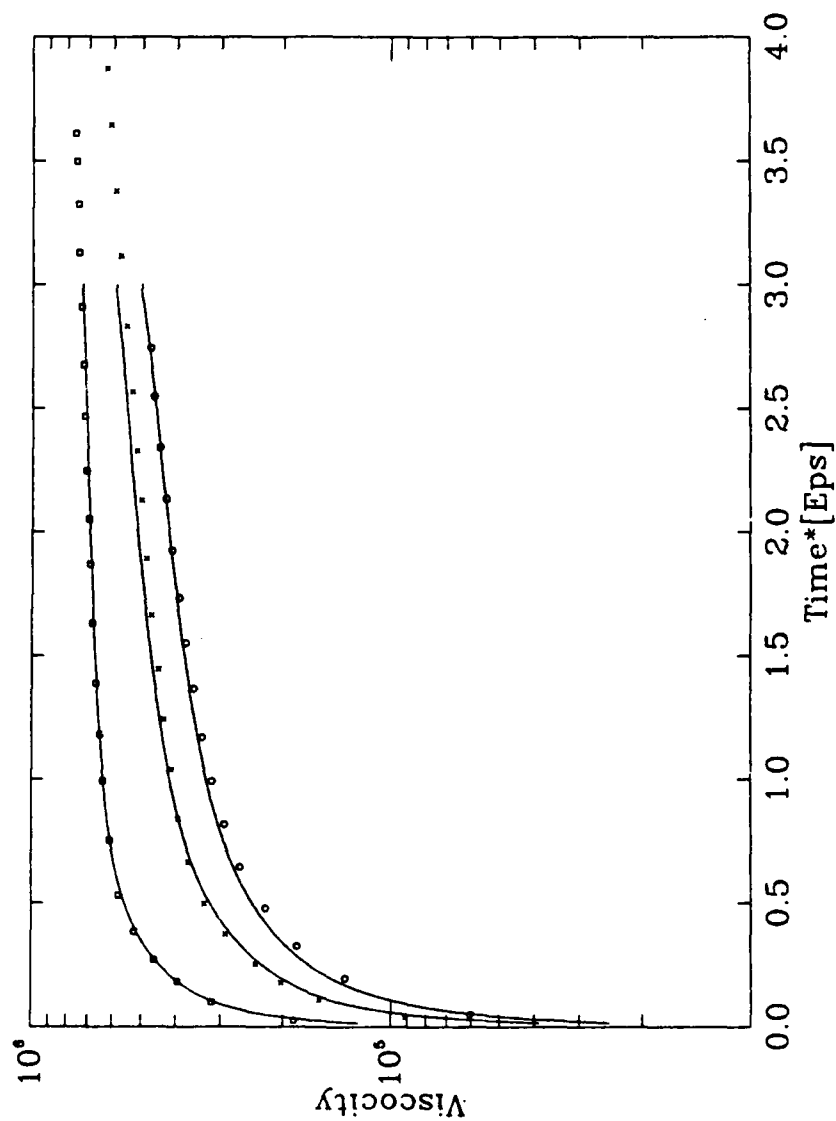
$$B = 0.3333 \text{ Gdot} = -0.122 - 0.065 - 0.012$$



< P L O T 7 9 > Release 1.6a 08-MAY-84 16:17:08

Fig. 22c

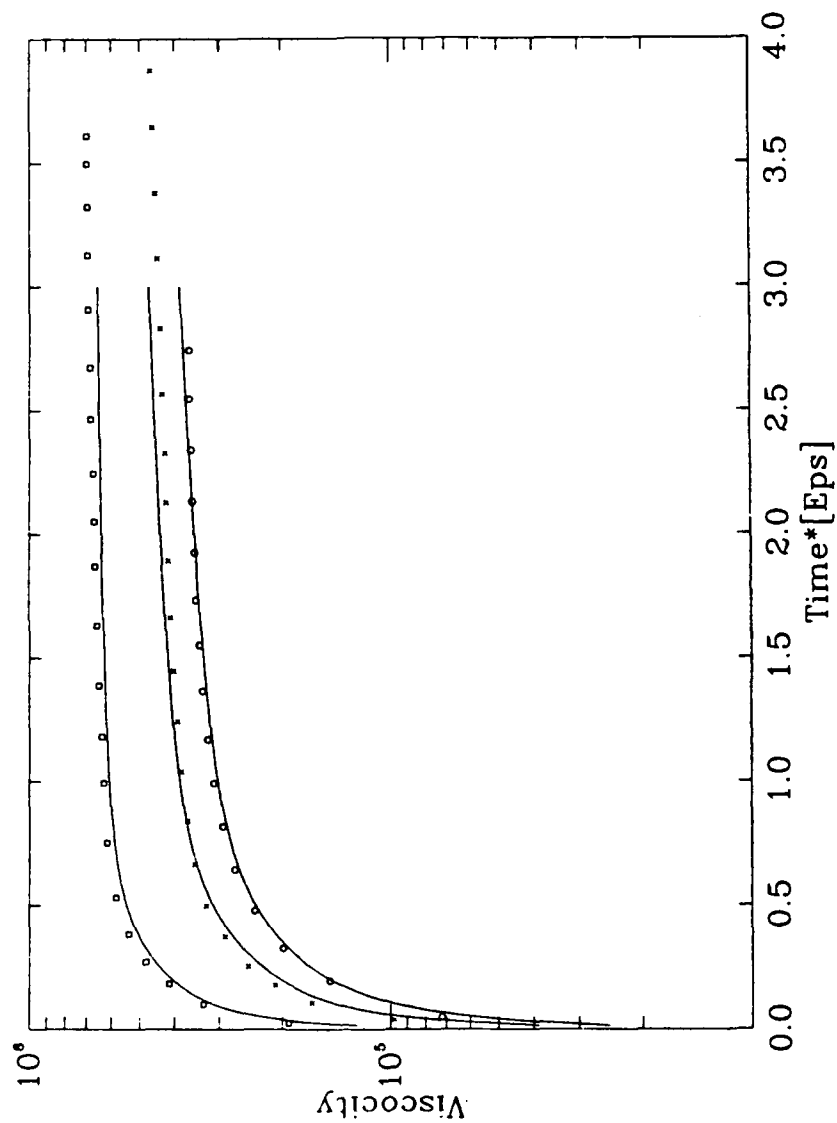
$$B = 0.3333 \text{ Eps} = -0.122 - 0.065 - 0.012$$



< P L O T 7 9 > Release 1.6a 09-MAY-84 08:54:01

Fig. 22d

$$B = 0.3333 \text{ Eps} = -0.122 - 0.065 - 0.012$$



< P L O T 7 9 > Release 1.6a 09-MAY-84 08:54:39

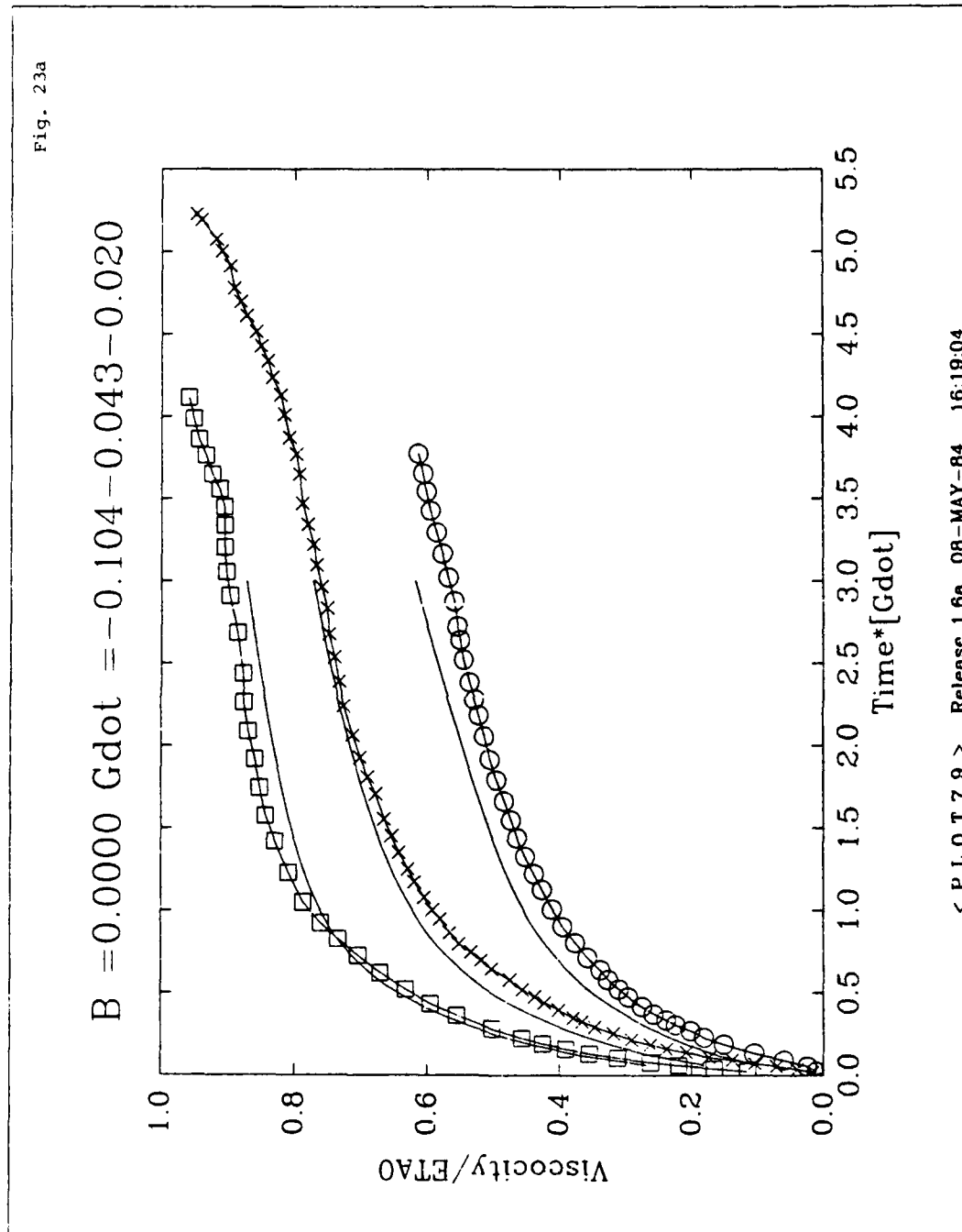
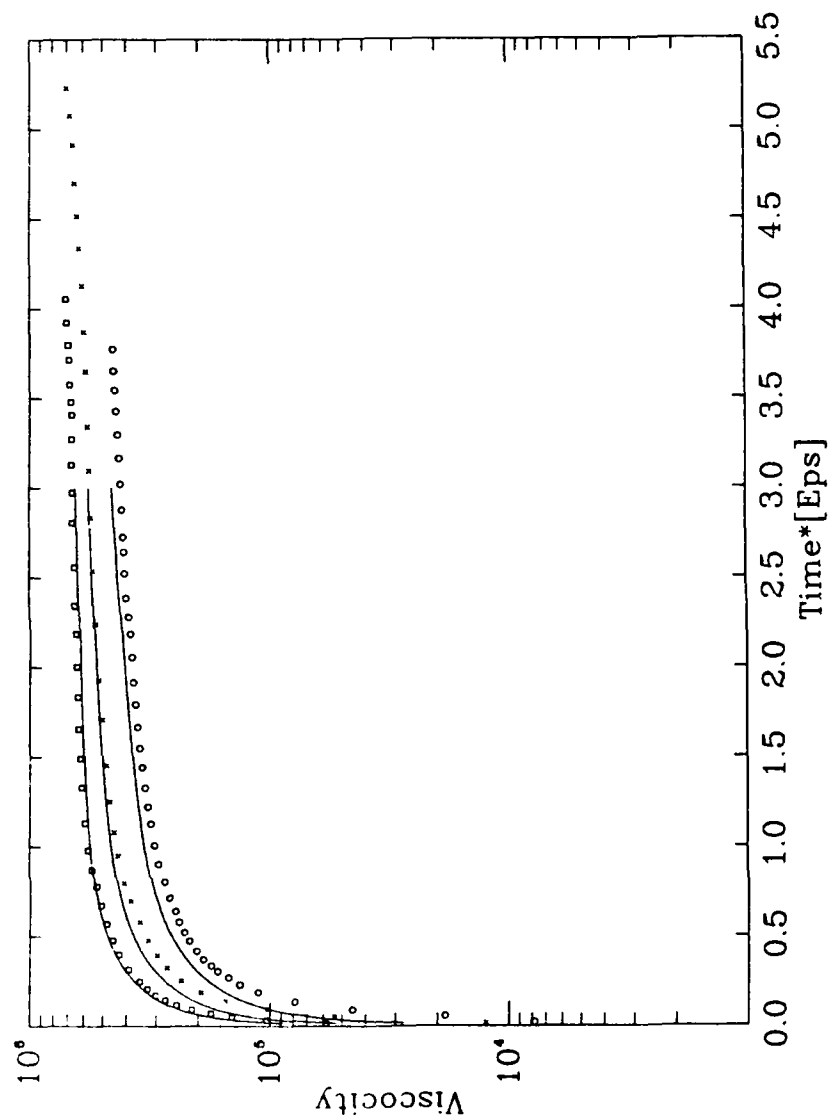


Figure 23. Comparison of model predictions (model (1.1)) and data ($\dot{\epsilon} = -0.104$, $X : \dot{\epsilon} = -0.043$ and $\dot{\epsilon} = -0.020$) in biaxial elongational flow. a) first viscosity function on a linear scale, b) first viscosity function on a logarithmic scale.

Fig. 23b

$B = 0.0000$ Eps $= -0.104 - 0.043 - 0.020$



< P L O T 7 9 > Release 1.6a 09-MAY-84 09:00:38

improvements, especially to the larger $\dot{\epsilon}$ - data. Apparently we do not sacrifice anything if we assume that the strain functions have to be the partial derivatives of the same function.

5. DISCUSSION

Our investigations of the factorized single integral constitutive equation suggests that the assumption of existence of a potential function for the strain functions does not limit the model in its ability to describe experiments. We find equally good descriptions of the general elongational data for the investigated PIB-polymer melt, with the assumption of a potential (Eq. 1.1) as without (Eq. 1.2).

We also found that with the factorized single integral constitutive equations and the linear viscoelastic memory function given by Demarmels (1983) it is impossible to adjust the strain functions to describe the experiments of Demarmels (1983) without significant systematic deviations. There may be several reasons for this:

- i) The linear viscoelastic memory function given by Demarmels may not be the optimal function. For example we do not feel comfortable with the oscillatory "measurements" in the frequency range from 10^{-3}s^{-1} and 10^{-2}s^{-1} artificially constructed from time temperature superposition. Also the shortest relaxation time, 10^{-3} sec. should be compared with the fact that a constant strain rate is not established in the experiments before after about 3 sec. It might have been preferable to represent relaxation times so short compared to typical times in the experiment by just a Newtonian contribution and estimate this contribution directly from the elongational flow experiment.
- ii) One can not rule out systematic errors in the experimental data. In particular what we fit is not raw data, but rather the results of some analysis applied to the measurements. This analysis is often different in different flow situations even for the same apparatus (Demarmels 1983, Ch. 5) and consequently a possibility for different types of systematic errors in the material functions arises.
- iii) The most interesting possibility, and the one we consider most likely is that the factorized single integral models with a memory function determined entirely from linear viscoelastic measurements, simply does not have sufficient flexibility to represent nonlinear material behavior over the entire invariant space. We

believe it is the first time that possibility has been so clearly established on the basis of experiments with "ever increasing deformations." The factorized single integral models are known (Demarmels 1983) to be unable to describe flows with sudden changes in flow type.

The strain functions calculated from the estimated potential function differ greatly from previously proposed strain functions; see Tables 1.1 and 1.2. The optimal strain functions for the particular PIB melt have maxima, with values well above 1, so the concept of the strain functions as being "damping-function" is not true for the particular model, and material. This point was noted also by Demarmels (1983). The general elongational flow data used here have the unique feature that they cover major parts of the invariant space. In contrast, the more common transient shear experiments are limited to $I_1 = I_2$. The general elongational experiments have two disadvantages, however. First it is not possible to obtain data for times that are even comparable to the smallest time constants of the fluid. The present rheometer can not give measurements with constant $\dot{\epsilon}$ for times smaller than approximately 3 sec., and the smallest time constant is 0.001 sec. Second it is not possible to obtain measurements for large $\dot{\epsilon}$ - values, or invariants.

If one were to search for a more general model our data comparison indicates that one should build on Eq. (1.1). We point out two possible generalizations:

i)

$$\tilde{\gamma}(t) = -n_s \dot{\gamma} + \int_{-\infty}^t M_i(t-t') \left[\frac{\partial W_i}{\partial I_1} \gamma_{[0]} + \frac{\partial W_i}{\partial I_2} \gamma_{[0]} \right] dt' \quad (5.1)$$

where

$$M_i(s) = \frac{n_i}{\lambda_i^2} \exp(-s/\lambda_i) \quad (5.2)$$

and $\dot{\gamma}$ is the rate-of-strain tensor. Here the short relaxation times have been "strangled" and represented by a Newtonian term. In other words to a first approximation $n_s = \sum n_i$ where the summation is on the relaxation times small compared to the shortest time in the experiment, here about 3 sec.

ii) One could add a term similar to the Curtiss-Bird (1981) ϵ -term. This involves the rate-of-strain tensor contracted twice with a fourth order tensor, and it is not immediately obvious how one would determine this fourth order tensor. The method proposed by Currie (1982) involves second derivatives of a potential function. Alfeld (1984b) has derived an explicit C^2 -Clough-Tocher scheme so this approach is feasible, but a serious question is if it is possible to implement models with this complexity in general flow programs.

REFERENCES

1. Alfeld, P. (1984a), "A Trivariate Clough-Tocher Scheme for Tetrahedral Data" to appear in "Computer Aided Geometric Design".
2. Alfeld, P. (1984b), "A Bivariate C^2 Clough-Tocher Scheme", MRC Technical Summary Report #2620, University of Wisconsin-Madison.
3. Bach, P. (1985), Ph.D. Thesis, The Technical University of Denmark.
4. Bernstein, B., Kearsley, E. and Zapos, L. (1963, Trans. Soc. Rheol. 7, 391-410.
5. Bird, R. B., Armstrong, R. C. and Hassager, O. (1985), Dynamics of Polymeric Liquids, Vol. 1, Fluid Mechanics, 2nd Ed., Wiley, New York.
6. Chacon, R. V. and Friedman, N. (1965), Arch. Ration. Mech. Anal., 18, 230-240.
7. Currie, P. K. (1982), J. Non-Newt. Fluid Mech., 11, 53-68.
8. Curtiss, C. F. and Bird, R. B. (1981), J. Chem. Phys. 74, 2016-2025, 74, 2036-2033.
9. Demarmels, A. (1983), "Das rheologische Verhalten von Polyisobutylen bei mehrachsigen Dehnströmungen und seine Beschreibung in der Netzwerktheorien" Abhandlung, ETH, Zürich, Switzerland.
10. Doi, M. and Edwards, S. F. (1978), J. Chem. Soc., Faraday Trans. II, 74, 1789-1801, 74, 1802-1817, 74, 1818-1832.
11. Doi, M. and Edwards, S. F. (1979), J. Chem. Soc., Faraday Trans. II, 75, 38-54.
12. Einaga, Y., Osaki, K. and Kurata, M. (1971), Polym. J. 2, 550.
13. Hassager, O. (1981), J. Non-Newt. Fluid Mech., 9, 321-328.
14. Kaye, A. (1962), College of Aeronautics Cranfield, Note No. 134.
15. Laun, H. M. (1978), Rheol. Acta., 17, 1-15.
16. Lodge, A. S. (1956), Trans. Faraday Soc., 52, 120-130.
Lodge, A. S. (1964), Elastic Liquids, Academic Press, London.
17. Martin, A. D. and Mizel, V. J. (1964), Arch. Ration. Mech. Anal., 15, 353-367.
18. Meissner, J., Stephenson, S. E., Demarmels, A. and Portmann, P. (1982), J. Non-Newt. Fluid Mech., 11, 221-237.
19. Papanastasiou, A. C., Scriven, L. E. and Macosko, C. W. (1983), J. Rheol. 27, 387-410.
20. Phillips, M. C. (1977), J. Non-Newt. Fluid Mech. 2, 109-121, 2, 123-137, 2, 139-149.

21. Renardy, M. (1984), "A local existence and uniqueness theorem for a K-BKZ fluid",
submitted to Arch. Rat. Mech. Anal.
22. Rivlin, R. S. and Saunders, D. W. (1951), Phil. Trans. A243, 251.
23. Rivlin, R. S. and Sawyers (1971), Ann. Rev. Fluid Mech. 3, 117-146.
24. Wagner, M. H. (1979), Rheol. Acta 18, 33-50.

A brief documentation

FORTRAN IV programs for the use in parameter estimation in a Kaye-BKZ polymer melt model. The theory and sample results for a specific PIB-polymer is given by Bach and Hassager (1984a).

Estimation programs.

The programs ESTIM, and ESTW are the main programs for estimation of two independent strainfunctions, and for estimation of a potential function respectively. The input is raw start-up data from any elongational flow. The time dependent behaviour is in the model assumed to be described by the linear viscoelastic memoryfunction, which is supplied as a FUNCTION. Only a very little programming effort is required to make the estimation programs take other material data, e.g. shear data (stress relaxation, stress growth experiments).

ESTIM estimates two independent strainfunctions Φ_1 and Φ_2 . These functions are defined by the shape functions belonging to an element mesh covering the invariant space. ESTIM uses the functions GPIB and FPIB. These are the relaxations modulus and the memory function respectively. When the linear least squares equation system is set up by ESTIM the IMSL routine LLSQF is called and finally the solution is written onto a file.

A number of routines from the Newtonian Flow program package NEWTON (Bach and Hassager (1984b)) have been used in ESTIM.

ESTW estimates the parameters in a C^1 Clough-Tocher scheme Alfeld (1984) for the potential function W . The Clough-Tocher scheme is implemented in the subroutine C1INT. This routine calculates the partial derivatives $\frac{\partial W}{\partial I^*}$ and $\frac{\partial W}{\partial II^*}$, and optional the potential function value, at any point in the covered invariant space. The invariant space is transformed to obtain a better distribution of data points. We use $I^* = \log(I - 2)$ and $II^* = \log(II - 2)$. The partial derivatives are related by :

$$\frac{\partial W}{\partial I} = \frac{\partial W}{\partial I^*} \frac{1}{(I - 2)} = \frac{\partial W}{\partial I^*} e^{-I^*}$$

$$\frac{\partial W}{\partial II} = \frac{\partial W}{\partial II^*} \frac{1}{(II - 2)} = \frac{\partial W}{\partial II^*} e^{-II^*}$$

It would in principle be possible to use the same method as in ESTIM but as the equations system would be very difficult to set up, a straight forward minimization method

is used instead. The IMSL routine ZXSSQ performs very well on the actual problem. The residuals are calculated by the FUNCTION FC2.

All subroutines used are described in the following. They are listed in alphabetic order. *All parameters in boldface are to be set by the user, and all underlined parameters are to be reset by the user, as they are changed by the routine.*

C1INT(X, Y, IOPR, MP, W, DW, DDW1, DDW2, DDW3, F, DFX, DFY, IER)

C1INT calculates the function value F (only for $IOPR = 0$), and the partial derivatives $\frac{\partial F}{\partial X} = DFX$, and $\frac{\partial F}{\partial Y} = DFY$ of the interpolant at (X,Y). If $IOPR > 0$ then C1INT assumes that (X,Y) is in element number = IOPR. If $IOPR \leq 0$ then C1INT searches all elements until the one containing (X,Y) is found. If no element is found IER equal to 1 will be returned, else IER = 0 is returned, and IOPR is set to the actual element number found. Note that this option can be used to enhance the effectiveness greatly in situations where C1INT is to be called with the same set of (X,Y) many times. Topology data is supplied in the C1DATA - COMMON block, and the data to be used in the interpolation scheme are supplied in W(MP), and DW(MP,2). The arrays DDW1(MP,2), DDW2(MP,2), and DDW3(MP,2) are the directional derivatives at the local nodes 1,2 and 3 respectively.

FC2(OMEGA, NRES, NPAR, RESV)

FC2 is the EXTERNAL routine required by ZXSSQ. The parameters are supplied in OMEGA(NPAR), and all residuals are to be returned in RESV(NRES) for any given parameter vector supplied by ZXSSQ. Every datapoint contribute with two residuals, except for flows with $B = 0$.

FMEMO(S, Td, G0)

FUNCTION FMEMO calculates the Doi-Edwards memory function. S is the independent argument of the memory function, and $Td := T_d$ is the disengagement time, and $G0 := G_0$ is the elastic modulus. The function value is returned in FMEMO.

FPIB(S, Td, G0)

FUNCTION FPIB calculates the memory function obtained by Demarmels (1983). S is the argument of the memory function, and here is G0 the zero shear rate viscosity η_0 . Td is not used. The function value is returned in FPIB.

GAUSSW(N, ROOT, WEIGHT)

SUBROUTINE GAUSSW calculates the N'th Gauss-Legendre rule; that is the abscissae: ROOT(N) in the interval $[-1, +1]$, and the corresponding weights: WEIGHT(N).

GMEMO(S, TD, G0)

FUNCTION GMEMO calculates the Doi-Edwards relaxation modulus. (See FMEMO for the explanation of the arguments).

GPIB(S, Td, G0)

FUNCTION GPIB calculates the relaxation modulus obtained by Demarmels (1983) for a commercial PIB polymer. (See FPIB for the explanation of the arguments).

LAMDA(I, II, L)

SUBROUTINE LAMDA calculates the eigenvalues in any flow using the analytical formulae derived by Currie (1982). I, II are the first and second invariants respectively. Note Currie's definitions ! It shall be noted that Currie's formulae are not suited for numerical evaluation for large invariants. Numerically it would be better to solve the cubic equation for the eigenvalues directly Bach (1985).

UPOT(I, II, N, L, FI1, FI2)

FUNCTION UPOT evaluates the Doi-Edwards potential function W using a N'th degree Gauss-Legendre quadrature formula. The partial derivatives of W with respect to the first (I) and second (II) invariant are calculated using the analytical formulae derived by Bach (1985). The eigenvalues L(3) are calculated by LAMDA. The partial derivatives $\frac{\partial W}{\partial I}$ and $\frac{\partial W}{\partial II}$ at (I, II) are returned in FI1 and FI2 respectively. The value of the W - function at (I, II) is returned in UPOT.

Utility programs.

The programs START and START1 are the interactive main programs used to calculate material functions and to test the obtained models.

START: Interactive MAIN program .

START calculates start-up material functions in shear flows, and in all kinds of elongational flows for 1) The exact Doi-Edwards model, 2) Currie's (1982) approximation to Doi-Edwards model. 3) General Kaye-BKZ models, with two independent strain functions given as nodalpoint values on an element mesh. The exact Doi-Edwards potential function is calculated by UPOT. The memory integral is evaluated by a very cautious Romberg routine called DCADRE (IMSL). START writes the necessary information to the PLOT79-interface routines (GPLT, GPLTL, GPLTLL). START can also be used to test model prediction against viscometric data.

START1 : Interactive MAIN program.

START1 calculates the start-up material functions in shear and all kinds of elongational flows for the Kaye-BKZ polymer melt model with a potential function W . W , and its derivatives, are calculated by C1INT. The memory integral is evaluated by DCADRE (IMSL-routine). START1 writes the necessary information to the PLOT79-interface routines (see START). START1 can also be used to test model predictions against viscometric data.

References.

- Alfeld, P. (1984): A trivariate Clough-Tocher scheme for tetrahedral data. Computer Aided Geometric Design, (to appear).
- Bach, P. and O. Hassager; (1984a) . MRC. report (to appear).
- Bach, P. and O. Hassager (1984b); USERS GUIDE to NEWTON; 5.ed. May 1984.
- Bach, P. (1985); Ph.D. thesis (to appear).
- Currie, P. K. (1982); Constitutive equations for polymer melts predicted by the Doi-Edwards and Curtiss-Bird kinetic theory models. Journal of Non-Newtonian Fluid Mechanics **11** 53-68.
- Demarmels, A. (1983); Diss. ETH Nr. 7345 Zürich. Das rheologische Verhalten von Polyisobutylen bei mehrachsigen Dehnströmungen und seine Beschreibung in den Netzwerktheorien.

REPORT DOCUMENTATION PAGE		READ INSTRUCTIONS BEFORE COMPLETING FORM
1. REPORT NUMBER 2755	2. GOVT ACCESSION NO. AD-A149410	3. RECIPIENT'S CATALOG NUMBER
4. TITLE (and Subtitle) SINGLE INTEGRAL CONSTITUTIVE EQUATIONS FOR VISCOELASTIC FLUIDS		5. TYPE OF REPORT & PERIOD COVERED Summary Report - no specific reporting period
		6. PERFORMING ORG. REPORT NUMBER
7. AUTHOR(s) Poul Bach and Ole Hassager		8. CONTRACT OR GRANT NUMBER(s) DAAG29-80-C-0041 16-3475, K-802
9. PERFORMING ORGANIZATION NAME AND ADDRESS Mathematics Research Center, University of 610 Walnut Street Wisconsin Madison, Wisconsin 53706		10. PROGRAM ELEMENT, PROJECT, TASK AREA & WORK UNIT NUMBERS Work Unit Number 2 - Physical Mathematics
11. CONTROLLING OFFICE NAME AND ADDRESS U. S. Army Research Office P.O. Box 12211 Research Triangle Park, North Carolina 27709		12. REPORT DATE September 1984
14. MONITORING AGENCY NAME & ADDRESS (if different from Controlling Office)		13. NUMBER OF PAGES 76
		15. SECURITY CLASS. (of this report) UNCLASSIFIED
15a. DECLASSIFICATION/DOWNGRADING SCHEDULE		
16. DISTRIBUTION STATEMENT (of this Report) Approved for public release; distribution unlimited.		
17. DISTRIBUTION STATEMENT (of the abstract entered in Block 20, if different from Report)		
18. SUPPLEMENTARY NOTES		
19. KEY WORDS (Continue on reverse side if necessary and identify by block number) Integral constitutive equations, Viscoelasticity, Rheology		
20. ABSTRACT (Continue on reverse side if necessary and identify by block number) It is demonstrated how the kernel functions of single integral constitutive equations may be determined from analysis of experiments in time dependent shear-free flows alone. It is assumed that the kernel functions may be factored into a product of a linear viscoelastic function and a finite-strain dependent function. No assumption is needed on the strain-dependent function except that it must be continuous within the attainable invariant space. The experimental data for ever-increasing deformations are not compatible with the assumptions inherent in single integral constitutive equations with factorized kernel functions.		

END

FILMED

2-85

DTIC